BIOLOGICAL SCIENCES: Cell Biology

Molecular basis of fatty acid selectivity in the zDHHC family of *S*-acyltransferases revealed by click chemistry

Short title: *Fatty acid selectivity of zDHHC S-acyltransferases*

Jennifer Greaves[1], Kevin R. Munro[2], Stuart C. Davidson[2], Matthieu Riviere[2], Justyna Wojno[2], Terry K. Smith[3], Nicholas C.O. Tomkinson[2], Luke H. Chamberlain[1]

[1]Strathclyde Institute of Pharmacy and Biomedical Sciences, University of Strathclyde, 161 Cathedral Street, Glasgow G4 0RE, UK.
[2]WestCHEM, Department of Pure and Applied Chemistry, University of Strathclyde, 295 Cathedral Street, Glasgow G1 1XL, UK.
[3]BSRC, Schools of Biology and Chemistry, University of St. Andrews, North Haugh, St. Andrews, Fife KY16 9ST, UK.

Correspondence to Luke H. Chamberlain: luke.chamberlain@strath.ac.uk

Keywords: *S*-acylation, palmitoylation, zDHHC, click chemistry, fatty acid, acyl-CoA

Abstract

***S*-Acylation is a major post-translational modification, catalysed by the zDHHC enzyme family. *S*-acylated proteins can be modified by different fatty acids; however, very little is known about how zDHHC enzymes contribute to acyl chain heterogeneity. Here, we employed fatty acid azide/alkyne labelling of mammalian cells, showing their transformation into acyl-CoAs and subsequent click chemistry-based detection, to demonstrate that zDHHC enzymes have marked differences in their fatty acid selectivity. This was apparent even for highly related enzymes such as zDHHC3 and zDHHC7, which displayed a marked difference in ability to use C18:0 acyl CoA as a substrate. Furthermore, we identified Isoleucine-182 in the third transmembrane domain of zDHHC3 as a key determinant limiting the use of longer chain acyl-CoAs by this enzyme. This is the first study to uncover differences in the fatty acid selectivity profiles of cellular zDHHC enzymes and to map molecular determinants governing this selectivity.**

Significance Statement

S-Acylation, the attachment of different fatty acids onto cysteine residues, regulates the activity of a diverse array of cellular proteins. This reversible post-translational modification is essential for normal physiology and defects are linked to human disease. S-acylation is catalysed by a large family of "zDHHC" S-acyltransferases that use a cellular pool of diverse fatty acyl CoAs as substrates. Using chemically-synthesised probes, we show that individual zDHHC enzymes have marked differences in fatty acid selectivity, and identify the underlying molecular basis for this. The study describes how acyl chain heterogeneity of S-acylated proteins is generated, and is significant because the chemical nature of the attached S-acyl chain can fundamentally impact protein behaviour.

\body

Introduction

S-Acylation is a reversible post-translational modification (PTM) involving the attachment of fatty acids onto cysteines(1, 2). This PTM occurs on both soluble and transmembrane (TM) proteins and exerts a number of important effects, such as mediating membrane binding (of soluble proteins or soluble loops of TM proteins), regulating protein trafficking and targeting to cholesterol-rich membrane micro-domains, and modulating protein stability(3, 4). These actions of *S*-acylation on a diverse array of cellular proteins impact many important physiological pathways, and defects in this process are linked to a number of major diseases and disorders(2, 5).

S-Acylation is mediated by the opposing actions of acyltransferases and thioesterases. *S*-Acyltransferase enzymes belong to the zDHHC protein family, which are encoded by twenty-four distinct genes(6-8). zDHHC enzymes are thought to share the same overall membrane topology, with 4-6 transmembrane domains and the N- and C-termini present in the cytosol(9). The catalytic DHHC cysteine-rich domain (CRD) of the enzymes lies in a cytosolic loop(9) allowing zDHHC enzymes to modify substrate cysteines present at the cytosol-membrane interface. The *S*-acylation reaction is thought to proceed through an enzyme-acyl intermediate, where the acyl chain is attached to the cysteine of the DHHC motif via a thioester linkage (often referred to as enzyme "autoacylation")(10, 11). The *S*-acyl chain is then transferred to a cysteine residue of a substrate protein(10, 11). This overall process is referred to as a "ping-pong" reaction mechanism. There has been progress identifying the zDHHC enzymes that are active against many substrate proteins(2), although we lack a detailed understanding of the protein substrate profiles of individual enzymes and how enzyme-substrate interaction specificity is achieved. Co-expression experiments have suggested that individual zDHHC enzymes might exhibit a level of overlap in their protein substrate profiles, suggesting some possible redundancy within the zDHHC family(2). Nevertheless, individual enzymes have been linked with many disorders, including intellectual disability, diabetes and cancer, suggesting that any functional redundancy is limited(2).

In contrast to the steadily increasing knowledge about the specific interactions of zDHHC enzymes with their protein substrates, we know relatively little about the fatty acid selectivity of these enzymes. The term *palmitoylation* is often used as a synonym for *S*-acylation. However this does not reflect the potential diversity of *S*-acyl chains added to substrate proteins. Indeed, an analysis of the acyl groups added to *S*-acylated proteins in platelets revealed that 74% were from palmitate (C16:0), 22% from stearate (C18:0) and 4% from oleate (C18:1)(12). Other studies have shown that *S*-acylated proteins can be modified by acyl chains from myristic acid (C14:0), palmitoleic acid (C16:1), linoleic acid (C18:2) and arachidonic acid (C20:4)(12-15). Furthermore, mass spectrometry analysis of the *S*-acyl chains attached to influenza haemagglutinin proteins has revealed that C16:0 and C18:0 fatty acids are attached in a site-specific manner(16). There is also potential for cell type specific differences in the fatty acid profiles of *S*-acylated proteins; for example, one study reported that in RAW26.7 cells less than 10% of the acyl-CoAs were greater than C20, whereas in MCF7 cells C24:0 and C26:0 acyl-CoAs were present at similar amounts to C16:0 and C18:0 acyl-CoAs(17). The identity of the added acyl chain is central to the regulatory effects of *S*-acylation as different acyl chains vary in affinity for membranes and for cholesterol-rich membrane micro-domains(18).

To-date, a single study has explored the potential role of zDHHC enzymes in differential protein *S*-acylation using purified recombinant zDHHC enzymes in detergent micelles(10). This study reported that zDHHC2 catalysed the *S*-acylation of substrate proteins with similar efficiency using palmitate (C16:0), stearate (C18:0) or C20 (C20:0, C20:4) fatty acids. In contrast, zDHHC3 displayed a marked preference for shorter chain length acyl-CoAs and incorporated C16:0 much more efficiently than either C18:0 or C20 fatty acids(10). This elegant study highlighted the potential for discrete patterns of fatty acid selectivity in the zDHHC family, but these questions have been challenging to address, particularly in a cellular context. Recent developments at the chemistry-biology interface have identified new approaches to investigate this poorly defined area of the *S*-acylation field. Specifically, azide and alkyne fatty acid probes have provided novel and highly-sensitive chemical tools to interrogate S-acylation by click chemistry(19-24). In this study, we report the use of chemically-synthesised azide and alkyne fatty acid probes to investigate fatty acid selectivity in the zDHHC enzyme family and determine the molecular mechanisms governing this selectivity.

Results

Azide fatty acids are good mimics of endogenous fatty acids

Fatty acid azide probes of different acyl chain length were synthesised as described in the SI Appendix. To assess their ability to be taken up by cells, the total fatty acid content of HEK293T cells treated with these synthesised azide fatty acids was determined (Figure 1). Untreated cells showed the expected range of saturated and unsaturated fatty acids, with C18:0 and C18:1 being the most abundant. Upon addition of the various azide fatty acids to the cells, it can clearly be seen that these were not only accumulated within the cells (with C16:0 and C18:0 azides being taken up significantly better than C14:0 and C20:0 azides), but also metabolised by the

cells. For example the C16:0 azide was elongated to C18:0, which was subsequently desaturated to C18:1, while the added C18:0 azide was also desaturated to C18:1 and to a very minor extent C18:2. However, C18:0 azide was not significantly elongated to C20:0.

As *S*-acylation of proteins involves acyl-CoA donors, it was deemed important that the impact on the cellular acyl-CoA pools be determined. This was achieved using a multiple reaction monitoring mass spectrometric method in conjunction with an internal non-natural (C17:0) acyl-CoA standard. This analysis revealed that in the untreated HEK293T cells, the C18:1- and C16:0-CoA were the most abundant, accounting for almost half of the total acyl-CoA pool (Figure 2). Upon addition of the various azide fatty acids, a significant amount of the corresponding acyl-CoA azides were formed, including some of the corresponding metabolised (elongated and desaturated) acyl-CoAs azides, reflecting the total fatty acid content. It is interesting to note that there were decreases in the corresponding endogenous acyl-CoA pools, suggesting clear competition for the acyl-CoA synthases that have a preference for particular acyl chain length.

Collectively, these data strongly suggest that the synthesised azide fatty acids are good mimics of the natural saturated fatty acids and can be used for downstream metabolic processes involving fatty acids, such as lipid metabolism and protein lipidation.

zDHHC enzymes display marked differences in fatty acid azide selectivity in cell-based substrate *S*-acylation assays

To test the ability of the synthesised azide fatty acid probes to reliably measure protein *S*-acylation, HEK293T cells were co-transfected with EGFP-SNAP25b and HA-zDHHC3 or an inactive mutant of this enzyme (C157S). Figure 3A shows that zDHHC3 promoted a marked increase in incorporation of the azide probes into SNAP25, whereas in the absence of active enzyme (either empty vector or the C157S mutant) only a low signal was detected, presumably representing SNAP25 that is modified by endogenously-expressed zDHHC enzymes. To test if the incorporated azide probes were attached to SNAP25 *via* a thioester linkage, transfected cells were treated overnight with 1M hydroxylamine (HA) pH 7, which led to a marked loss of labelling, whereas incubation with 1M Tris (pH 7) as a control had no effect (Figure 3B).

The results presented in Figure 3 suggest that the level of C18:0 incorporation into SNAP25 by zDHHC3 is markedly lower than C14:0 and C16:0. Our previous work and others' has shown that five zDHHC enzymes are active against SNAP25 in similar co-expression assays: zDHHC2, zDHHC3, zDHHC7, zDHHC15 and zDHHC17(25). Thus, we undertook a quantitative comparison of SNAP25 *S*-acylation by these five zDHHC enzymes to examine for the first time if zDHHC enzymes exhibit any differences in fatty acid selectivity when expressed in cells. The results shown in Figure 4A (*top left panel*) confirm that zDHHC3 has a marked preference for C14:0/C16:0 over C18:0-azide. Interestingly, zDHHC7 which is highly related to zDHHC3 at sequence level (67.8% identical for mouse) incorporated C18:0-azide into SNAP25 more efficiently than zDHHC3 did, although there was still a significant reduction in C18:0-azide incorporation relative to C14:0/C16:0 azides with this enzyme (Figure 4A, *top panel*). zDHHC2 and zDHHC15, also displayed interesting differences in fatty acid azide selectivity despite being highly related at amino acid level (65.4% identical): zDHHC2 exhibited no significant preference whereas C18:0 incorporation into SNAP25 by zDHHC15 was markedly lower than C14:0/C16:0 azides (Figure 4A, *middle panel*). Finally, zDHHC17 showed a preference for longer chain fatty acids and incorporated C16:0 and C18:0 with higher efficiency than C14:0 (Figure 4A, *bottom right panel*). We also synthesised the corresponding *alkyne* probes and assayed their incorporation into SNAP25 by zDHHC-3, -7 and -17, which revealed the same distinct profiles as seen with the azide probes (Figure 4B). To avoid confusion, the number of carbon groups given in the name for the alkyne probes reflects those of the fatty acid minus the alkyne group. Thus, C14:0-alkyne is a C14 fatty acid chain plus an alkyne group (16 carbon atoms total). Synthesis of these alkyne probes and their correct IUPAC nomenclature is given in the SI Appendix.

To generate a more comprehensive understanding of the limits of zDHHC fatty acid selectivity, we also examined C20:0 and C22:0 azide probes. zDHHC3 showed no difference in ability to transfer C18:0, C20:0 or C22:0 (low incorporation for each), whereas zDHHC7 and zDHHC17 displayed a gradual decline in azide incorporation as chain length was increased (Figure 5A). We also used competition assays to test the ability of unlabelled fatty acids to block C16:0 azide incorporation into SNAP25 by zDHHC3 and zDHHC17. Consistent with the observation that zDHHC3 did not incorporate the C18:0 azide probe with high efficiency, neither stearic acid (C18:0) nor oleic acid (C18:1) could block incorporation of C16:0 azide into SNAP25 catalysed by this enzyme, whereas myristic acid (C14:0), palmitic acid (C16:0) and palmitoleic acid (C16:1) were all effective inhibitors (Figure 5B). In contrast to zDHHC3, stearic acid effectively blocked C16:0 azide incorporation into SNAP25 by zDHHC17, whereas myristic acid and palmitic acid had no significant inhibitory effect (Figure 5B). Furthermore, oleic acid and linoleic acid (C18:2) also blocked incorporation of C16:0 azide, and indeed even arachidonic acid (C20:4) was effective at blocking C16:0 azide incorporation by zDHHC17 (Figure 5B). The inhibitory effects of these longer chain unsaturated fatty acids are interesting given that significant amounts of the respective acyl CoAs are present in HEK293T cells (Figure 2). In contrast, lignoceric acid (C24:0) did not inhibit C16:0

azide incorporation, consistent with the results presented in Figure 5A showing that C22:0 azide displayed a marked reduction in incorporation by zDHHC17 compared with shorter chain azide probes. Autoacylation of all zDHHC enzymes tested was dependent on an intact DHHC motif (SI Appendix, Supplementary Figure 1).

Different fatty acid selectivities of zDHHC enzymes correspond to autoacylation status

The *S*-acylation reaction proceeds via an enzyme-acyl intermediate (referred to as "autoacylation") and is followed by transfer of the acyl chain to a substrate protein(10). We therefore tested if the different substrate *S*-acylation profiles observed in Figures 4 and 5 correspond with the autoacylation status of zDHHC enzymes. Figure 6A reveals that the autoacylation profiles of zDHHC-2, -3, -7 and -15 were essentially identical to the profiles observed for these enzymes with SNAP25 *S*-acylation (Figure 4). Despite repeated attempts, we were unable to reliably detect autoacylation of zDHHC17 and therefore could not compare the autoacylation profile of this enzyme with its substrate *S*-acylation profile. As enzyme autoacylation reliably reports on fatty acid selectivity of zDHHC enzymes, we extended this analysis to provide a more comprehensive study of the zDHHC family. Further distinct fatty acid azide selectivity profiles were identified for a set of zDHHC enzymes for which autoacylation was readily detectable: zDHHC5 and zDHHC11 exhibited a preference for C14:0/C16:0 azides, zDHHC4 showed no preference for C14:0/C16:0/C18:0 azides and zDHHC23 displayed a marked preference for C18:0-azide over C14:0 and C16:0 azides (Figure 6B).

Differences in fatty acid selectivities of zDHHC3 and zDHHC7 are linked to residues in the third transmembrane domain

To understand how differences in fatty acid selectivity might be encoded at the molecular level, we undertook a systematic domain swapping analysis of zDHHC3 and zDHHC7. These enzymes are highly conserved and thus we reasoned that domain swapping between these two isoforms should be less likely to produce deleterious effects on protein folding than similar analyses of other zDHHC enzymes. zDHHC3 and zDHHC7 exhibited a marked difference in ability to incorporate the C18:0 azide probe (Figure 7A) and therefore we focused on this distinction between these two enzymes. This distinction was observed for SNAP25 *S*-acylation (Figure 4), enzyme autoacylation (Figure 6), and we also confirmed it using a different substrate protein (cysteine-string protein; SI Appendix, Supplementary Figure 2). zDHHC3 and zDHHC7 consist of four predicted transmembrane domains with cytosolic N- and C-termini and a central intracellular loop containing the 51-amino acid catalytic DHHC-CRD (See Figure 7B). Interestingly, replacing either the N- or C-terminal domain or the DHHC-CRD of zDHHC3 with the same domains from zDHHC7 had no detectable effect on the fatty acid selectivity profile of zDHHC3 (Figure 7C). In contrast, replacing all four transmembrane domains of zDHHC3 with those from zDHHC7 or only the second and third transmembrane domains resulted in a significant increase in C18:0 azide incorporation into SNAP25 by these mutant enzymes (Figure 7D), mirroring the fatty acid profile of zDHHC7 (see Figure 7A). Further analysis revealed that substituting only transmembrane domain three of zDHHC3 with the same domain from zDHHC7 was sufficient to change the C18:0 selectivity profile of zDHHC3 (Figure 7E).

To pinpoint the specific features of TMD3 that are important for dictating the fatty acid selectivity profile of zDHHC3, we compared the amino acid sequences of this domain from zDHHC3 and zDHHC7 (Figure 8A). There are four differences in amino acid sequence between mammalian zDHHC3 and zDHHC7 isoforms in this region and thus we generated two mutants containing either I182S/L184V or M189L/V190C mutations. Figure 8B shows that the I182S/L184V mutation led to a marked increase in C18:0 azide incorporation into SNAP25 by zDHHC3, whereas the M189L/V190C mutations had no effect. Thus, we subsequently generated single I182S and L184V mutations, which clearly showed that the I182S mutation in zDHHC3 significantly enhanced the level of C18:0 incorporation by zDHHC3 whereas the L184V mutation had no effect (Figure 8C). It is interesting to note that zDHHC7 in *Danio rerio* has an isoleucine rather than a serine residue at this position (see Figure 8A). When autoacylation and substrate *S*-acylation profiles of zDHHC3 and zDHHC7 from this species were examined, we found no significant difference, with both enzymes weakly incorporating the C18:0 azide (SI Appendix, Supplementary Figure 3). This further supports the key role played by these residues in determining fatty acid selectivity profiles of zDHHC enzymes.

Finally, to exclude the possibility that any findings with the fatty acid azide probes were related to the presence of the azide/alkyne group, we examined incorporation of [^{3}H]-palmitic acid and [^{3}H]-stearic acid into SNAP25 by zDHHC3, zDHHC7 and the zDHHC3 (I182S) mutant. Figure 9 shows that the level of incorporation of [^{3}H]palmitic acid catalysed by these zDHHC enzymes was similar. In contrast, zDHHC7 more effectively incorporated [^{3}H]stearic acid than zDHHC3, and the zDHHC3 (I182S) mutant displayed a significant increase in [^{3}H]stearic acid incorporation compared with wild-type zDHHC3 and to a similar level as seen with zDHHC7. Thus, the results of these experiments fully support the results obtained with the fatty acid azides.

Discussion

This study provides the first analysis of zDHHC enzyme fatty acid selectivity in cells. The only other study to examine how zDHHC enzymes handle acyl CoA substrates explored *S*-acylation by purified zDHHC2 and zDHHC3 in detergent

micelles(10). Jennings and Linder demonstrated that zDHHC3 has a strong preference for C16:0 over C18:0 acyl CoA, whereas zDHHC2 displays no overt preference(10). Importantly, this present study has shown that these differences are also seen when zDHHC2 and zDHHC3 are expressed in mammalian cells. zDHHC3 is Golgi-localised(26), whereas zDHHC2 associates with the plasma membrane and endosomes(27). Therefore, the acyl CoA selectivity profiles of zDHHC2/3 are preserved irrespective of whether they are in detergent micelles or native membranes and irrespective of localisation to distinct cellular compartments.

zDHHC autoacylation provides a robust measure of fatty acid selectivity as we clearly showed that the autoacylation profile of zDHHC2, -3, -7 and -15 closely match their respective substrate *S*-acylation profiles. This allowed us to investigate the acyl CoA selectivity of an additional set of enzymes by measuring their autoacylation. The results of this analysis showed that zDHHC-3, -5, -7, -11 and -15 prefer C14/C16 over C18, zDHHC-2 and -4 display no clear fatty acid preference, zDHHC17 prefers C16/C18 over C14, and zDHHC23 exhibits a strong preference for C18. These observations re-emphasise that acyl CoA specificities do not show any correlation with intracellular localisation, for example, zDHHC-3, -7, -15, -17 and -23 all localise to the Golgi (26, 28), whereas zDHHC-2 and -5 are localised to the plasma membrane(25), and zDHHC4 is ER-localised(29).

zDHHC-3 and -7 are highly related at the sequence level, localise to Golgi membranes and share many common protein substrates. Yet these enzymes have a significant difference in acyl CoA selectivity, with zDHHC7 having an increased ability to incorporate C18:0 chains relative to zDHHC3. The high sequence conservation of zDHHC-3 and -7 provided an opportunity to undertake a comprehensive domain swapping analysis to pinpoint features that underpin acyl CoA selectivity. This analysis identified a single amino acid in the third transmembrane domain of zDHHC3 as a critical determinant limiting use of longer chain fatty acids. When Ile-182 was replaced by a serine, which is present at the same position in zDHHC7, a significant increase in the ability of the mutant protein to incorporate C18:0 was noted. We confirmed the importance of this residue using both C16:0/C18:0 azides with click chemistry detection and [^{3}H]palmitic acid/stearic acid labelling. It is interesting that neither the azide or alkyne group present on the probes appeared to influence acyl chain selectivity, perhaps suggesting that these chemical groups have a flexible character that does not impede association with zDHHC enzymes. Consistent with this, we also found that the fatty acid azides selectively competed for formation of endogenous acyl-CoA of the same chain length when added to HEK293T cells. This shows that the azide probes compete with and are very good mimics of endogenous fatty acids, and are therefore excellent tools with which to interrogate aspects of fatty acid biology such as *S*-acylation.

Although we performed a comprehensive domain-swapping analysis between zDHHC3 and zDHHC7, the high similarity of these two enzymes means that other factors that are important for acyl chain selectivity could have been missed. Nevertheless, the approach taken here provides an important first step towards understanding the basis for acyl CoA selectivity in the zDHHC family. Interestingly, a lysine was identified in the transmembrane domain of an elongase component of the yeast very long-chain fatty acid synthase complex that was also a key determinant of the final length of fatty acid acyl CoA chain synthesised by this enzyme complex(30). In addition, a subsequent mutational analysis of the related rat elongases Elovl2 and Elovl5 highlighted the importance of the transmembrane domains of these enzymes in setting the substrate specificity profiles. Elovl2 is required for synthesis of omega-3 docosahexaenoic acid (DHA; 22:6n-3) as this elongase (but not Elovl5) can elongate docosapentaenoic acid (22:5n-3) to 24:5n-3, a precursor of DHA. This difference in substrate specificity between Elovl2 and Elovl5 was shown to involve a region encompassing transmembrane domains 6 and 7, with a cysteine-to-tryptophan switch in transmembrane domain 7 proving to be particularly important in setting specificity(31).

It is tempting to speculate that the transmembrane domains of zDHHC enzymes form “channels” that accommodate specific acyl CoA molecules. This could involve different transmembrane domains in the same zDHHC molecule or might require dimerization and multimerisation of zDHHC enzymes(32). As isoleucine occupies more space that serine, it is possible that this amino acid in TMD3 of zDHHC3 limits the length of acyl chain that can be accommodated by blocking the acyl-CoA channel. This idea is consistent with the position of the isoleucine residue in zDHHC3, which is present in the middle of TMD3. Indeed, the catalytic DHHC-CRD of zDHHC enzymes is present immediately preceding TMD3, suggesting that the cysteine in the DHHC active site could be positioned close to the channel opening.

Mass spectrometry analysis of haemaglutinin (HA) from influenza has shown that C18:0 is added specifically to a cysteine present in the transmembrane domain, whereas C16:0 is attached to cysteines in a membrane proximal region (33). It is not clear how this highly selective process is achieved but our results suggest that the modified cysteines in HA might be targets of different zDHHC enzymes with distinct acyl CoA specificities. It is also possible that there is sometimes a contribution made by the substrate in determining which fatty acids are attached. Thus, for transmembrane proteins, the sequence of the transmembrane domain could affect which fatty acids are

added to membrane-proximal cysteines in a similar way as seen here for zDHHC enzymes.

There are two major properties of *S*-acylation that are thought to be central to its various effects on modified proteins: hydrophobicity and affinity for cholesterol-rich membranes(3, 34). Hydrophobicity is fundamental to the effects of *S*-acylation on reversible membrane binding of many soluble proteins and in regulating the membrane association of soluble loops of transmembrane proteins(3). Association with cholesterol-rich membranes is thought to influence aspects of protein trafficking and membrane compartmentalisation. It is well established from *in vitro* studies that saturated phospholipids cluster together with cholesterol, whereas unsaturated phospholipids are excluded from these domains(35). Although the effects of saturated versus unsaturated *S*-acyl chains have not been studied in such detail, it is clear that *S*-acylation is a major signal for association with cholesterol-rich domains at least *in vitro*(36). It is likely that the addition of saturated versus unsaturated acyl chains onto proteins have distinct influences on membrane partitioning and subsequent trafficking and function in the cell. Furthermore, the acyl chain added to *S*-acylated proteins is also likely to affect the strength of membrane association. Although two tandem lipid modifications (e.g. myristoylation/palmitoylation or prenylation/palmitoylation) provide a strong membrane anchor, a single lipid group (e.g. myristoyl or prenyl) is not sufficient for membrane association (37). However, single myristate, palmitate or stearate groups added to an *S*-acylated protein could have different effects on membrane association. Indeed, stearate has a significantly stronger interaction with phospholipid membranes than palmitate(12).

This study identified clear differences in the acylation profiles of different zDHHC enzymes and their substrates expressed in HEK293T cells. In future work it will be important to further advance understanding of this area and the functional significance of fatty acid heterogeneity by investigating fatty acid selectivity of endogenous proteins and how this is impacted by a dynamic and heterogeneous acyl CoA pool. The distribution of different pools of acyl-CoAs and their availability for use in *S*-acylation reactions is unclear, and this is also an important area for future investigations.

Materials and Methods

Materials

Mouse GFP antibody was from Clontech (CA, USA). Rat HA antibody was from Roche (West Sussex, UK). *Danio rerio* zDHHC3 and zDHHC7 coding sequences were synthesised by GeneArt (Thermo Fisher). IR-dye conjugated secondary antibodies and alkyne/azide probes were purchased from LI-COR (Cambridge UK). [9,10-^{3}H] palmitic acid and [9,10-^{3}H] stearic acid (specific activity for each 1.11-2.22 TBq/mmol) were from Hartmann Analytic (Braunschweig, Germany).

Cell transfection

For substrate *S*-acylation assays, HEK293T cells plated on 24-well plates were transfected using Lipofectamine 2000 (Invitrogen) with 0.8 μg of EGFP-SNAP25 and 1.6 μg of zDHHC plasmid (in pEF-BOS-HA backbone). For autoacylation assays, 3 μg of zDHHC plasmid was used. Cells were labelled and processed the day after transfection.

Quantification of fatty acids and acyl-CoAs

Cells were collected by centrifugation and washed with serum-free DMEM, prior to incubation at 37 °C for 15 min with DMEM only, followed by the addition of defatted BSA coupled to the appropriate fatty acid azide (100 μM final concentration) and incubated for 4 hours at 37ºC. Cells were then harvested by centrifugation and either washed in ice-cold PBS and freeze-dried for total fatty acid determination or processed for acyl-CoA extraction (see below).

For total fatty acid determination, the freeze-dried cells were subjected to acid hydrolysis using constant boiling HCl (6 M, 200 μL) vortexing/sonication followed by incubation for 16 h at 110 °C. After cooling, the samples were spiked with 100 pmoles of C17:0 fatty acid (as an internal control) and processed and derivatised to fatty acid methyl esters (FAMEs), prior to analysis by gas chromatography-mass spectrometry (GC-MS) as described previously(38). The individual azide fatty acids were also converted to their corresponding FAMEs and analysed by GC-MS to determine retention time and fragmentation patterns.

For acyl-CoA extraction and quantification, the absolute number of cells was determined (typically between 2-4 x 10^{7} cells). Cells were harvested by centrifugation at 15,000 x g for 1 min at room temperature and the supernatant media removed. The pellet was washed with 200 μl of ice-cold PBS and completely lysed with ice-cold TCA (100 μl, 1 M) and vortexing, and stored on ice to prevent sample hydrolysis.

The internal standard C17:0-CoA (150 pmol) was added to the lysate and the sample centrifuged (15,000g, 10 min, 4°C). The resulting supernatant was transferred to a fresh pre-cooled tube. EDTA (25 μl, 10 mM, pH 7.0) was added followed by chloroform (50 μL) triethylammonium acetate (50 μl), and the mixture was vortexed and centrifuged (15,000 x g, 10 min, 4°C). The upper phase was carefully removed to a fresh Eppendorf tube, flash frozen in liquid nitrogen and freeze-dried. The dried sample was kept at -80°C prior to analysis by electrospray-mass spectrometry (ES-MS), using multiple reaction monitoring (MRM) similar to the method of Haynes et al(17).

Samples were suspended in 15 μl of a 1:2 (v/v) chloroform / methanol and 5 μl of acetonitrile / isopropanol / water (6:7:2) and delivered using a NanoMate (Advion) to a AB Sciex 4000

QTRAP triple quadrupole mass-spectrometry with a nanoelectrospray source, using nitrogen as the collision gas. A MRM approach was utilized to quantify acyl CoA. MRM mass transition (SI Appendix, Table 1) for the acyl-CoAs was determined in positive ion mode, (EP 8 eV, CXP 12 eV, an interface temperature of 30 °C , gas pressure 0.5 psi and a tip voltage of 1.25-1.5kV, dwell time 500 mS), spectra were acquired for 2 minutes. All MRM data were normalized relative to the internal standard before generating standard curves (0.1-500 pmoles) for the acyl-CoAs (C14:0. C16:0, C17:0, C18:0, C20 and C20:4) which were obtained from either Sigma or Avanti Polar Lipids (Alabaster, AL), allowing their own response factor to be determined. Samples were analysed in the same manner, allowing quantification of the extracted acyl-CoAs.

Cell labelling with fatty acid azide and alkyne probes for analysis of *S*-acylation

HEK293T cells were incubated with 100 μM of the fatty acid azide probes (in DMEM with 1 mg/ml defatted BSA) for 4 h at 37 °C. For competition experiments, transfected cells were labelled with 100 μM of the C16:0 azide probe in the presence of a 3-fold excess (300 μM) of the relevant fatty acid. For cell labelling with [^{3}H]palmitic acid and [^{3}H]stearic acid (Hartmann Analytic), transfected cells were incubated in DMEM/BSA containing 0.5 mCi/ml of the tritiated fatty acid probes for 4 h at 37 °C.

Detection of fatty acid azide and alkyne probes in *S*-acylated proteins

Cells were washed twice in PBS then lysed on ice in 100 μl of 50mM Tris pH 8.0 containing 0.5% SDS and protease inhibitors (Roche, West Sussex UK). Conjugation of azide or alkyne IR-800 Dye (LI-COR, Cambridge UK) to fatty acid azide or alkyne probes was carried out for 1 h at room temperature with end-over-end rotation by adding an equal volume (100 μl) of freshly mixed click chemistry reaction mixture containing 10 μM IRDye® 800CW azide or alkyne Infrared Dye, 4 mM $CuSO_4$, 400 μM Tris[(1-benzyl-1*H*-1,2,3-triazol-4-yl)methyl]amine and 8 mM ascorbic Acid in dH_20. Proteins were isolated by acetone precipitation and resuspended in 100 μl SDS sample buffer containing 25 mM DTT. Samples were incubated at 95 °C for 5 min and 10-15 μl was resolved by SDS-PAGE.

For detection of [^{3}H] fatty acid probes, cell lysates were resolved by SDS-PAGE and transferred to duplicate nitrocellulose membranes. One membrane was used for immunoblotting, the other was exposed to light-sensitive film in the presence of a Kodak Biomax Transcreen LE intensifier screen for detection of [^{3}H].

Generation of mutant zDHHC constructs

The zDHHC3 chimeras containing the N- and C-terminal domains (zDHHC3/CN7) or intracellular domain including the zDHHC cysteine-rich domain of zDHHC7 (zDHHC3/CRD7) were generated within the HA-tagged constructs by inserting *Nhe*1 and *Sal*1 restriction sites at the boundaries of the domains that were swapped (upstream of C47 and F235 in zDHHC3 and C50 and F238 in zDHHC7 for zDHHC3/CN7, and S93 and T176 in zDHHC3 and S96 and T179 in zDHHC7 for zDHHC3/CRD7) by site-directed mutagenesis. The regions were then swapped by restriction/ligation and the *Nhe*1/*Sal*1 restriction sites removed using site-directed mutagenesis. The zDHHC3 chimeras containing the transmembrane domains of zDHHC7 were constructed by GeneArt and sub-cloned into pEF-BOS-HA vector using *Bam*H1 restrictions sites. The transmembrane domains predicted by UniProt were defined as follows: zDHHC3 A48-V68 (TMD1), Y73-S93 (TMD2), F172-F192 (TMD3), I215-F235 (TMD4); zDHHC7 A51-L71 (TMD1), F76-S96 (TMD2), F175-G194 (TMD3), I218-F238 (TMD4). Site-directed mutants were generated using PCR. The validity of all clones was confirmed by sequencing.

Data Quantification and Statistical Analysis

Quantification of all click chemistry experiments was performed by expressing the click signal relative to the corresponding protein signal (immunoblot). For substrate *S*-acylation assays, this was then normalised to empty vector control. Statistical analysis used a one-way ANOVA with a Tukey post-test (Graphpad Prism software).

Acknowledgements

We are grateful to Mike Shipston and Heather McClafferty for the zDHHC23 cysteine mutant. This work was funded by BBSRC grant (BB/L022087/1) to LHC, NCT and TKS, and Wellcome Trust grant (093228) to TKS. We thank the EPSRC Mass Spectrometry Service, Swansea, for high-resolution spectra.

Author contributions

JG and TKS: conceived and performed experiments, analysed data and wrote the manuscript; KRM, SCD MR and JW: synthesised chemical probes; LHC and NCOT: conceived experiments and wrote the manuscript.

References

1. Smotrys JE, Linder ME (2004) Palmitoylation of intracellular signalling proteins: Regulation and Function. *Ann Rev Biochem* **73**(1):559-587.
2. Chamberlain LH, Shipston MJ (2015) The physiology of protein S-acylation. *Physiol Rev* **95**(2):341-376.
3. Salaun C, Greaves J, Chamberlain LH (2010) The intracellular dynamic of protein palmitoylation. *J Cell Biol* **191**(7):1229-1238.
4. Linder ME, Deschenes RJ (2007) Palmitoylation: policing protein stability and traffic. *Nat Rev Mol Cell Biol* **8**(1):74-84.
5. Greaves J, Chamberlain LH (2011) DHHC palmitoyl transferases: substrate interactions and (patho)physiology. *Trends Biochem Sci* **36**:245-253.

6. Fukata M, Fukata Y, Adesnik H, Nicoll RA, Bredt DS (2004) Identification of PSD-95 Palmitoylating Enzymes. *Neuron* **44**(6):987-996.
7. Lobo S, Greentree WK, Linder ME, Deschenes RJ (2002) Identification of a Ras Palmitoyltransferase in Saccharomyces cerevisiae. *J. Biol. Chem.* **277**(43):41268-41273.
8. Roth AF, Feng Y, Chen L, Davis NG (2002) The yeast DHHC cysteine-rich domain protein Akr1p is a palmitoyl transferase. *J. Cell Biol.* **159**(1):23-28.
9. Politis EG, Roth AF, Davis NG (2005) Transmembrane Topology of the Protein Palmitoyl Transferase Akr1. *J Biol Chem* **280**(11):10156-10163.
10. Jennings BC, Linder ME (2012) DHHC protein S-acyltransferases use a similar ping-pong kinetic mechanism but display different Acyl CoA specificities. *J Biol Chem* **287**(10):7236-7245.
11. Mitchell DA, Mitchell G, Ling Y, Budde C, Deschenes RJ (2010) Mutational analysis of Saccharomyces cerevisiae Erf2 reveals a two-step reaction mechanism for protein palmitoylation by DHHC enzymes. *J Biol Chem* **285**(49):38104-38114.
12. Muszbek L, Haramura G, Cluette-Brown J, Van Cott E, Laposata M (1999) The pool of fatty acids covalently bound to platelet proteins by thioester linkages can be altered by exogenously supplied fatty acids. *Lipids* **34**(0):S331-S337.
13. Hallak H*, et al.* (1994) Covalent binding of arachidonate to G protein alpha subunits of human platelets. *J Biol Chem* **269**(7):4713-4716.
14. O'Brien PJ, Zatz M (1984) Acylation of bovine rhodopsin by [3H]palmitic acid. *J Biol Chem* **259**(8):5054-5057.
15. Veit M, Reverey H, Schmidt MF (1996) Cytoplasmic tail length influences fatty acid selection for acylation of viral glycoproteins. *Biochem J* **318**(1):163-172.
16. Brett K*, et al.* (2014) Site-specific S-acylation of influenza virus hemagglutinin: the location of the acylation site relative to the membrane border is the decisive factor for attachment of stearate. *J Biol Chem* **289**(50):34978-34989.
17. Haynes CA*, et al.* (2008) Quantitation of fatty acyl-coenzyme As in mammalian cells by liquid chromatography-electrospray ionization tandem mass spectrometry. *J Lipid Res* **49**(5):1113-1125.
18. Liang X*, et al.* (2001) Heterogeneous Fatty Acylation of Src Family Kinases with Polyunsaturated Fatty Acids Regulates Raft Localization and Signal Transduction. *J Biol Chem* **276**(33):30987-30994.
19. Hang HC*, et al.* (2007) Chemical Probes for the Rapid Detection of Fatty-Acylated Proteins in Mammalian Cells. *J Am Chem Soc* **129**(10):2744-2745.
20. Charron G*, et al.* (2009) Robust fluorescent detection of protein fatty-acylation with chemical reporters. *J Am Chem Soc* **131**(13):4967-4975.
21. Hannoush RN, Arenas-Ramirez N (2009) Imaging the Lipidome: Alkynyl Fatty Acids for Detection and Cellular Visualization of Lipid-Modified Proteins. *ACS Chemical Biology* **4**(7):581-587.
22. Hannoush RN, Sun J (2010) The chemical toolbox for monitoring protein fatty acylation and prenylation. *Nat Chem Biol* **6**(7):498-506.
23. Yap MC*, et al.* (2010) Rapid and selective detection of fatty acylated proteins using {omega}-alkynyl-fatty acids and click chemistry. *J. Lipid Res.* **51**(6):1566-1580.
24. Hang HC, Linder ME (2011) Exploring protein lipidation with chemical biology. *Chemical reviews* **111**(10):6341-6358.
25. Greaves J, Gorleku OA, Salaun C, Chamberlain LH (2010) Palmitoylation of the SNAP25 protein family: specificty and regulation by DHHC palmitoyl transferases. *J Biol Chem* **285**(32):24629-24238.
26. Greaves J, Salaun C, Fukata Y, Fukata M, Chamberlain LH (2008) Palmitoylation and Membrane Interactions of the Neuroprotective Chaperone Cysteine-string Protein. *J Biol Chem* **283**(36):25014-25026.
27. Greaves J, Carmichael JA, Chamberlain LH (2011) The palmitoyl transferase DHHC2 targets a dynamic membrane cycling pathway: regulation by a C-terminal domain. *Mol. Biol. Cell* **22**(11):1887-1895.
28. Tian L, McClafferty H, Knaus H-G, Ruth P, Shipston MJ (2012) Distinct Acyl Protein Transferases and Thioesterases Control Surface Expression of Calcium-activated Potassium Channels. *J Biol Chem* **287**(18):14718-14725.
29. Gorleku OA, Barns A-M, Prescott GR, Greaves J, Chamberlain LH (2011) Endoplasmic Reticulum Localization of DHHC Palmitoyltransferases Mediated by Lysine-based Sorting Signals. *J Biol Chem* **286**(45):39573-39584.
30. Denic V, Weissman JS (2007) A molecular caliper mechanism for determining very long-chain fatty acid length. *Cell* **130**(4):663-677.
31. Gregory MK, Cleland LG, James MJ (2013) Molecular basis for differential elongation of omega-3 docosapentaenoic acid by the rat Elovl5 and Elovl2. *J Lipid Res* **54**(10):2851-2857.
32. Lai J, Linder ME (2013) Oligomerization of DHHC Protein S-Acyltransferases. *J Biol Chem* **288**(31):22862-22870.
33. Kordyukova LV, Serebryakova MV, Baratova LA, Veit M (2010) Site-specific attachment of palmitate or stearate to cytoplasmic versus transmembrane cysteines is a common feature of viral spike proteins. *Virology* **398**(1):49-56.
34. Resh MD (2006) Trafficking and signaling by fatty-acylated and prenylated proteins. *Nature Chemical Biology* **2**(11):584-590.
35. Brown DA, London E (2000) Structure and Function of Sphingolipid- and Cholesterol-rich Membrane Rafts. *J Biol Chem* **275**(23):17221-17224.
36. Melkonian KA, Ostermeyer AG, Chen JZ, Roth MG, Brown DA (1999) Role of lipid modifications in targeting proteins to detergent-resistant membrane

rafts. Many raft proteins are acylated, while few are prenylated. *J Biol Chem* **274**(6):3910-3917.

37. Shahinian S, Silvius J (1995) Doubly-lipid-modified protein sequence motifs exhibit long-lived anchorage to lipid bilayer membranes. *Biochemistry* **34**:3813-3822.

38. Trindade S*, et al.* (2016) Trypanosoma brucei Parasites Occupy and Functionally Adapt to the Adipose Tissue in Mice. *Cell host & microbe* **19**(6):837-848.

Figure Legends

Figure 1: Relative percentage of the total fatty acid content of cells with and without treatments of azide-fatty acids.
HEK293T cells were incubated with or without fatty acid azides. Fatty acids released from cellular lipids and protein by acid were then converted to methyl esters and analysed by GC-MS as described in material and methods. Values shown are means ± SEM (n=3).

Figure 2: Quantification of the acyl-CoA content of HEK293T cells with and without treatments of azide-fatty acids.
HEK293T cells were incubated with or without fatty acid azides and acyl-CoAs were then quantified as described in materials and methods. Values shown are means ± SEM (n=3).

Figure 3: *S*-acylation of EGFP-SNAP25B by zDHHC3.
HEK293T cells were transfected with EGFP-SNAP25B and pEF-BOS-HA (*vector*), HA-zDHHC3, or HA-zDHHC(C157S), or were left untransfected. Cells were then incubated with C14:0, C16:0 or C18:0 fatty acid azides for 4 h at 37 °C. Incorporated fatty acid azides were detected by click chemistry using an alkyne-800 infrared dye. Isolated proteins were resolved by SDS-PAGE and transferred to nitrocellulose membranes. Representative images are shown. (a) Upper panel: click chemistry signal. Middle panel: anti-GFP immunoblot. Lower panel: anti-HA immunoblot. *Arrowheads* denote the position of the EGFP-SNAP25 band (top and middle panels) and hA-zDHHC3 band (lower panel). (b) Following click chemistry, samples were incubated in hydroxylamine (+) or Tris (-) at a final concentration of 1 M overnight prior to SDS-PAGE. Upper panel: click chemistry signal. Lower panel: anti-GFP immunoblot. Position of molecular weight markers is shown.

Figure 4: *S*-acylation of EGFP-SNAP25B by different zDHHC enzymes.
HEK293T cells were transfected with EGFP-SNAP25B and pEF-BOS-HA (*vector*), HA-zDHHC-2, -3, -7, -15 or -17. Cells were then incubated with C14:0, C16:0 or C18:0 fatty acid azides or alkynes as indicated for 4 h at 37 °C. Fatty acid azides/alkynes were labelled by click chemistry using an alkyne- or azide-800 infrared dye. Isolated proteins were then resolved by SDS-PAGE and transferred to nitrocellulose membranes. (a) *S*-acylation analysis of EGFP-SNAP25B using fatty acid-azides. Representative images are shown in the left panel with position of molecular mass standards indicated; graphs showing mean ± SEM shown are in the right panel. zDHHC3: n = 46; zDHHC7: n = 26; zDHHC2: n= 10; zDHHC15: n = 9; zDHHC17: n = 22. **p < 0.01; ***p < 0.001. (b) *S*-acylation analysis of EGFP-SNAP25B in HEK293T cells labelled with fatty acid-alkynes. Graphs show mean ± SEM (n=10). ns = not significant; **p < 0.01; ***p < 0.001.

Figure 5: *S*-acylation of EGFP-SNAP25B by longer-chain saturated and unsaturated fatty acids.
(a) *S*-acylation analysis of EGFP-SNAP25B by HA-zDHHC3, HA-zDHHC7 and HA-zDHHC17 in HEK293T cells with C14:0, C16:0, C18:0, C20:0 and C22:0 fatty acid-azides. Representative images are shown and position of molecular mass standards indicated. Upper panel: click chemistry signal. Middle panel: anti-GFP immunoblot. Lower panel: quantified data. n ≥ 3, mean ± SEM. (b) Competition analysis of EGFP-SNAP25B *S*-acylation by HA-zDHHC3 (upper panel) or HA-zDHHC17 (lower panel) in HEK293T cells labelled with C16:0-azide in the presence of 3-fold excess of the indicated unlabelled (u) fatty acids. Position of molecular mass standards is shown. Graphs show mean values ± SEM (n ≥ 3). ns = not significant; *p < 0.05; **p < 0.01; ***p < 0.001.

Figure 6: Autoacylation of zDHHC enzymes by fatty-acid azides.
HEK293T cells transfected with HA-tagged zDHHC constructs were incubated with C14:0, C16:0 or C18:0 fatty acid azides for 4h at 37 °C. Fatty acid azides were then labelled by click chemistry using an alkyne-800 infrared dye. Isolated proteins were resolved by SDS-PAGE and transferred to nitrocellulose membranes. Representative click signals and western blots with position of molecular mass standards indicated, together with quantified data (mean ± SEM) are shown for each zDHHC enzyme. (a) Autoacylation of zDHHC enzymes active against SNAP25B. zDHHC2: n = 6; zDHHC3: n = 14; zDHHC7: n = 11; zDHHC15: n = 6. (b) Autoacylation of additional zDHHC enzymes. n ≥ 6. ns = not significant; *p < 0.05; **p < 0.01; ***p < 0.001. The arrowhead on the zDHHC5 blot indicates the zDHHC5 band.

Figure 7: *S*-acylation of EGFP-SNAP25B by zDHHC3/zDHHC7 chimeras.
HEK293T cells were transfected with EGFP-SNAP25B and pEF-BOS-HA (*vector*) or the indicated wild-type or mutant zDHHC constructs. Cells were then incubated with C14:0, C16:0 or C18:0 fatty acid azides for 4h at 37 ºC. Fatty acid azides were labelled by

click chemistry using an alkyne-800 infrared dye. Isolated proteins were then resolved by SDS-PAGE and transferred to nitrocellulose membranes for analysis. (a) Quantification of the relative levels of C14:0-, C16:0- or C18:0-azide incorporation into EGFP-SNAP25B by zDHHC3 or zDHHC7 (mean ± SEM). n ≥ 26. (b) Schematic illustration detailing the zDHHC3/zDHHC7 chimeras that were constructed. (c-e) Analysis of EGFP-SNAP25B *S*-acylation by zDHHC3 chimeras with fatty acid-azides. Representative images are shown on the left, graphs showing mean ± SEM are on the right. (c) n ≥ 4. (d) n = 6. (e) n ≥ 12. ns = not significant, ***p < 0.001.

Figure 8: *S*-acylation of EGFP-SNAP25B by zDHHC3 TMD3 mutants.
HEK293T cells were transfected with EGFP-SNAP25B and pEF-BOS-HA (*vector*) or the indicated wild-type or mutant zDHHC constructs. Cells were then incubated with C14:0, C16:0 or C18:0 fatty acid azides for 4 h at 37 °C. Fatty acid azides were labelled by click chemistry using an alkyne-800 infrared dye. Isolated proteins were resolved by SDS-PAGE and transferred to nitrocellulose membranes. (a) Sequence alignment of amino acids in the third transmembrane domain of zDHHC3 and zDHHC7; the blue boxes highlight Isoleucine-182 in zDHHC3 and Serine-185 in zDHHC7. (b) and (c) Analysis of EGFP-SNAP25B *S*-acylation by zDHHC3 TMD3 mutants with fatty acid-azides. Representative images are shown on the left, graphs showing mean ± SEM are on the right. (b) n ≥ 6. (c) n ≥ 8. ns = not significant, ***p < 0.001.

Figure 9: Incorporation of [^{3}H]palmitic and [^{3}H]stearic acid into EGFP-SNAP25B by zDHHC3 and zDHHC7.
HEK293T cells were transfected with pEGFPC2 or EGFP-SNAP25B together with pEF-BOS-HA (*vector*), HA-zDHHC3, HA-zDHHC7, or HA-zDHHC3(I182S). Cells were labelled with either [^{3}H]palmitic acid (Left panel) or [^{3}H]stearic acid (Right panel), lysed, and resolved by SDS-PAGE. Top panel: [^{3}H] fatty acid incorporation. Upper middle panel: expression levels of EGFP-SNAP25B. Lower middle panel: zDHHC protein expression. Molecular weight markers are shown on the left. Lower panel: Quantification of [^{3}H] fatty acid incorporation normalised to EGFP-SNAP25B protein levels expressed as mean ± SEM. n = 3, ns = not significant. **p < 0.01; ***p < 0.001.

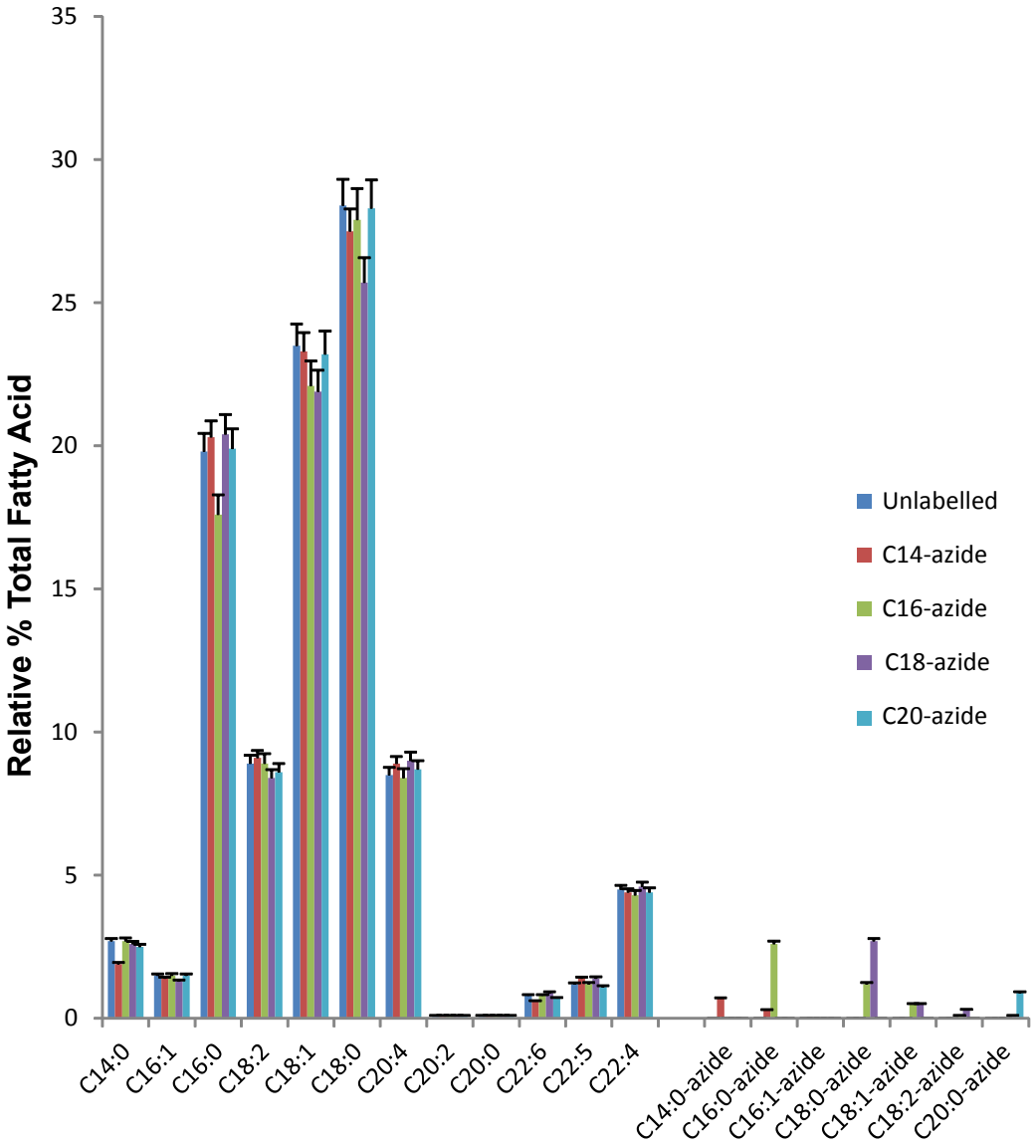
Relative % Total Fatty Acid
35
30
25
20
15
10
5
0
Unlabelled
C14-azide
C16-azide
C18-azide
C20-azide
C14:0
C16:1
C16:0
C18:2
C18:1
C18:0
C20:4
C20:2
C20:0
C22:6
C22:5
C22:4
C14:0-azide
C16:0-azide
C16:1-azide
C18:0-azide
C18:1-azide
C18:2-azide
C20:0-azide

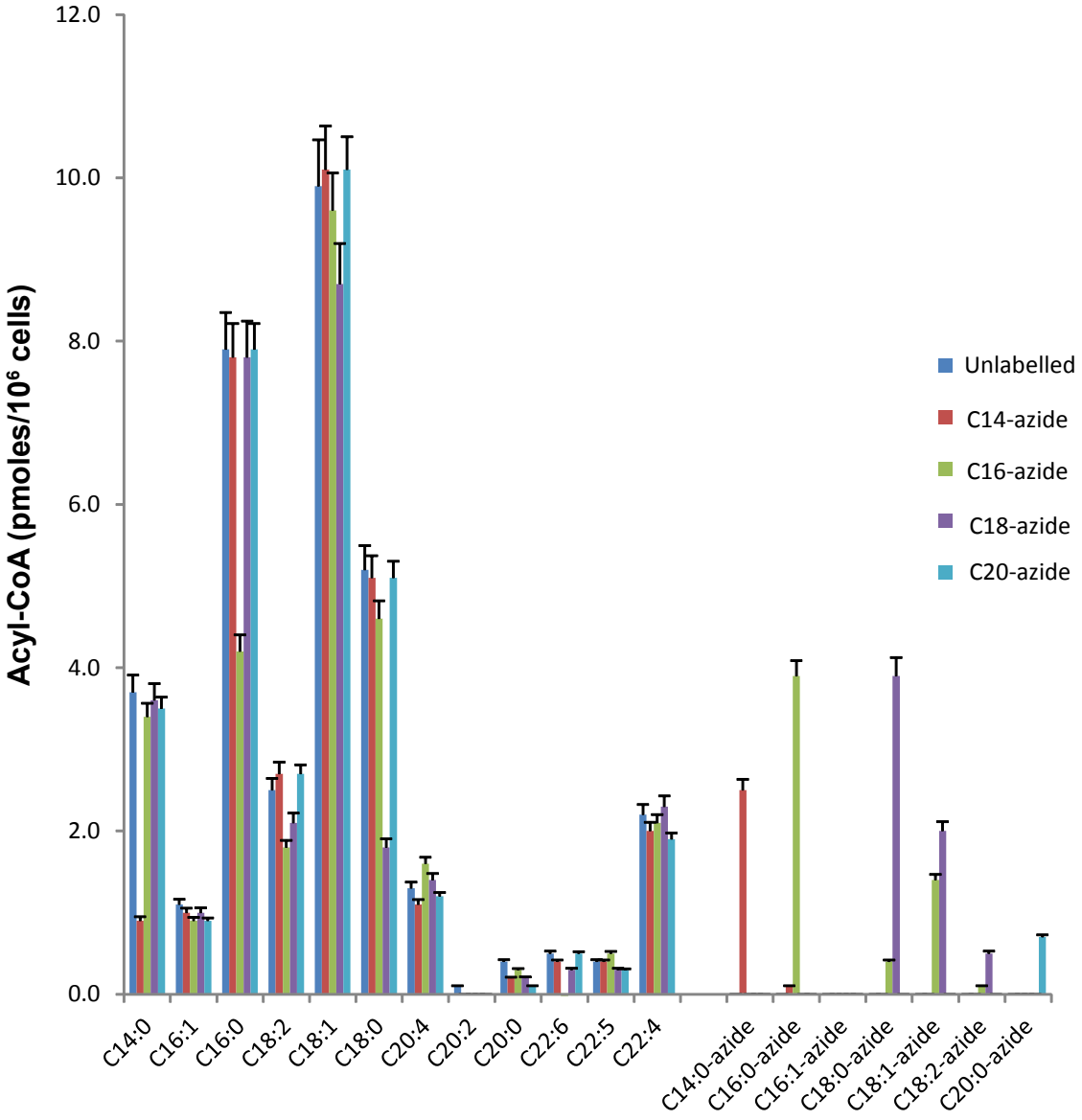
Acyl-CoA (pmoles/10⁶ cells)
12.0
10.0
8.0
6.0
4.0
2.0
0.0
Unlabelled
C14-azide
C16-azide
C18-azide
C20-azide
C14:0
C16:1
C16:0
C18:2
C18:1
C18:0
C20:4
C20:2
C20:0
C22:6
C22:5
C22:4
C14:0-azide
C16:0-azide
C16:1-azide
C18:0-azide
C18:1-azide
C18:2-azide
C20:0-azide

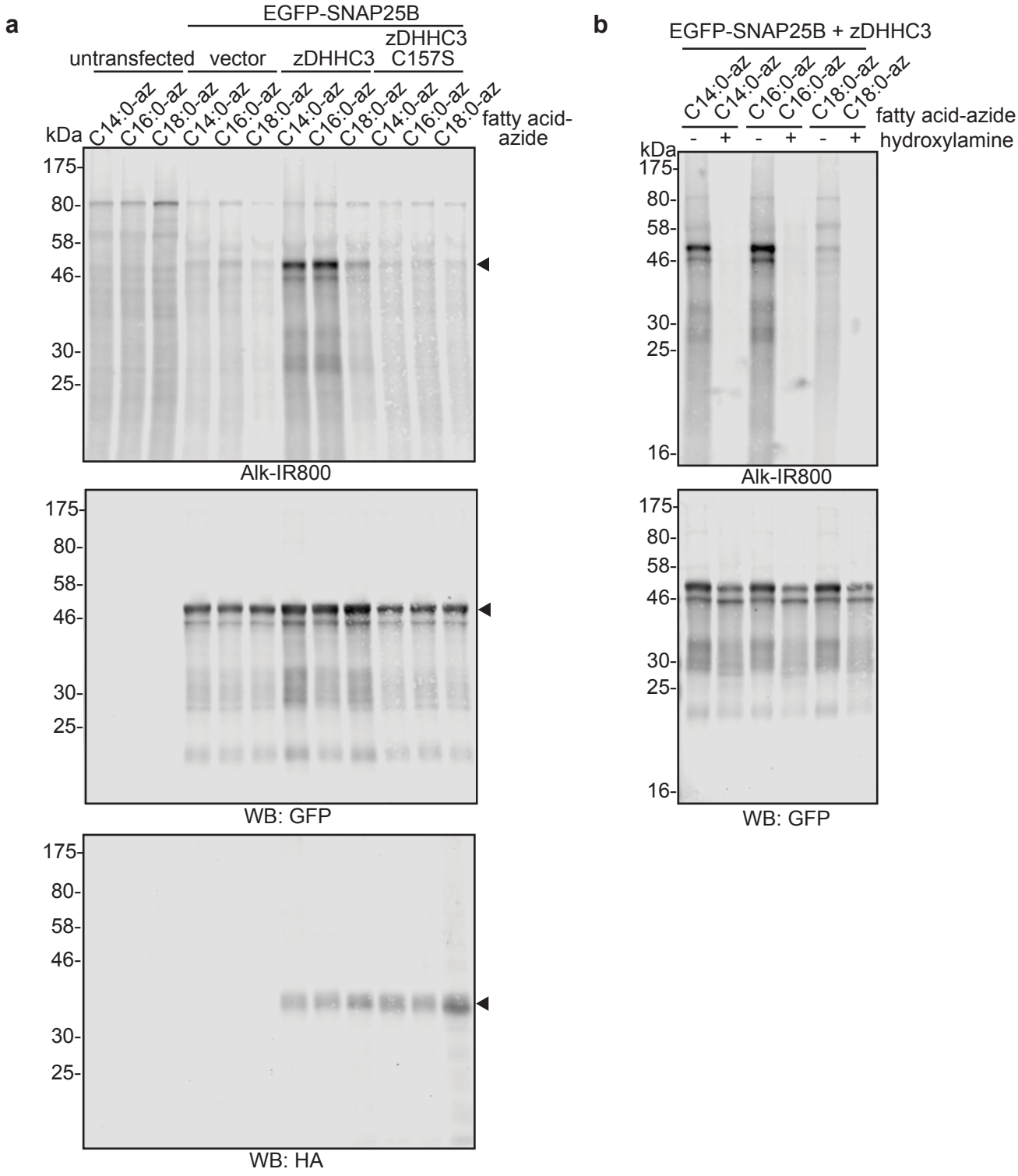
a
EGFP-SNAP25B
zDHHC3
C157S
untransfected
vector
zDHHC3
C14:0-az
C16:0-az
C18:0-az
fatty acid-azide
kDa
175
80
58
46
30
25
Alk-IR800
WB: GFP
WB: HA
b
EGFP-SNAP25B + zDHHC3
fatty acid-azide
hydroxylamine
-
+
16

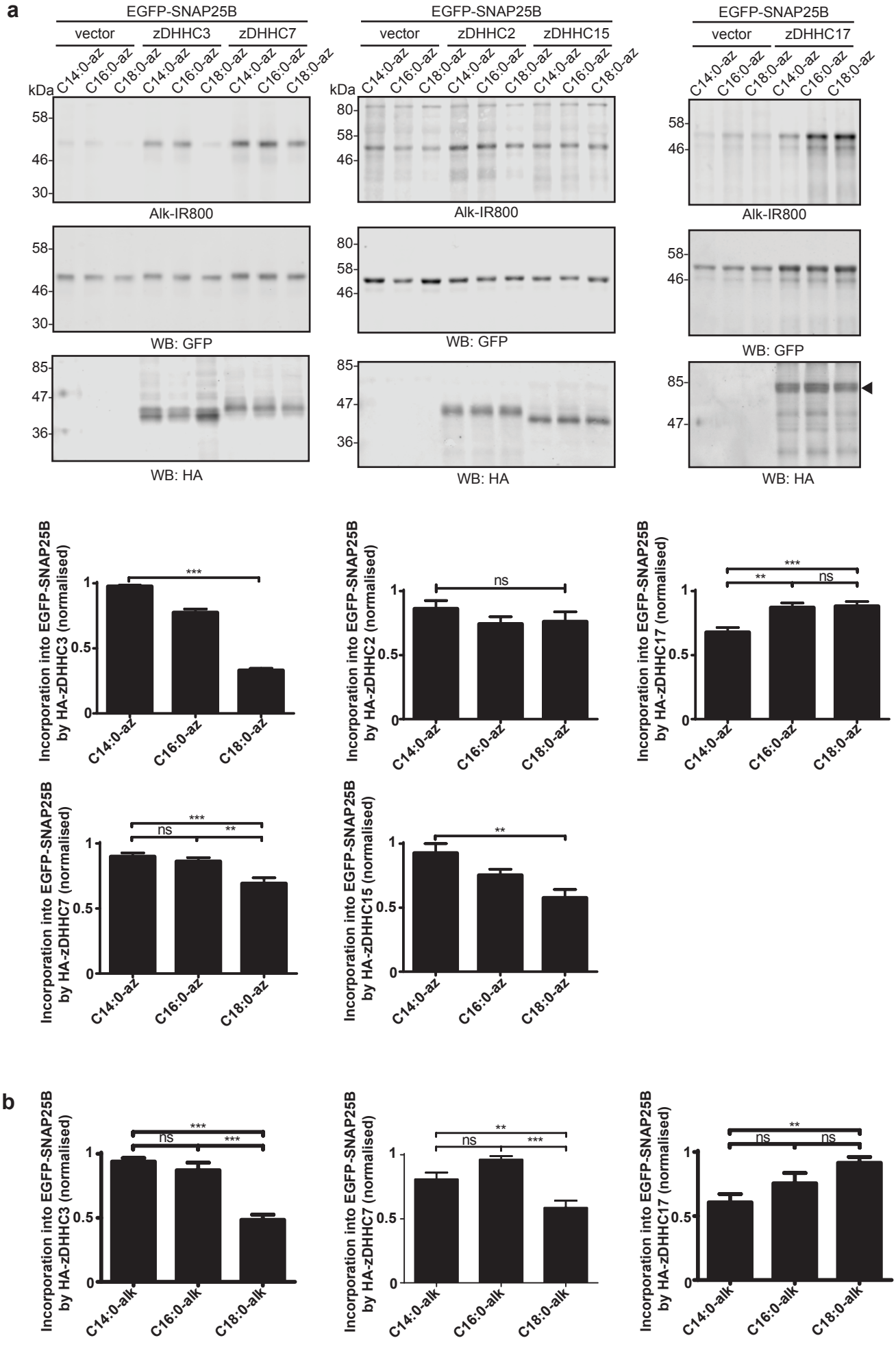
a
EGFP-SNAP25B
vector
zDHHC3
zDHHC7
zDHHC2
zDHHC15
zDHHC17
C14:0-az
C16:0-az
C18:0-az
kDa
Alk-IR800
WB: GFP
WB: HA
Incorporation into EGFP-SNAP25B by HA-zDHHC3 (normalised)
Incorporation into EGFP-SNAP25B by HA-zDHHC2 (normalised)
Incorporation into EGFP-SNAP25B by HA-zDHHC17 (normalised)
Incorporation into EGFP-SNAP25B by HA-zDHHC7 (normalised)
Incorporation into EGFP-SNAP25B by HA-zDHHC15 (normalised)
***
**
ns
b
C14:0-alk
C16:0-alk
C18:0-alk

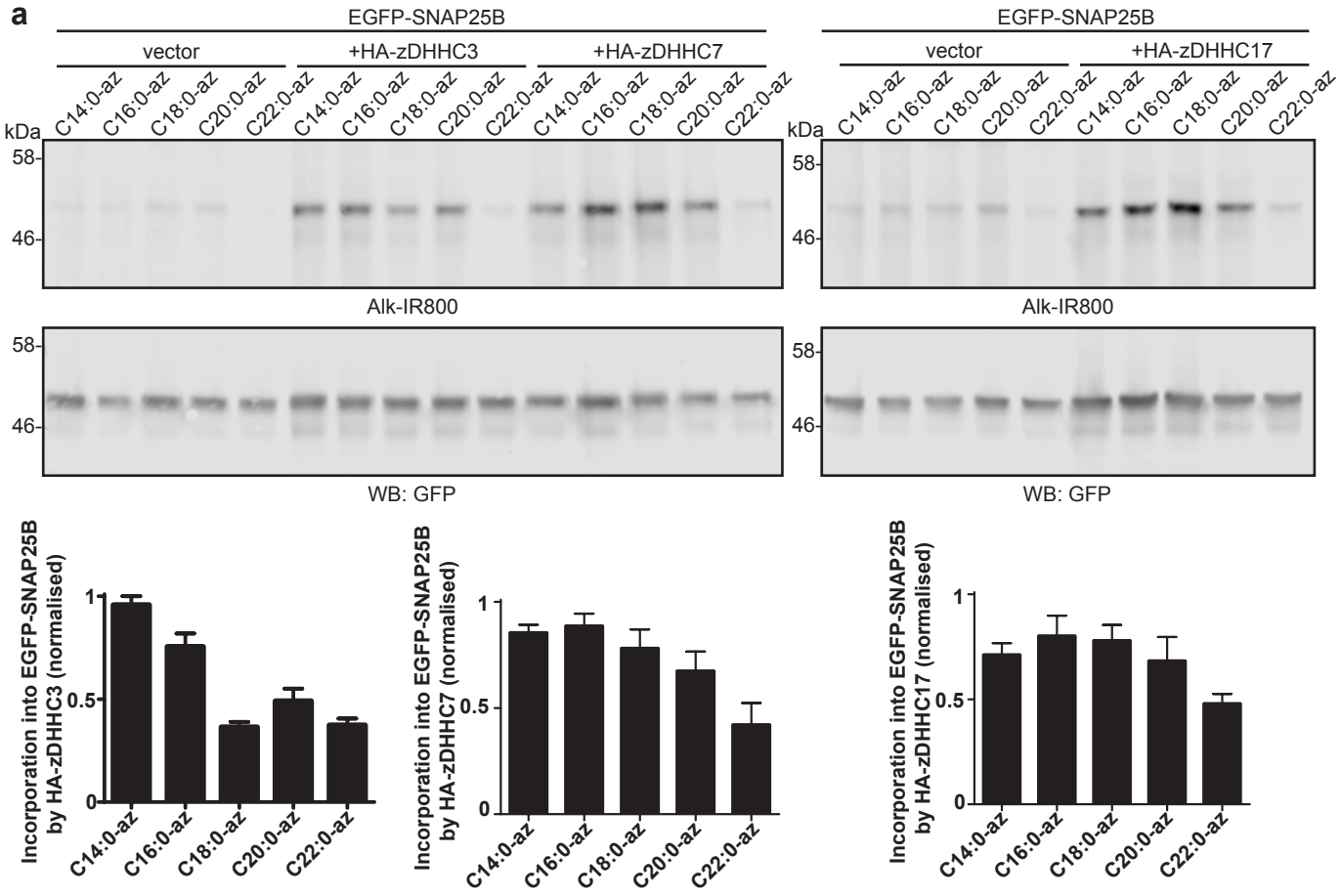
a
EGFP-SNAP25B
vector
+HA-zDHHC3
+HA-zDHHC7
EGFP-SNAP25B
vector
+HA-zDHHC17
C14:0-az
C16:0-az
C18:0-az
C20:0-az
C22:0-az
kDa
58
46
Alk-IR800
WB: GFP
Incorporation into EGFP-SNAP25B by HA-zDHHC3 (normalised)
Incorporation into EGFP-SNAP25B by HA-zDHHC7 (normalised)
Incorporation into EGFP-SNAP25B by HA-zDHHC17 (normalised)
1
0.5
0

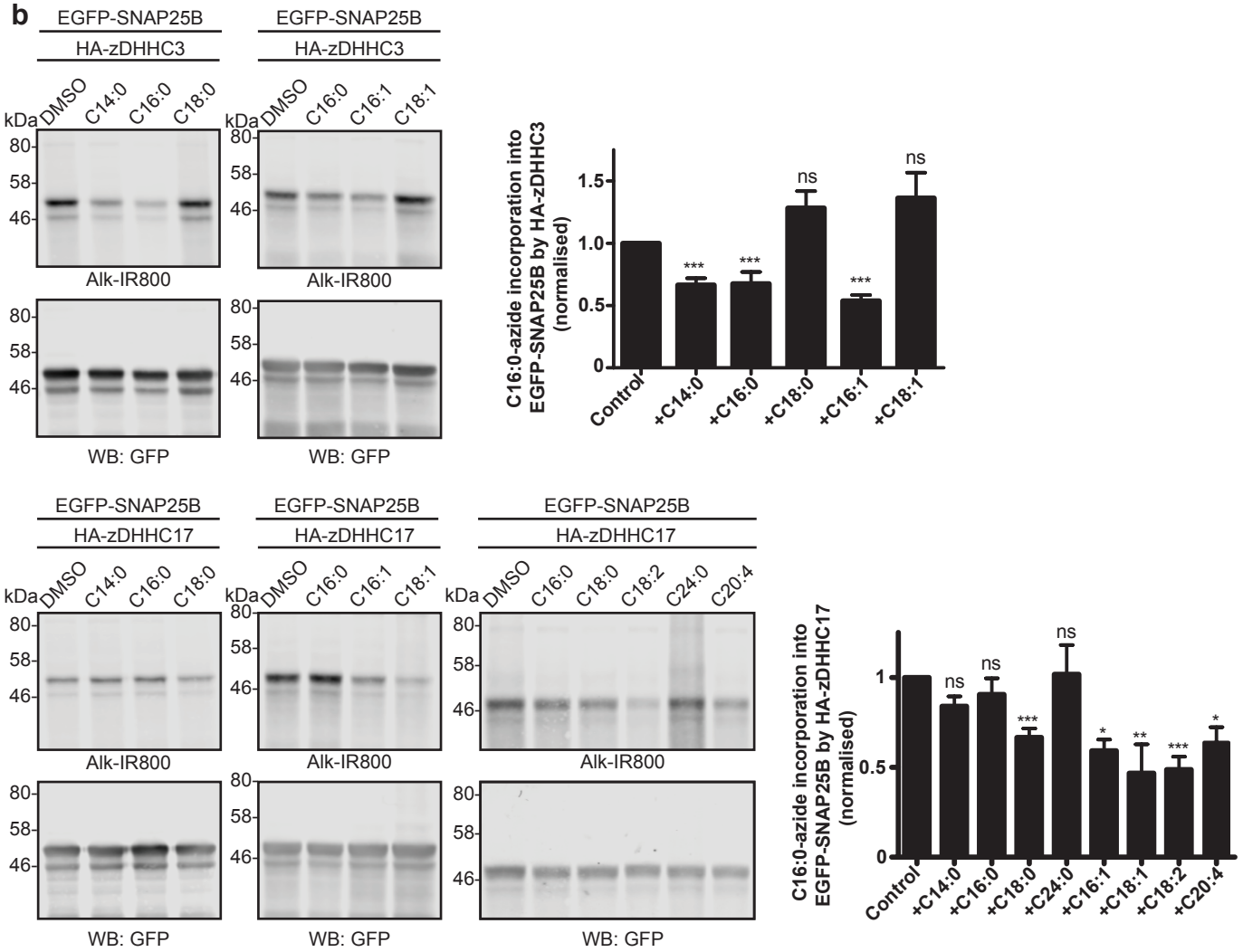
b
EGFP-SNAP25B
HA-zDHHC3
HA-zDHHC17
DMSO
C14:0
C16:0
C18:0
C16:1
C18:1
C18:2
C24:0
C20:4
kDa
80
58
46
Alk-IR800
WB: GFP
C16:0-azide incorporation into EGFP-SNAP25B by HA-zDHHC3 (normalised)
C16:0-azide incorporation into EGFP-SNAP25B by HA-zDHHC17 (normalised)
Control
+C14:0
+C16:0
+C18:0
+C16:1
+C18:1
+C24:0
+C18:2
+C20:4
ns
***
**
*

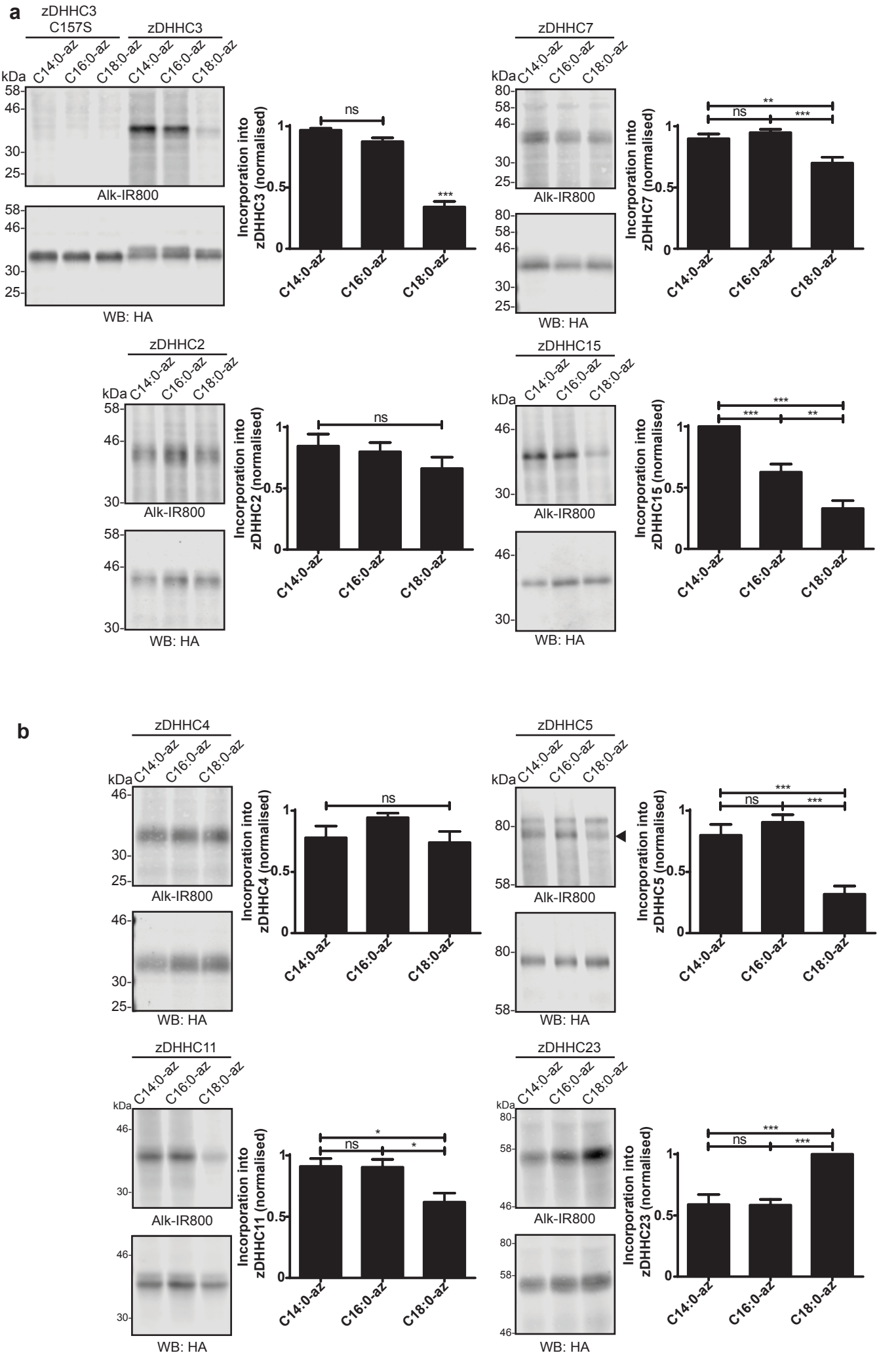
a
zDHHC3 C157S
zDHHC3
C14:0-az
C16:0-az
C18:0-az
kDa
58
46
30
25
Alk-IR800
WB: HA
Incorporation into zDHHC3 (normalised)
ns
***
zDHHC7
80
58
46
30
25
Incorporation into zDHHC7 (normalised)
**
ns
***
zDHHC2
Incorporation into zDHHC2 (normalised)
zDHHC15
Incorporation into zDHHC15 (normalised)
b
zDHHC4
Incorporation into zDHHC4 (normalised)
zDHHC5
Incorporation into zDHHC5 (normalised)
zDHHC11
Incorporation into zDHHC11 (normalised)
*
zDHHC23
Incorporation into zDHHC23 (normalised)

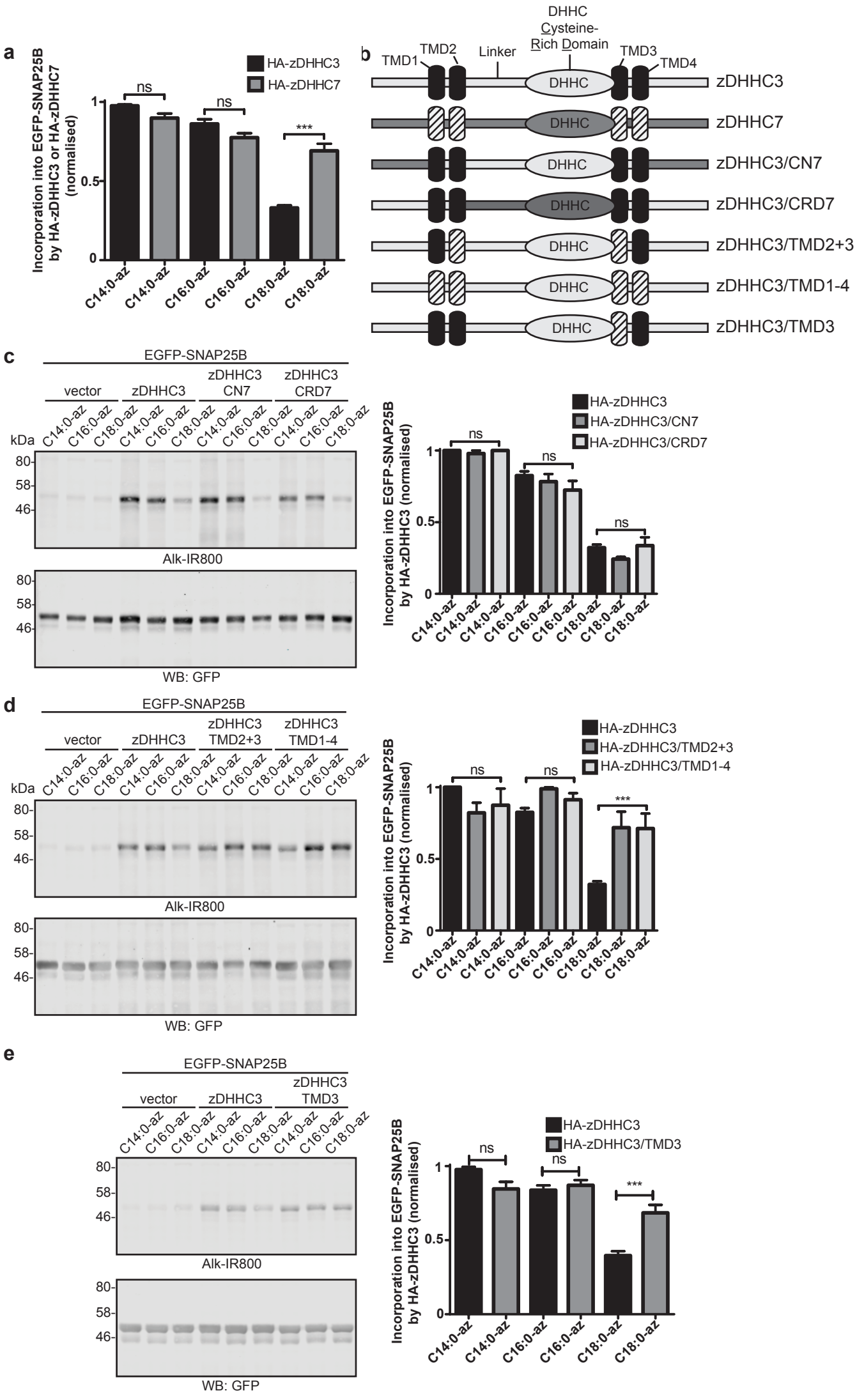
a
HA-zDHHC3
HA-zDHHC7
Incorporation into EGFP-SNAP25B by HA-zDHHC3 or HA-zDHHC7 (normalised)
ns
ns
***
C14:0-az
C14:0-az
C16:0-az
C16:0-az
C18:0-az
C18:0-az
b
DHHC Cysteine-Rich Domain
TMD1
TMD2
Linker
TMD3
TMD4
DHHC
zDHHC3
zDHHC7
zDHHC3/CN7
zDHHC3/CRD7
zDHHC3/TMD2+3
zDHHC3/TMD1-4
zDHHC3/TMD3
c
EGFP-SNAP25B
vector
zDHHC3
zDHHC3 CN7
zDHHC3 CRD7
kDa
Alk-IR800
WB: GFP
HA-zDHHC3
HA-zDHHC3/CN7
HA-zDHHC3/CRD7
Incorporation into EGFP-SNAP25B by HA-zDHHC3 (normalised)
d
EGFP-SNAP25B
vector
zDHHC3
zDHHC3 TMD2+3
zDHHC3 TMD1-4
Alk-IR800
WB: GFP
HA-zDHHC3
HA-zDHHC3/TMD2+3
HA-zDHHC3/TMD1-4
Incorporation into EGFP-SNAP25B by HA-zDHHC3 (normalised)
e
EGFP-SNAP25B
vector
zDHHC3
zDHHC3 TMD3
Alk-IR800
WB: GFP
HA-zDHHC3
HA-zDHHC3/TMD3
Incorporation into EGFP-SNAP25B by HA-zDHHC3 (normalised)

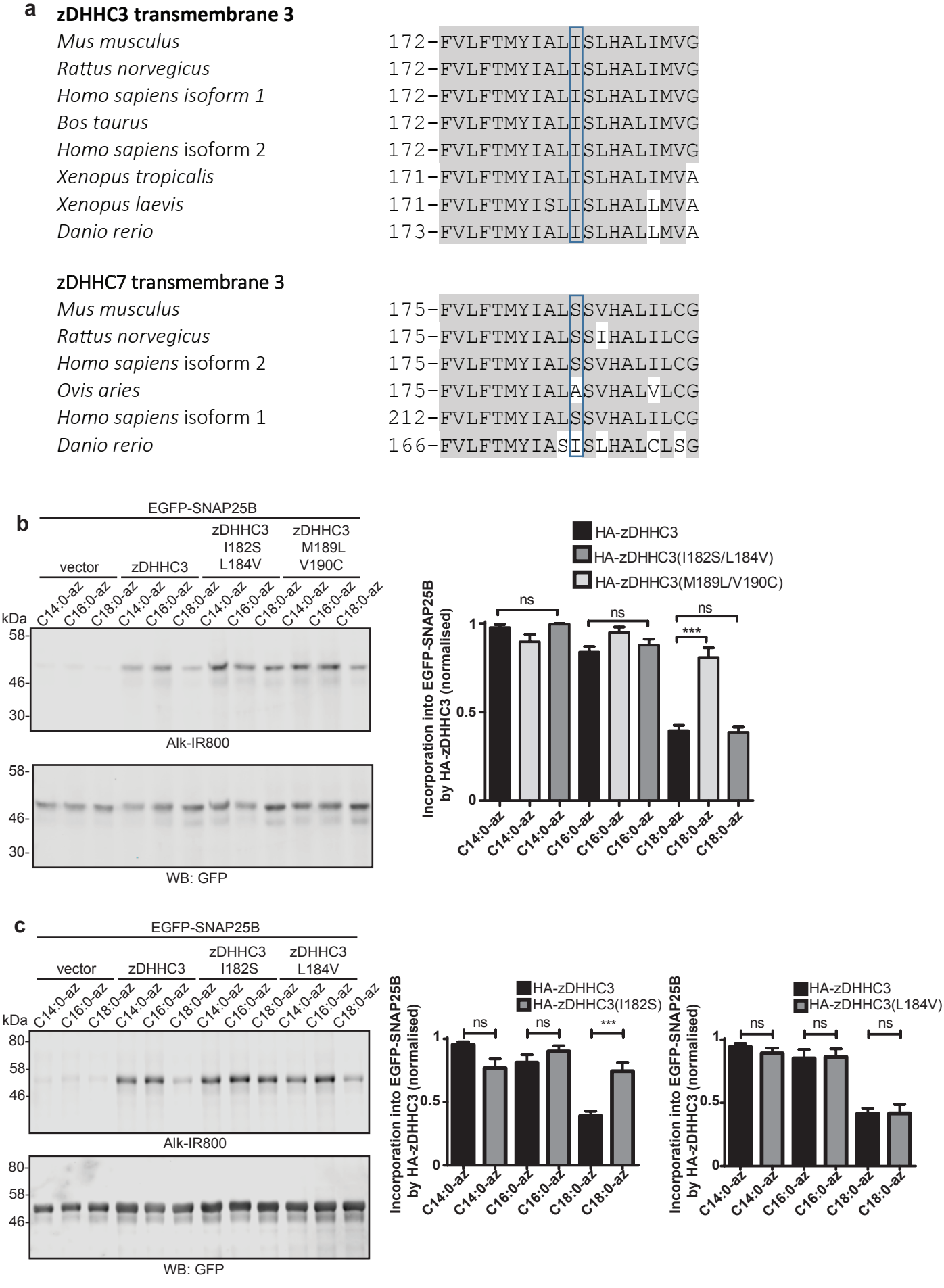
a
zDHHC3 transmembrane 3
Mus musculus 172-FVLFTMYIALISLHALIMVG
Rattus norvegicus 172-FVLFTMYIALISLHALIMVG
Homo sapiens isoform 1 172-FVLFTMYIALISLHALIMVG
Bos taurus 172-FVLFTMYIALISLHALIMVG
Homo sapiens isoform 2 172-FVLFTMYIALISLHALIMVG
Xenopus tropicalis 171-FVLFTMYIALISLHALIMVA
Xenopus laevis 171-FVLFTMYISLISLHALLMVA
Danio rerio 173-FVLFTMYIALISLHALLMVA
zDHHC7 transmembrane 3
Mus musculus 175-FVLFTMYIALSSVHALILCG
Rattus norvegicus 175-FVLFTMYIALSSIHALILCG
Homo sapiens isoform 2 175-FVLFTMYIALSSVHALILCG
Ovis aries 175-FVLFTMYIALASVHALVLCG
Homo sapiens isoform 1 212-FVLFTMYIALSSVHALILCG
Danio rerio 166-FVLFTMYIASISLHALCLSG
b
EGFP-SNAP25B
vector
zDHHC3
zDHHC3 I182S L184V
zDHHC3 M189L V190C
C14:0-az
C16:0-az
C18:0-az
kDa
58
46
30
Alk-IR800
WB: GFP
HA-zDHHC3
HA-zDHHC3(I182S/L184V)
HA-zDHHC3(M189L/V190C)
Incorporation into EGFP-SNAP25B by HA-zDHHC3 (normalised)
ns
***
c
zDHHC3 I182S
zDHHC3 L184V
80
HA-zDHHC3(I182S)
HA-zDHHC3(L184V)

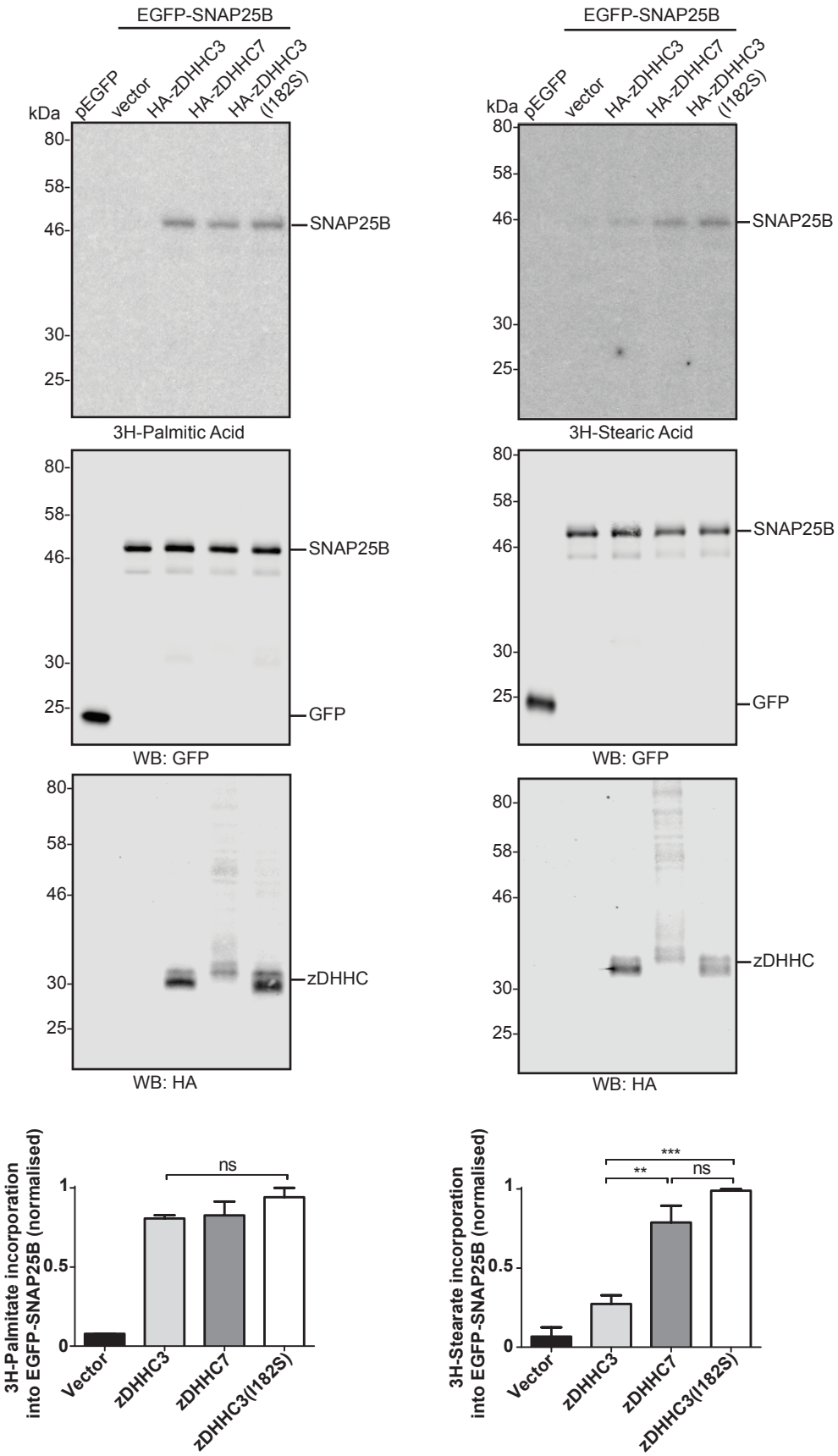
EGFP-SNAP25B
kDa
pEGFP
vector
HA-zDHHC3
HA-zDHHC7
HA-zDHHC3 (I182S)
80
58
46
30
25
SNAP25B
3H-Palmitic Acid
3H-Stearic Acid
GFP
WB: GFP
zDHHC
WB: HA
3H-Palmitate incorporation into EGFP-SNAP25B (normalised)
3H-Stearate incorporation into EGFP-SNAP25B (normalised)
ns
**
***
1
0.5
0
Vector
zDHHC3
zDHHC7
zDHHC3(I182S)

Molecular basis of fatty acid selectivity in the zDHHC family of S-acyltransferases revealed by click chemistry

Greaves et al

SUPPLEMENTARY INFORMATION APPENDIX

General Experimental Details

Unless otherwise stated, all commercially available reagents were used as supplied without any further purification. ^{n}BuLi was purchased as a 2.5 M solution, and the solution was titrated with diphenylacetic acid prior to use. Dry THF was used directly from a PureSolv MD 5 Solvent Purification System by Innovative Technology Inc., and handled under inert atmosphere. 1,3-Dimethyl-3,4,5,6-tetrahydro-2(1*H*)-pyrimidinone) (DMPU) was dried by heating to reflux over calcium hydride and distilling under vacuum before being purged with, and stored under N_2 over 4 Å molecular sieves. Flash chromatography was carried out using Merck Kieselgel 60 H silica. Analytical thin layer chromatography was carried out using aluminium-backed plates coated with Merck Kieselgel 60 GF_{254} that were visualised using *p*-anisaldehyde. Nuclear magnetic resonance (NMR) spectra were recorded on a 400 MHz Ultrashield Magnet, Prodigy liquid nitrogen cryoprobe, AVIII console and a Z420 HP workstation running TopSpin 3.X running at 400 MHz (^{1}H NMR) and 101 MHz (^{13}C NMR); an 500 MHz Ascend magnet, BBO multi nuc' Smart probe, AVIIIHD500 console and Z420 HP workstation running TopSpin 3.X running at 500 MHz (^{1}H NMR) and 126 MHz (^{13}C NMR) or a 600 MHz Ultrashield magnet, BBO multi nuc' probe, AVII+ console and a Z420 HP workstation running TopSpin 3.X running at 600 MHz (^{1}H NMR) or 151 MHz (^{13}C NMR). Chemical shifts are reported in parts per million (ppm) in the scale relative to $CDCl_3$, 7.26 ppm for ^{1}H NMR and 77.16 for ^{13}C NMR; DMSO-d_6, 2.50 ppm for ^{1}H NMR and 39.52 for ^{13}C NMR. Coupling constants are measured in Hertz (Hz). Low-resolution mass spectra (LRMS) were recorded on an Agilent 6130 single quadrupole with APCI/ESI dual source, on a ThermoQuest Finnigan LCQ DUO electrospray, or on an Agilent 7890A GC system, equipped with a 30 m DB5MS column connected to a 5975C inert XL CI MSD with Triple-Axis Detector. MALDI were performed on an Axima-CFR from Kratos-Shimadzu. High-resolution mass spectra (HRMS) were obtained courtesy of the EPSRC National Mass Spectrometry Facility at Swansea University, UK. Infrared spectra were recorded on an Agilent 5500a FTIR equipped with ATR (Attenuated Total Reflectance) and were reported in cm^{-1}. *In vacuo* refers to evaporation under reduced pressure using a rotary evaporator connected to a diaphragm pump, followed by the removal of trace volatiles using a high vacuum (oil) pump. Melting points were determined with a Gallenkamp SG92 melting point apparatus and are uncorrected.

Preparation of fatty acid azide and alkyne chemical probes

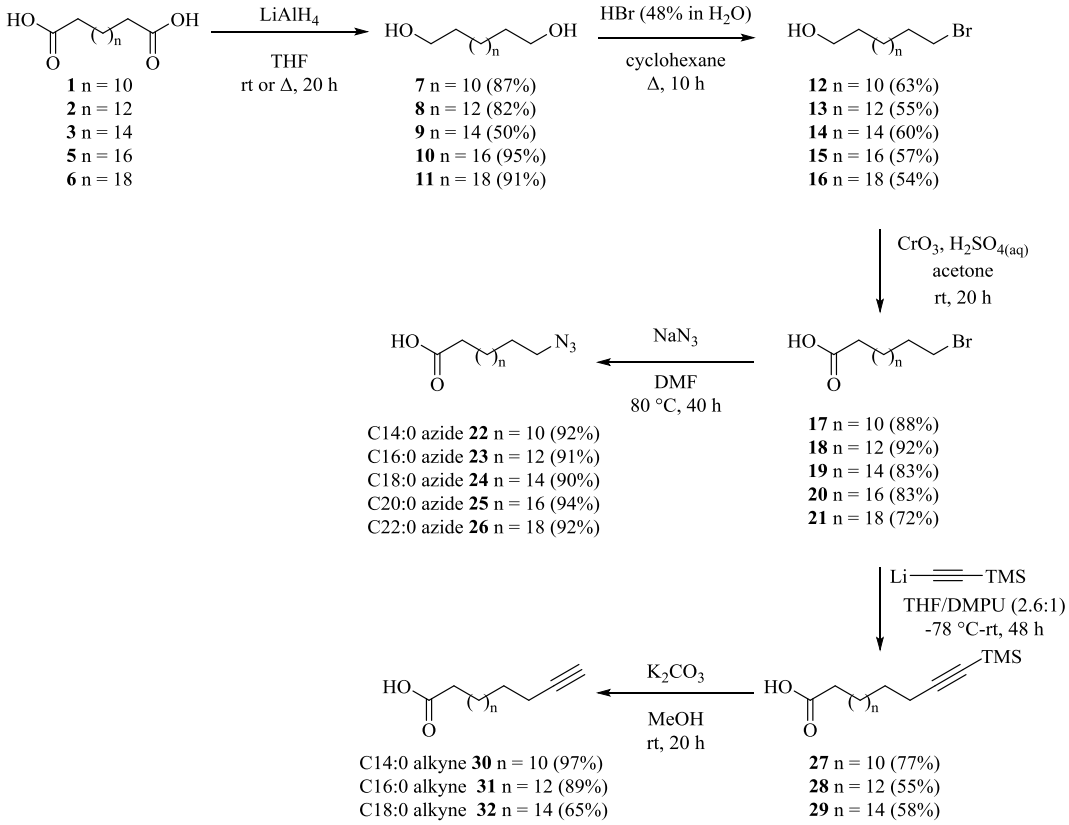

1 n = 10
2 n = 12
3 n = 14
5 n = 16
6 n = 18

7 n = 10 (87%)
8 n = 12 (82%)
9 n = 14 (50%)
10 n = 16 (95%)
11 n = 18 (91%)

12 n = 10 (63%)
13 n = 12 (55%)
14 n = 14 (60%)
15 n = 16 (57%)
16 n = 18 (54%)

17 n = 10 (88%)
18 n = 12 (92%)
19 n = 14 (83%)
20 n = 16 (83%)
21 n = 18 (72%)

C14:0 azide **22** n = 10 (92%)
C16:0 azide **23** n = 12 (91%)
C18:0 azide **24** n = 14 (90%)
C20:0 azide **25** n = 16 (94%)
C22:0 azide **26** n = 18 (92%)

27 n = 10 (77%)
28 n = 12 (55%)
29 n = 14 (58%)

C14:0 alkyne **30** n = 10 (97%)
C16:0 alkyne **31** n = 12 (89%)
C18:0 alkyne **32** n = 14 (65%)

Preparation of 1,14-tetradecanediol 7(1)

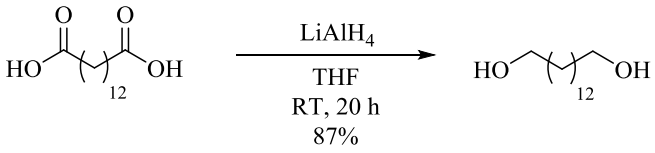

Reaction performed under a N_2 atmosphere.

Solid $LiAlH_4$ (1.47 g, 38.7 mmol) was added to a solution of 1,14-tetradecanedioic acid (5.00 g, 19.35 mmol) in THF (194 mL) at 0 °C. The reaction was allowed to warm to room temperature and stirred at room temperature for 20 h. Upon completion, wet $NaSO_4$ was added portion-wise until the grey suspension turned white. The suspension was stirred at room temperature until the white solid was free-flowing, and solid $MgSO_4$ was added. The reaction was filtered and the filter cake washed with Et_2O (5 × 50 mL). The solvent was evaporated *in vacuo* to afford the product (3.88 g, 87%) as a white solid.

δ_H (600 MHz, DMSO-d_6) 4.29 (t, 2H, *J* 5.0 Hz, 2 × O*H*), 3.35–3.38 (m, 4H, 2 × C*H*$_2$OH), 1.36–1.42 (m, 4H, 2 × C*H*$_2$CH$_2$OH), 1.22–1.29 (m, 20H, 10 × C*H*$_2$).

δ_C (151 MHz, DMSO-d_6) 60.7, 32.5, 29.1, 29.0, 29.0, 28.9, 25.5.

LR-MS (MALDI-TOF) 253.2 ($[M+Na]^+$)

HR-MS calcd for $C_{14}H_{31}O_2^+$ ($[M+H]^+$) 231.2318, found 231.2318.

υ_{max} (thin film, cm^{-1}) 3410, 3351, 2921, 2891, 2850.

Mp 88–90 °C (lit. 87–89 °C)(1)

Preparation of 14-bromotetradecan-1-ol 12(2, 3)

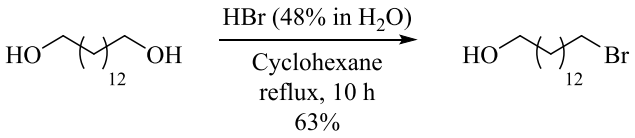

HBr (48% in H_2O, 41 mL) was added to a suspension of diol **7** (3.57 g, 15.5 mmol) in cyclohexane (41 mL). The biphasic mixture was heated to reflux for 10 h before being cooled to room temperature. The layers were separated and the aqueous phase extracted with CH_2Cl_2 (4 × 30 mL). The combined organics were washed with $NaHCO_3$ (4 × 20 mL of a saturated aqueous solution), brine (20 mL), dried over $MgSO_4$, filtered and concentrated *in vacuo*. The crude residue was purified by column chromatography, eluting with 95:5 petrol/EtOAc then 70:30 petrol/EtOAc, to afford the product (2.85 g, 63%) as a pale yellow solid.

δ_H (400 MHz, $CDCl_3$) 3.64 (t, 2H, *J* 6.6 Hz, C*H*$_2$OH), 3.40 (t, 2H, *J* 6.9 Hz, C*H*$_2$Br), 1.80–1.90 (m, 2H, C*H*$_2$CH$_2$Br), 1.53–1.60 (m, 2H, C*H*$_2$CH$_2$OH), 1.25–1.46 (m, 20H, 10 × C*H*$_2$).

δ_C (101 MHz, $CDCl_3$) 63.2, 34.2, 33.0, 33.0, 29.7, 29.7, 29.6, 28.3, 28.9.

LR-MS (EI+) 294.9 ([M(^{81}Br)+H]$^+$), 292.9 ([M(^{79}Br)+H]$^+$), 276.9 ([M(^{81}Br)-H_2O+H]$^+$), 292.9 ([M(^{79}Br)-H_2O+H]$^+$), 213.9 ([M-Br+H]$^+$).

HR-MS calcd for $C_{14}H_{33}ON^{79}Br^+$ ([M+NH_4]$^+$) 310.1740, found 310.1744.

υ_{max} (thin film, cm^{-1}) 3274, 2919, 2850.

Mp 46–48 °C (lit. 42–43 °C)(3)

Preparation of 14-bromotetradecanoic acid 17(4, 5)

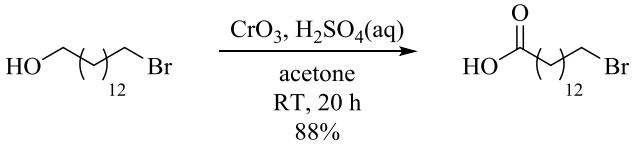

CrO_3 (3.89 g, 38.92 mmol) was dissolved in concentrated H_2SO_4 (7.2 mL). Cold H_2O (16.2 mL) was added slowly and the solution stirred at room temperature for 10 min. The resulting solution was added drop-wise to a solution of alcohol **12** (2.85 g, 9.73 mmol) in acetone (243 mL). The reaction was stirred at room temperature for 20 h before being H_2O (100 mL) and CH_2Cl_2 (40 mL) were added. The layers were separated and the aqueous phase extracted with CH_2Cl_2 (4 × 30 mL). The combined organics were washed with brine (30 mL), dried over $MgSO_4$, filtered and concentrated *in vacuo*. The crude residue was purified by column chromatography, eluting with 90:10 petrol/EtOAc (+0.1% AcOH), to afford the product (2.63 g, 88%) as a white solid.

δ_H (400 MHz, $CDCl_3$) 3.41 (t, 2H, *J* 6.9 Hz, C*H*$_2$Br), 2.35 (t, 2H, *J* 7.5 Hz, C*H*$_2$CO$_2$H), 1.81–1.89 (m, 2H, C*H*$_2$CH$_2$Br), 1.59–1.68 (m, 2H, C*H*$_2$CH$_2$CO$_2$H), 1.24–1.45 (m, 18H, 9 × C*H*$_2$).

δ_C (101 MHz, $CDCl_3$) 179.0, 34.2, 34.0, 33.0, 29.7, 29.7, 29.6, 29.4, 29.2, 28.9, 28.3, 24.8.

LR-MS (EI+) 309.0 ([M(^{81}Br)+H]$^+$), 307.0 ([M(^{79}Br)+H]$^+$), 291.0 ([M(^{81}Br)-H_2O+H]$^+$), 289.0 ([M(^{79}Br)-H_2O+H]$^+$), 227.1 ([M-Br+H]$^+$).

HR-MS calcd for $C_{14}H_{26}O^{79}Br^-$ ([M-H]$^-$) 305.1122, found 305.1123.

υ_{max} (thin film, cm^{-1}) 3036, 2917, 2852, 1696

Mp 63–66 °C (lit. 64–65 °C)(5)

Preparation of 14-azidotetradecanoic acid 22(4, 6)

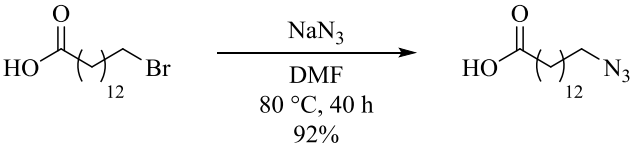

Reaction performed under a N_2 atmosphere

NaN_3 (636 mg, 9.78 mmol) was added to a solution of bromide **17** (500 mg, 1.63 mmol) in DMF (6.5 mL). The reaction was stirred at 80 °C for 40 h before being cooled to room temperature. A 1:1 mixture of EtOAc/H_2O (20 mL) was added, the layers separated and the aqueous phase extracted with EtOAc (3 × 10 mL). The combined organics were washed with brine (10 mL), dried

over $MgSO_4$, filtered and concentrated *in vacuo*. The crude residue was purified by column chromatography, eluting with 90:10 petrol/EtOAc (+0.1% AcOH), to afford the product (403 mg, 92%) as a white solid.

δ_H (400 MHz, $CDCl_3$) 3.25 (t, 2H, *J* 7.0 Hz, CH_2N_3), 2.34 (t, 2H, *J* 7.5 Hz, CH_2CO_2H), 1.55–1.68 (m, 4H, $CH_2CH_2N_3$, $CH_2CH_2CO_2H$), 1.23–1.38 (m, 18H, 9 × CH_2).

δ_C (101 MHz, $CDCl_3$) 180.1, 51.6, 34.2, 29.7, 29.6, 29.6, 29.5, 29.4, 29.3, 29.2, 29.0, 26.9, 24.8.

LR-MS (ES-) 268.1 ($[M-H]^-$), 240.1 ($[M-N_2-H]^-$).

HR-MS calcd for $C_{14}H_{26}N_3O_2^-$ ($[M-H]^-$) 268.2031, found 268.2028.

υ_{max} (thin film, cm^{-1}) 3016, 2915, 2848, 2101, 1701.

Mp 38–40 °C.

Preparation of 16-(trimethylsilyl)hexadec-15-ynoic acid 27

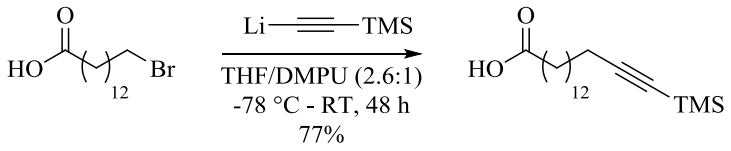

Reaction performed under a N_2 atmosphere.

^{n}BuLi (2.19 M, 7.46 mL, 16.3 mmol) was added drop-wise to a solution of (trimethylsilyl)acetylene (1.6 g, 2.3 mL, 16.3 mmol) in THF (10 mL) at -78 °C. The reaction was stirred at -78 °C for 1 h before DMPU (18 mL) was added and the reaction stirred for a further 30 min. A solution of bromide **17** (500 mg, 1.63 mmol) in THF (37 mL) was added drop-wise and the reaction stirred at room temperature for 48 h. Upon completion, the reaction was quenched with HCl (20 mL of a 1 M solution). The layers were separated and the aqueous phase extracted with Et_2O (4 × 20 mL). The combined organics were washed with brine (3 × 20 mL), dried over $MgSO_4$, filtered and concentrated *in vacuo*. The crude residue was purified by column chromatography, eluting with 90:10 petrol/EtOAc (+0.1% AcOH), to afford the product (407 mg, 77%) as a white solid.

δ_H (400 MHz, $CDCl_3$) 2.34 (t, 2H, *J* 7.5 Hz, CH_2CO_2H), 2.20 (t, 2H, *J* 7.2 Hz, $CH_2C{\equiv}CSi$), 1.58–1.67 (m, 2H, $CH_2CH_2CO_2H$), 1.46–1.55 (m, 2H, $CH_2CH_2C{\equiv}CSi$), 1.25–1.39 (m, 18H, 9 × CH_2), 0.14 (s, 9H, $Si(CH_3)_3$).

δ_C (101 MHz, $CDCl_3$) 180.3, 107.9, 84.4, 34.2, 29.7, 29.6, 29.6, 29.4, 29.2, 28.9, 28.8, 24.8, 20.0, 0.3.

LR-MS (ES-) 323.2 ($[M-H]^-$).

HR-MS calcd for $C_{19}H_{35}O_2Si^-$ ($[M-H]^-$) 323.2412, found 323.2408.

υ_{max} (thin film, cm^{-1}) 2939, 2921, 2852, 2178, 1714, 1699.

Mp 37–40 °C

Preparation of hexadec-15-ynoic acid 30(7, 8)

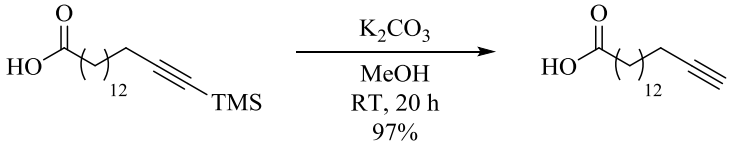

K_2CO_3 (285 mg, 2.06 mmol) was added to a solution of TMS-alkyne **27** (268 mg, 0.82 mmol) in methanol (8.2 mL) at room temperature. The reaction was stirred at room temperature for 20 h before the solvent was evaporated *in vacuo*. The residue was dissolved in EtOAc (15 mL) and HCl (15 mL of a 1 M aqueous solution) added. The layers were separated and the aqueous phase extracted with EtOAc (3 × 20 mL). The combined organics were washed with brine (20 mL), dried over $MgSO_4$, filtered and concentrated *in vacuo*. The crude residue was purified by column chromatography, eluting with 90:10 petrol/EtOAc (+0.1% AcOH), to afford the product (200 mg, 97%) as a white solid.

δ_H (400 MHz, $CDCl_3$) 2.34 (t, 2H, *J* 7.5 Hz, C*H*$_2$CO$_2$H), 2.18 (td, 2H, *J* 7.1 Hz, ^4J 2.7 Hz, C*H*$_2$C≡CH), 1.93 (t, 1H, ^4J 2.7 Hz, C≡C*H*), 1.58–1.67 (m, 2H, C*H*$_2$CH$_2$CO$_2$H), 1.47–1.55 (m, 2H, C*H*$_2$CH$_2$C≡CH), 1.25–1.43 (m, 18H, 9 × C*H*$_2$).

δ_C (101 MHz, $CDCl_3$) 180.3, 85.0, 68.2, 34.2, 29.7, 29.6, 29.6, 29.4, 29.2, 29.2, 28.9, 28.6, 24.8, 18.5.

LR-MS (ES-) 251.2 ([M-H]$^-$).

HR-MS calcd for $C_{16}H_{27}O_2^-$ ([M-H]$^-$) 251.2017, found 251.2017.

υ_{max} (thin film, cm^{-1}) 3285, 3042, 2917, 2852, 2115, 1694.

Mp 59–61 °C.

Preparation of 1,16-hexadecanediol 8(9)

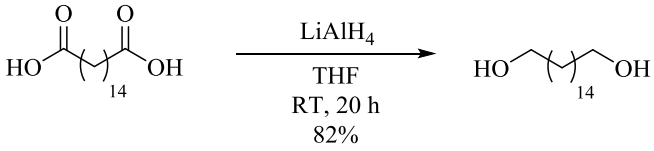

Reaction performed under a N_2 atmosphere.

Solid $LiAlH_4$ (1.33 g, 34.9 mmol) was added to a solution of 1,16-hexadecanedioic acid (5.00 g, 17.46 mmol) in THF (175 mL) at 0 °C. The reaction was allowed to warm to room temperature and stirred at room temperature for 20 h. Upon completion, wet $NaSO_4$ was added portion-wise until the grey suspension turned white. The suspension was stirred at room temperature until the white solid was free-flowing, and solid $MgSO_4$ was added. The reaction was filtered and the filter cake washed with Et_2O (5 × 50 mL). The solvent was evaporated *in vacuo* to afford the product (3.68 g, 82%) as a white solid.

δ_H (600 MHz, DMSO-d_6) 4.29 (t, 2H, *J* 4.9 Hz, 2 × O*H*), 3.34–3.39 (m, 4H, 2 × C*H*$_2$OH), 1.36–1.42 (m, 4H, 2 × C*H*$_2$CH$_2$OH), 1.22–1.29 (m, 24H, 12 × C*H*$_2$).

δ_C (151 MHz, DMSO-d_6) 60.7, 32.5, 29.1, 29.0, 29.0, 29.0, 28.9, 25.5.

LR-MS (MALDI-TOF) 281.3 ([M+Na]$^+$), 297.3 ([M+K]$^+$).

HR-MS calcd for $C_{16}H_{35}O_2^+$ ([M+H]$^+$) 259.2632, found 259.2632.

υ_{max} (thin film, cm^{-1}) 3414, 3353, 2919, 2891, 2848.

Mp 91-94 °C (lit. 93–94 °C)(9)

Preparation of 16-bromohexadecan-1-ol 13(10, 11)

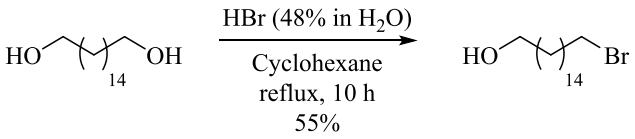

HBr (48% in H_2O, 36 mL) was added to a suspension of diol **8** (3.48 g, 13.5 mmol) in cyclohexane (36 mL). The biphasic mixture was heated to reflux for 10 h before being cooled to room temperature. The layers were separated and the aqueous phase extracted with CH_2Cl_2 (4 × 30 mL). The combined organics were washed with $NaHCO_3$ (4 × 20 mL of a saturated aqueous solution), brine (20 mL), dried over $MgSO_4$, filtered and concentrated *in vacuo*. The crude residue was purified by column chromatography, eluting with 95:5 petrol/EtOAc then 70:30 petrol/EtOAc, to afford the product (2.40 g, 55%) as a pale yellow solid.

δ_H (400 MHz, $CDCl_3$) 3.64 (t, 2H, *J* 6.6 Hz, C*H*$_2$OH), 3.41 (t, 2H, *J* 6.9 Hz, C*H*$_2$Br), 1.80–1.91 (m, 2H, C*H*$_2$CH$_2$Br), 1.52–1.62 (m, 2H, C*H*$_2$CH$_2$OH), 1.25–1.46 (m, 24H, 12 × C*H*$_2$).

δ_C (101 MHz, $CDCl_3$) 63.3, 34.2, 33.0, 33.0, 29.8, 29.8, 29.7, 29.6, 28.9, 28.3, 25.9.

LR-MS (EI+) 320.9 ([M(^{81}Br)+H]$^+$), 318.9 ([M(^{79}Br)+H]$^+$), 304.9 ([M(^{81}Br)-H$_2$O+H]$^+$), 302.9 ([M(^{79}Br)-H$_2$O+H]$^+$), 241.8 ([M-Br+H]$^+$).

HR-MS calcd for $C_{16}H_{37}{}^{79}BrON^+$ ([M+NH$_4$]$^+$) 338.2053, found 338.2056.

υ_{max} (thin film, cm^{-1}) 3274, 2917, 2850.

Mp 54-56 °C (lit. 54–56 °C)(12)

Preparation of 16-bromohexadecanoic acid 18(13)

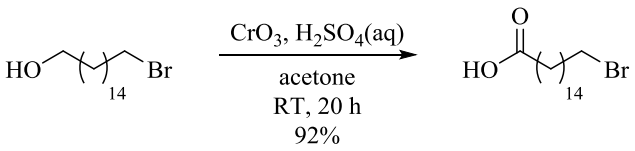

CrO_3 (3.00 g, 30.0 mmol) was dissolved in concentrated H_2SO_4 (5.5 mL). Cold H_2O (12.5 mL) was added slowly and the solution stirred at room temperature for 10 min. The resulting solution was added drop-wise to a solution of alcohol **13** (2.40 g, 7.50 mmol) in acetone (188 mL). The reaction was stirred at room temperature for 20 h before being H_2O (100 mL) and CH_2Cl_2 (40 mL) were added. The layers were separated and the aqueous phase extracted with CH_2Cl_2 (4 × 30 mL). The combined organics were washed with brine (30 mL), dried over $MgSO_4$, filtered and

concentrated *in vacuo*. The crude residue was purified by column chromatography, eluting with 90:10 petrol/EtOAc (+0.1% AcOH), to afford the product (2.30 g, 92%) as a white solid.

δ_H (400 MHz, $CDCl_3$) 3.41 (t, 2H, *J* 6.9 Hz, C*H*$_2$Br), 2.35 (t, 2H, *J* 7.5 Hz, C*H*$_2$CO$_2$H), 1.80–1.90 (m, 2H, C*H*$_2$CH$_2$Br), 1.59–1.68 (m, 2H, C*H*$_2$CH$_2$CO$_2$H), 1.25–1.48 (m, 22H, 11 × C*H*$_2$).

δ_C (101 MHz, $CDCl_3$) 178.6, 34.2, 33.9, 33.0, 29.8, 29.7, 29.6, 29.4, 29.2, 28.9, 28.3, 24.8.

LR-MS (EI+) 337.0 ([M(^{81}Br)+H]$^+$), 335.0 ([M(^{79}Br)+H]$^+$), 317.0 ([M(^{81}Br)-H_2O+H]$^+$), 315.0 ([M(^{79}Br)-H_2O+H]$^+$), 257.1 ([M-Br+H]$^+$), 237.1 ([M-Br-H_2O+H]$^+$).

HR-MS calcd for $C_{16}H_{30}{}^{79}BrO^-$ ([M-H]$^-$) 333.1435, found 333.1430.

υ_{max} (thin film, cm^{-1}) 3034, 2917, 2850, 1696

Mp 72-74 °C (lit. 71 °C)(11)

Preparation of 16-azidohexadecanoic acid 23(6)

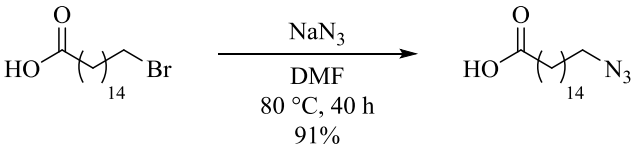

Reaction performed under a N_2 atmosphere

NaN_3 (582 mg, 8.96 mmol) was added to a solution of bromide **18** (500 mg, 1.49 mmol) in DMF (6 mL). The reaction was stirred at 80 °C for 40 h before being cooled to room temperature. A 1:1 mixture of EtOAc/H_2O (20 mL) was added, the layers separated and the aqueous phase extracted with EtOAc (3 × 10 mL). The combined organics were washed with brine (10 mL), dried over $MgSO_4$, filtered and concentrated *in vacuo*. The crude residue was purified by column chromatography, eluting with 90:10 petrol/EtOAc (+0.1% AcOH), to afford the product (402 mg, 91%) as a white solid.

δ_H (400 MHz, $CDCl_3$) 3.25 (t, 2H, *J* 7.0 Hz, C*H*$_2$N$_3$), 2.34 (t, 2H, *J* 7.5 Hz, C*H*$_2$CO$_2$H), 1.55–1.67 (m, 4H, C*H*$_2$CH$_2$N$_3$, C*H*$_2$CH$_2$CO$_2$H), 1.24–1.40 (m, 22H, 11 × C*H*$_2$).

δ_C (101 MHz, $CDCl_3$) 180.0, 51.7, 34.2, 29.8, 29.7, 29.7, 29.6, 29.6, 29.4, 29.3, 29.3, 29.2, 29.2, 29.0, 26.9, 24.8.

LR-MS (ES-) 268.2 ([M-N_2-H]$^-$), 296.2 ([M-H]$^-$).

HR-MS calcd for $C_{16}H_{32}NO_2^+$ ([M-N_2+H]$^+$) 270.2440, found 270.2433.

υ_{max} (thin film, cm^{-1}) 3014, 2915, 2848, 2103, 1701.

Mp 48–50 °C

Preparation of 18-(trimethylsilyl)octadec-17-ynoic acid 28

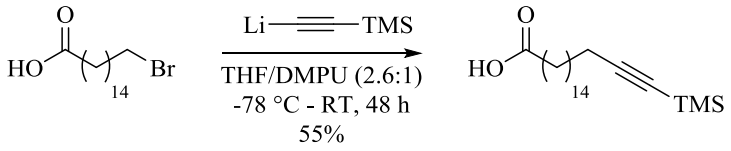

Reaction performed under a N_2 atmosphere.

^{n}BuLi (2.09 M, 3.6 mL, 7.46 mmol) was added drop-wise to a solution of (trimethylsilyl)acetylene (773 mg, 1.05 mL, 7.46 mmol) in THF (4.6 mL) at -78 °C. The reaction was stirred at -78 °C for 1 h before DMPU (8.3 mL) was added and the reaction stirred for a further 30 min. A solution of bromide **18** (500 mg, 1.49 mmol) in THF (16.7 mL) was added drop-wise and the reaction stirred at room temperature for 48 h. Upon completion, the reaction was quenched with HCl (20 mL of a 1 M solution). The layers were separated and the aqueous phase extracted with Et_2O (4 × 20 mL). The combined organics were washed with brine (3 × 20 mL), dried over $MgSO_4$, filtered and concentrated *in vacuo*. The crude residue was purified by column chromatography, eluting with 90:10 petrol/EtOAc (+0.1% AcOH), to afford the product (288 mg, 55%) as a white solid.

δ_H (400 MHz, $CDCl_3$) 2.34 (t, 2H, *J* 7.5 Hz, C*H*$_2$CO$_2$H), 2.20 (t, 2H, *J* 7.2 Hz, C*H*$_2$C≡CSi), 1.58–1.69 (m, 2H, C*H*$_2$CH$_2$CO$_2$H), 1.46–1.56 (m, 2H, C*H*$_2$CH$_2$C≡CSi), 1.24–1.40 (m, 22H, 11 × C*H*$_2$), 0.14 (s, 9H, Si(C*H*$_3$)$_3$).

δ_C (101 MHz, $CDCl_3$) 179.8, 108.0, 84.4, 34.1, 29.8, 29.7, 29.6, 29.6, 29.4, 29.2, 29.0, 28.8, 24.8, 20.0, 0.3.

LR-MS (ES-) 351.3 ([M-H]$^-$).

HR-MS calcd for $C_{21}H_{39}O_2Si^-$ ([M-H]$^-$) 251.2725, found 351.2718.

υ_{max} (thin film, cm^{-1}) 2937, 2919, 2850, 2178, 1714, 1699.

Mp 50–53 °C

Preparation of octadec-17-ynoic acid 31(14)

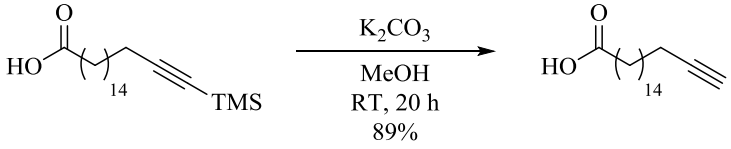

K_2CO_3 (223 mg, 1.61 mmol) was added to a solution of TMS-alkyne **28** (228 mg, 0.65 mmol) in methanol (6.5 mL) at room temperature. The reaction was stirred at room temperature for 20 h before the solvent was evaporated *in vacuo*. The residue was dissolved in EtOAc (15 mL) and HCl (15 mL of a 1 M aqueous solution) added. The layers were separated and the aqueous phase extracted with EtOAc (3 × 20 mL). The combined organics were washed with brine (20 mL), dried over $MgSO_4$, filtered and concentrated *in vacuo*. The crude residue was purified by column chromatography, eluting with 90:10 petrol/EtOAc (+0.1% AcOH), to afford the product (161 mg, 89%) as a white solid.

δ_H (400 MHz, $CDCl_3$) 2.34 (t, 2H, *J* 7.5 Hz, C*H*$_2$CO$_2$H), 2.18 (td, 2H, *J* 7.1 Hz, ^{4}*J* 2.6 Hz, C*H*$_2$C≡CH), 1.93 (t, 1H, ^{4}*J* 2.6 Hz, C≡C*H*), 1.59–1.67 (m, 2H, C*H*$_2$CH$_2$CO$_2$H), 1.48–1.56 (m, 2H, C*H*$_2$CH$_2$C≡CH), 1.24–1.44 (m, 22H, 11 × C*H*$_2$).

δ_C (101 MHz, $CDCl_3$) 180.1, 85.0, 68.2, 34.2, 29.8, 29.7, 29.6, 29.6, 29.4, 29.3, 29.2, 28.9, 28.7, 28.4, 18.5.

LR-MS (ES-) 279.2 ($[M-H]^-$).

HR-MS calcd for $C_{18}H_{31}O_2^-$ ($[M-H]^-$) 279.2330, found 279.2331.

υ_{max} (thin film, cm^{-1}) 3284, 3042, 2917, 2850, 2115, 1694.

Mp 70–72 °C

Preparation of 1,18-octadecanediol 9(15-17)

Method A

Reaction performed under a N_2 atmosphere.

Solid $LiAlH_4$ (1.21 g, 31.8 mmol) was added to a solution of 1,18-octadecanedioic acid (5.00 g, 15.9 mmol) in THF (160 mL) at 0 °C. The reaction was allowed to warm to room temperature and stirred at room temperature for 20 h. Upon completion, wet $NaSO_4$ was added portion-wise until the grey suspension turned white. The suspension was stirred at room temperature until the white solid was free-flowing, and solid $MgSO_4$ was added. The reaction was filtered and the filter cake washed with Et_2O (5 × 50 mL). The solvent was evaporated *in vacuo* to afford the product (2.26 g, 50%) as a white solid.

Method B

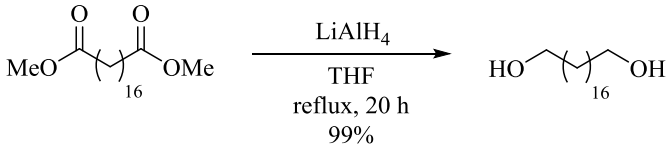

Reaction performed under a N_2 atmosphere.

Solid $LiAlH_4$ (1.44 g, 37.96 mmol) was added to a vigorously stirred solution of dimethyl octadecanedioate (5.00 g, 14.9 mmol) at room temperature. The reaction was heated to reflux and stirred at reflux for 20 h. Upon completion, the reaction was cooled to room temperature and wet $NaSO_4$ was added portion-wise until the grey suspension turned white. The suspension was stirred at room temperature until the white solid was free-flowing, and solid $MgSO_4$ was added. The reaction was filtered and the filter cake washed with Et_2O (5 × 50 mL). The solvent was evaporated *in vacuo* to afford the product (4.15 g, 99%) as a white solid.

δ_H (600 MHz, DMSO-d_6) 4.30 (t, 2H, *J* 5.1 Hz, 2 × O*H*), 3.34–3.39 (m, 4H, 2 × CH_2OH), 1.35–1.43 (m, 4H, 2 × CH_2CH$_2$OH), 1.23 (app. br. s., 28H, 14 × CH_2).

δ_C (151 MHz, DMSO-d_6) 60.6, 32.3, 28.8, 28.8, 28.7, 25.3.

LR-MS (MALDI-TOF) 293.3 ([M+Li]$^+$), 309.3 ([M+Na]$^+$).

HR-MS calcd for $C_{18}H_{39}O_2^+$ ([M+H]$^+$) 287.2945, found 287.2946.

υ_{max} (thin film, cm^{-1}) 3416, 3353, 2919, 2891.

Mp 103–106 °C (lit. 98–99 °C)(16, 17)

Preparation of 18-bromooctadecan-1-ol 14(12)

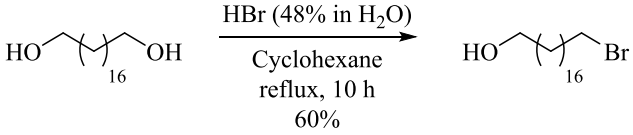

HBr (48% in H_2O, 21 mL) was added to a suspension of diol **9** (2.26 g, 7.9 mmol) in cyclohexane (21 mL). The biphasic mixture was heated to reflux for 10 h before being cooled to room temperature. The layers were separated and the aqueous phase extracted with CH_2Cl_2 (4 × 20 mL). The combined organics were washed with $NaHCO_3$ (4 × 20 mL of a saturated aqueous solution), brine (20 mL), dried over $MgSO_4$, filtered and concentrated *in vacuo*. The crude residue was purified by column chromatography, eluting with 95:5 petrol/EtOAc then 70:30 petrol/EtOAc, to afford the product (1.65 g, 60%) as a pale yellow solid.

δ_H (400 MHz, $CDCl_3$) 3.64 (t, 2H, *J* 6.6 Hz, CH_2OH), 3.40 (t, 2H, *J* 6.9 Hz, CH_2Br), 1.81–1.89 (m, 2H, CH_2CH$_2$Br), 1.53–1.60 (m, 2H, CH_2CH$_2$OH), 1.25–1.46 (m, 28H, 14 × CH_2).

δ_C (101 MHz, $CDCl_3$) 63.3, 34.2, 33.0, 33.0, 29.8, 29.8, 29.7, 29.6, 28.9, 28.3, 25.9.

LR-MS (ES+) 332.5 ([M(^{81}Br)-H_2O+H]$^+$), 330.5 ([M(^{79}Br)-H_2O+H]$^+$).

HR-MS calcd for $C_{18}H_{41}{}^{79}BrON^+$ ([M+NH_4]$^+$) 366.2366, found 336.2368.

υ_{max} (thin film, cm^{-1}) 3274, 2917, 2850.

Mp 59–61 °C (lit. 60–62 °C)(12)

Preparation of 18-bromooctadecanoic acid 19(12, 18)

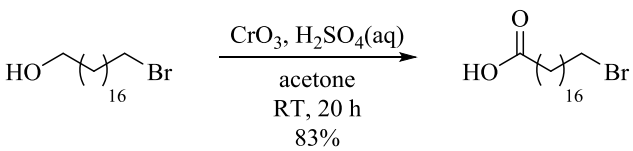

CrO_3 (1.42 g, 14.2 mmol) was dissolved in concentrated H_2SO_4 (3.5 mL). Cold H_2O (7.9 mL) was added slowly and the solution stirred at room temperature for 10 min. The resulting solution was added drop-wise to a solution of alcohol **14** (1.65 g, 4.73 mmol) in acetone (120 mL). The reaction was stirred at room temperature for 20 h before being H_2O (60 mL) and CH_2Cl_2 (40 mL) were added. The layers were separated and the aqueous phase extracted with CH_2Cl_2 (4 × 20 mL). The combined

organics were washed with brine (20 mL), dried over $MgSO_4$, filtered and concentrated *in vacuo*. The crude residue was purified by column chromatography, eluting with 90:10 petrol/EtOAc (+0.1% AcOH), to afford the product (1.43 g, 83%) as a white solid.

δ_H (400 MHz, $CDCl_3$) 3.41 (t, 2H, *J* 6.9 Hz, C*H*$_2$Br), 2.35 (t, 2H, *J* 7.5 Hz, C*H*$_2$CO$_2$H), 1.81–1.90 (m, 2H, C*H*$_2$CH$_2$Br), 1.59–1.68 (m, 2H, C*H*$_2$CH$_2$CO$_2$H), 1.25–1.46 (m, 26H, 13 × C*H*$_2$).

δ_C (101 MHz, $CDCl_3$) 179.6, 34.2, 34.1, 33.0, 29.8, 29.7, 29.7, 29.6, 29.4, 29.2, 28.9, 28.3, 24.8.

LR-MS (EI+) 365.0 ([M(^{81}Br)+H]$^+$), 363.0 ([M(^{79}Br)+H]$^+$), 347.0 ([M(^{81}Br)-H$_2$O+H]$^+$), 345.0 ([M(^{79}Br)-H$_2$O+H]$^+$), 284.0 ([M-Br+H]$^+$), 265.1 ([M-Br-H$_2$O+H]$^+$).

HR-MS calcd for $C_{18}H_{34}{}^{79}BrO_2^-$ ([M-H]$^-$) 361.1748, found 361.1741.

υ_{max} (thin film, cm^{-1}) 3034, 2915, 2850, 1696

Mp 77–80 °C (lit. 80 °C)(18)

Preparation of 18-azidooctadecanoic acid 24

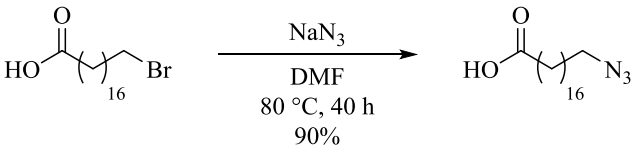

Reaction performed under a N_2 atmosphere

NaN_3 (537 mg, 8.3 mmol) was added to a solution of bromide **19** (500 mg, 1.38 mmol) in DMF (5.5 mL). The reaction was stirred at 80 °C for 40 h before being cooled to room temperature. A 1:1 mixture of EtOAc/H_2O (30 mL) was added, the layers separated and the aqueous phase extracted with EtOAc (3 × 10 mL). The combined organics were washed with brine (10 mL), dried over $MgSO_4$, filtered and concentrated *in vacuo*. The crude residue was purified by column chromatography, eluting with 90:10 petrol/EtOAc (+0.1% AcOH), to afford the product (403 mg, 90%) as a white solid.

δ_H (400 MHz, $CDCl_3$) 3.25 (t, 2H, *J* 7.0 Hz, C*H*$_2$N$_3$), 2.34 (t, 2H, *J* 7.5 Hz, C*H*$_2$CO$_2$H), 1.55–1.67 (m, 4H, C*H*$_2$CH$_2$N$_3$, C*H*$_2$CH$_2$CO$_2$H), 1.25–1.39 (m, 26H, 13 × C*H*$_2$).

δ_C (101 MHz, $CDCl_3$) 180.1, 51.6, 34.2, 29.8, 29.7, 29.7, 29.6, 29.6, 29.4, 29.4, 29.3, 29.2, 29.0, 26.7, 24.8.

LR-MS (ES-) 296.3 ([M-N$_2$-H]$^-$), 324.1 ([M-H]$^-$).

HR-MS calcd for $C_{18}H_{34}N_3O_2^-$ ([M-H]$^-$) 324.2657, found 324.2649.

υ_{max} (thin film, cm^{-1}) 3040, 2915, 2850, 2098, 1696.

Mp 56–58 °C

Preparation of 20-(trimethylsilyl)icos-19-ynoic acid 29

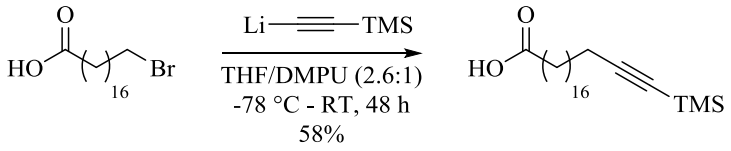

Reaction performed under a N_2 atmosphere.

^{n}BuLi (2.00 M, 6.9 mL, 13.8 mmol) was added drop-wise to a solution of (trimethylsilyl)acetylene (1.36 g, 1.95 mL, 13.8 mmol) in THF (20 mL) at -78 °C. The reaction was stirred at -78 °C for 1 h before DMPU (15.3 mL) was added and the reaction stirred for a further 30 min. A solution of bromide **19** (500 mg, 1.38 mmol) in THF (14.5 mL) was added drop-wise and the reaction stirred at room temperature for 48 h. Upon completion, the reaction was quenched with HCl (20 mL of a 1 M solution). The layers were separated and the aqueous phase extracted with Et_2O (4 × 20 mL). The combined organics were washed with brine (3 × 20 mL), dried over $MgSO_4$, filtered and concentrated *in vacuo*. The crude residue was purified by column chromatography, eluting with 90:10 petrol/EtOAc (+0.1% AcOH), to afford the product (305 mg, 58%) as a white solid.

δ_H (400 MHz, $CDCl_3$) 2.34 (t, 2H, *J* 7.5 Hz, C*H*$_2$CO$_2$H), 2.21 (t, 2H, *J* 7.2 Hz, C*H*$_2$C≡CSi), 1.59–1.67 (m, 2H, C*H*$_2$CH$_2$CO$_2$H), 1.47–1.55 (m, 2H, C*H*$_2$CH$_2$C≡CSi), 1.25–1.39 (m, 26H, 13 × C*H*$_2$), 0.14 (s, 9H, Si(C*H*$_3$)$_3$).

δ_C (101 MHz, $CDCl_3$) 179.8, 108.0, 84.4, 34.1, 29.8, 29.7, 29.6, 29.6, 29.4, 29.2, 29.0, 28.8, 24.8, 20.0, 0.3.

LR-MS (ES-) 379.3 ([M-H]$^-$).

HR-MS calcd for $C_{23}H_{43}O_2^-$ ([M-H]$^-$) 379.3038, found 379.3030.

υ_{max} (thin film, cm^{-1}) 2937, 2917, 2850, 2178, 1714, 1699.

Mp 58–60 °C

Preparation of icos-19-ynoic acid 32

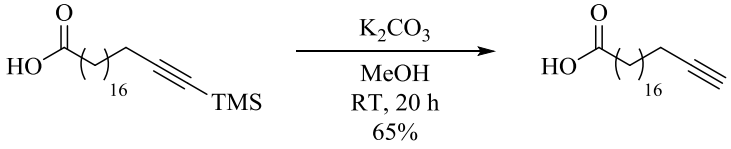

K_2CO_3 (233 mg, 1.69 mmol) was added to a solution of TMS-alkyne **29** (257 mg, 0.67 mmol) in methanol (6.7 mL) at room temperature. The reaction was stirred at room temperature for 20 h before the solvent was evaporated *in vacuo*. The residue was dissolved in EtOAc (15 mL) and HCl (15 mL of a 1 M aqueous solution) added. The layers were separated and the aqueous phase extracted with EtOAc (3 × 20 mL). The combined organics were washed with brine (20 mL), dried over $MgSO_4$, filtered and concentrated *in vacuo*. The crude residue was purified by column chromatography, eluting with 90:10 petrol/EtOAc (+0.1% AcOH), to afford the product (134 mg, 65%) as a white solid.

δ_H (400 MHz, $CDCl_3$) 2.34 (t, 2H, *J* 7.5 Hz, CH_2CO$_2$H), 2.18 (td, 2H, *J* 7.1 Hz, ^4J 2.6 Hz, CH_2C≡CH), 1.93 (t, 1H, ^4J 2.6 Hz, C≡C*H*), 1.58–1.68 (m, 2H, CH_2CH$_2$CO$_2$H), 1.48–1.56 (m, 2H, CH_2CH$_2$C≡CH), 1.24–1.43 (m, 26H, 13 × CH_2).

δ_C (101 MHz, $CDCl_3$) 179.9, 85.0, 68.2, 34.1, 29.8, 29.7, 29.7, 29.6, 29.4, 29.3, 29.2, 28.9, 28.7, 24.8, 18.5.

LR-MS (ES-) 307.2 ($[M-H]^-$).

HR-MS calcd for $C_{20}H_{35}O_2^-$ ($[M-H]^-$) 307.2643, found 307.2636.

υ_{max} (thin film, cm^{-1}) 3282, 2915, 2850, 2115, 1694.

Mp 76–78 °C

Preparation of 1,20-icosanediol 10(19-22)

Method A

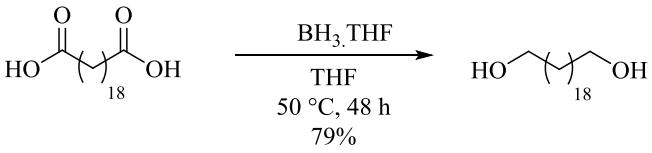

Reaction performed under a N_2 atmosphere.

BH_3.THF (1 M, 8.8 mL, 8.8 mmol) was added to a solution of icosanedioic acid (1.00 g, 2.92 mmol) in THF (58 mL). The reaction was heated to 50 °C for 24 h before additional BH_3.THF (1 M, 2.9 mL, 2.9 mmol) was added. The reaction was heated for a further 24 h before being cooled to 0 °C, quenched with MeOH (20 mL) and stirred for 30 min. HCl (20 mL of a 2 M aqueous solution) was added and the mixture stirred for 1 h. The solvent was evaporated *in vacuo* and the remaining aqueous phase extracted with $CHCl_3$ (3 × 30 mL). The combined organic phase was washed with H_2O (30 mL), brine (30 mL), dried over $MgSO_4$, filtered and concentrated *in vacuo* to afford the product (724 mg, 79%) as white solid.

Method B

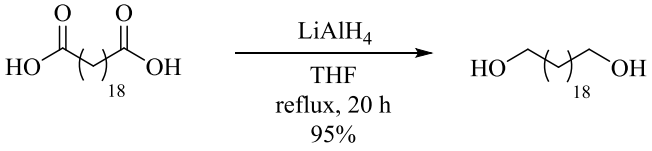

Reaction performed under a N_2 atmosphere.

Solid $LiAlH_4$ (1.44 g, 37.96 mmol) was added to a vigorously stirred solution of icosanedioic acid (5.00 g, 14.6 mmol) at room temperature. The reaction was heated to reflux and stirred at reflux for 20 h. Upon completion, the reaction was cooled to room temperature and wet $NaSO_4$ was added portion-wise until the grey suspension turned white. The suspension was stirred at room temperature until the white solid was free-flowing, and solid $MgSO_4$ was added. The reaction was filtered and the

filter cake washed with Et_2O (5 × 50 mL). The solvent was evaporated *in vacuo* to afford the product (4.35 g, 95%) as a white solid.

δ_H (600 MHz, DMSO-d_6) 3.38 (t, 4H, *J* 6.5 Hz, 2 × CH_2OH), 1.37–1.45 (m, 4H, 2 × CH_2CH_2OH), 1.23 (app. br. s., 32H, 16 × CH_2).

δ_C (151 MHz, DMSO-d_6) 60.6, 32.3, 28.8, 28.7, 28.7, 25.3.

LR-MS (MALDI-TOF) 337.3 ($[M+Na]^+$).

HR-MS calcd for $C_{20}H_{43}O_2^+$ ($[M+H]^+$) 315.3258, found 315.3259.

υ_{max} (thin film, cm^{-1}) 3252, 2915, 2848.

Mp 103–105 °C (lit. 102–105 °C)(20)

Preparation of 20-bromoicosan-1-ol 15

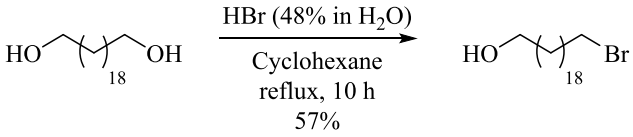

HBr (48% in H_2O, 36 mL) was added to a suspension of diol **10** (4.35 g, 13.6 mmol) in cyclohexane (86 mL). The biphasic mixture was heated to reflux for 10 h before being cooled to room temperature. The layers were separated and the aqueous phase extracted with CH_2Cl_2 (4 × 50 mL). The combined organics were washed with $NaHCO_3$ (4 × 30 mL of a saturated aqueous solution), brine (30 mL), dried over $MgSO_4$, filtered and concentrated *in vacuo*. The crude residue was purified by column chromatography, eluting with 95:5 petrol/EtOAc then 70:30 petrol/EtOAc, to afford the product (2.94 g, 57%) as a pale yellow solid.

δ_H (400 MHz, $CDCl_3$) 3.64 (t, 2H, *J* 6.6 Hz, CH_2OH), 3.41 (t, 2H, *J* 6.9 Hz, CH_2Br), 1.81–1.89 (m, 2H, CH_2CH_2Br), 1.53–1.59 (m, 2H, CH_2CH_2OH), 1.25–1.45 (m, 32H, 16 × CH_2).

δ_C (101 MHz, $CDCl_3$) 63.3, 34.2, 33.0, 33.0, 29.8, 29.8, 29.7, 29.6, 28.9, 28.3, 25.9.

LR-MS (EI+) 376.4 ($[M(^{81}Br)+H]^+$), 374.4 ($[M(^{79}Br)+H]^+$), 361.1 ($[M(^{81}Br)-H_2O+H]^+$), 359.1 ($[M(^{79}Br)-H_2O+H]^+$,), 296.6 ($[M-Br+H]^+$).

HR-MS calcd for $C_{20}H_{40}{}^{79}Br^+$ ($[M-H_2O+H]^+$) 359.2313, found 359.2313.

υ_{max} (thin film, cm^{-1}) 3270, 2915, 2846.

Mp 66–68 °C

Preparation of 20-bromoicosanoic acid 20

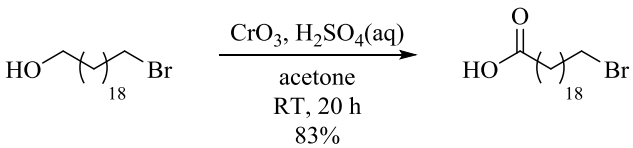

CrO_3 (3.12 g, 31.2 mmol) was dissolved in concentrated H_2SO_4 (5.7 mL). Cold H_2O (13 mL) was added slowly and the solution stirred at room temperature for 10 min. The resulting solution was added drop-wise to a solution of alcohol **15** (2.94 g, 7.8 mmol) in acetone (195 mL). The reaction was stirred at room temperature for 20 h before being H_2O (100 mL) and CH_2Cl_2 (50 mL) were added. The layers were separated and the aqueous phase extracted with CH_2Cl_2 (4 × 50 mL). The combined organics were washed with brine (50 mL), dried over $MgSO_4$, filtered and concentrated *in vacuo*. The crude residue was purified by column chromatography, eluting with 90:10 petrol/EtOAc (+0.1% AcOH), to afford the product (2.53 g, 83%) as a white solid.

δ_H (400 MHz, $CDCl_3$) 3.41 (t, 2H, *J* 6.9 Hz, C*H*$_2$Br), 2.35 (t, 2H, *J* 7.5 Hz, C*H*$_2$CO$_2$H), 1.81–1.90 (m, 2H, C*H*$_2$CH$_2$Br), 1.59–1.68 (m, 2H, C*H*$_2$CH$_2$CO$_2$H), 1.25–1.46 (m, 30H, 15 × C*H*$_2$).

δ_C (101 MHz, $CDCl_3$) 178.9, 34.2, 34.0, 33.0, 29.8, 29.7, 29.6, 29.4, 29.2, 28.9, 28.3, 24.8.

LR-MS (EI+) 393.0 ([M(^{81}Br)+H]$^+$), 391.0 ([M(^{79}Br)+H]$^+$), 375.0 ([M(^{81}Br)-H_2O+H]$^+$), 373.0 ([M(^{79}Br)-H_2O+H]$^+$), 312.0 ([M-Br+H]$^+$), 293.1 ([M-Br-H_2O+H]$^+$).

HR-MS calcd for $C_{20}H_{38}{}^{79}BrO^-$ ([M-H]$^-$) 389.2061, found 389.2057.

υ_{max} (thin film, cm^{-1}) 2914, 2848, 1693.

Mp 81–83 °C

Preparation of 20-azidoicosanoic acid 25

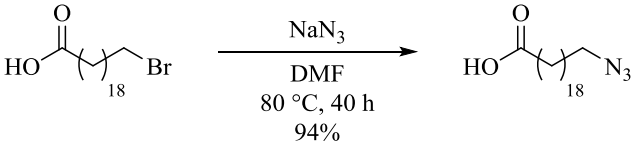

Reaction performed under a N_2 atmosphere

NaN_3 (499 mg, 7.7 mmol) was added to a solution of bromide **20** (500 mg, 1.28 mmol) in DMF (5 mL). The reaction was stirred at 80 °C for 40 h before being cooled to room temperature. A 1:1 mixture of EtOAc/H_2O (30 mL) was added, the layers separated and the aqueous phase extracted with EtOAc (3 × 15 mL). The combined organics were washed with brine (15 mL), dried over $MgSO_4$, filtered and concentrated *in vacuo*. The crude residue was purified by column chromatography, eluting with 90:10 petrol/EtOAc (+0.1% AcOH), to afford the product (425 mg, 94%) as a white solid.

δ_H (400 MHz, $CDCl_3$) 3.25 (t, 2H, *J* 7.0 Hz, C*H*$_2$N$_3$), 2.35 (t, 2H, *J* 7.5 Hz, C*H*$_2$CO$_2$H), 1.55–1.67 (m, 4H, C*H*$_2$CH$_2$N$_3$, C*H*$_2$CH$_2$CO$_2$H), 1.25–1.39 (m, 30H, 15 × C*H*$_2$).

δ_C (101 MHz, $CDCl_3$) 179.6, 51.7, 34.1, 29.8, 29.8, 29.7, 29.7, 29.6, 29.6, 29.4, 29.3, 29.2, 29.0, 26.9, 24.8.

LR-MS (ES-) 324.3 ([M-N_2-H]$^-$), 352.3 ([M-H]$^-$).

HR-MS calcd for $C_{20}H_{38}N_3O_2^-$ ([M-H]$^-$) 352.2970, found 352.2963.

υ_{max} (thin film, cm^{-1}) 3012, 2915, 2848, 2111, 1701.

Mp 63–65 °C

Preparation of 1,22-docosanediol 11(23)

Method A

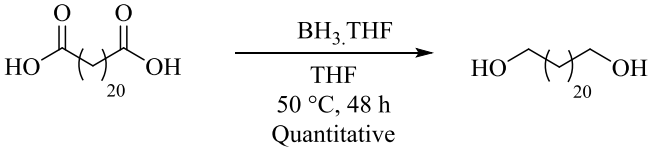

Reaction performed under a N_2 atmosphere.

BH_3.THF (1 M, 8.2 mL, 8.2 mmol) was added to a solution of docosanedioic acid (1.00 g, 2.70 mmol) in THF (51 mL). The reaction was heated to 50 °C for 24 h before additional BH_3.THF (1 M, 2.7 mL, 2.7 mmol) was added. The reaction was heated for a further 24 h before being cooled to 0 °C, quenched with MeOH (20 mL) and stirred for 30 min. HCl (20 mL of a 2 M aqueous solution) was added and the mixture stirred for 1 h. The solvent was evaporated *in vacuo* and the remaining aqueous phase extracted with $CHCl_3$ (3 × 30 mL). The combined organic phase was washed with H_2O (30 mL), brine (30 mL), dried over $MgSO_4$, filtered and concentrated *in vacuo* to afford the product (974 mg, 100%) as white solid.

Method B

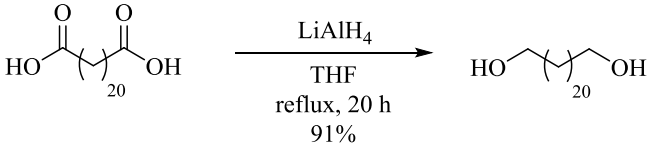

Reaction performed under a N_2 atmosphere.

Solid $LiAlH_4$ (1.36 g, 35.9 mmol) was added to a vigorously stirred solution of docosanedioic acid (5.12 g, 13.8 mmol) at room temperature. The reaction was heated to reflux and stirred at reflux for 20 h. Upon completion, the reaction was cooled to room temperature and wet $NaSO_4$ was added portion-wise until the grey suspension turned white. The suspension was stirred at room temperature until the white solid was free-flowing, and solid $MgSO_4$ was added. The reaction was filtered and the filter cake washed with Et_2O (5 × 50 mL). The solvent was evaporated *in vacuo* to afford the product (4.30 g, 91%) as a white solid.

δ_H (600 MHz, DMSO-d_6) 4.17 (t, 2H, *J* 5.1 Hz, 2 × O*H*), 3.36–3.40 (m, 4H, 2 × CH_2OH), 1.38–1.44 (m, 4H, 2 × CH_2CH_2OH), 1.25 (app. br. s., 36H, 18 × CH_2).

δ_C (151 MHz, DMSO-d_6) 60.6, 32.3, 28.8, 28.8, 28.7, 25.3.

LR-MS (MALDI-TOF) 365.4 ($[M+Na]^+$).

HR-MS calcd for $C_{22}H_{47}O_2^+$ ($[M+H]^+$) 343.3571, found 343.3574.

υ_{max} (thin film, cm^{-1}) 3255, 2915, 2848.

Mp 98–100 °C (lit. 96–98 °C)(23)

Preparation of 22-bromodocosan-1-ol 16(24)

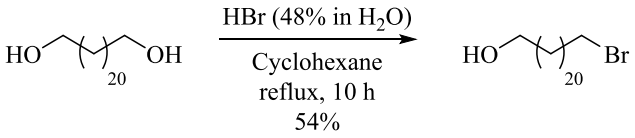

HBr (48% in H_2O, 32 mL) was added to a suspension of diol **11** (4.16 g, 12.2 mmol) in cyclohexane (64 mL). The biphasic mixture was heated to reflux for 10 h before being cooled to room temperature. The layers were separated and the aqueous phase extracted with CH_2Cl_2 (4 × 50 mL). The combined organics were washed with $NaHCO_3$ (4 × 30 mL of a saturated aqueous solution), brine (30 mL), dried over $MgSO_4$, filtered and concentrated *in vacuo*. The crude residue was purified by column chromatography, eluting with 95:5 petrol/EtOAc then 70:30 petrol/EtOAc, to afford the product (2.65 g, 54%) as a pale yellow solid.

δ_H (400 MHz, $CDCl_3$) 3.64 (t, 2H, *J* 6.6 Hz, C*H*$_2$OH), 3.40 (t, 2H, *J* 6.9 Hz, C*H*$_2$Br), 1.81–1.89 (m, 2H, C*H*$_2$CH$_2$Br), 1.53–1.60 (m, 2H, C*H*$_2$CH$_2$OH), 1.25–1.44 (m, 36H, 18 × C*H*$_2$).

δ_C (101 MHz, $CDCl_3$) 63.3, 34.2, 33.0, 33.0, 29.8, 29.8, 29.7, 29.6, 28.9, 28.3, 25.9.

LR-MS (EI+) 405.5 ([M(^{81}Br)+H]$^+$), 403.5 ([M(^{79}Br)+H]$^+$), 388.5 ([M(^{81}Br)-H_2O+H]$^+$), 386.5 ([M(^{79}Br)-H_2O+H]$^+$), 324.4 ([M-Br+H]$^+$).

HR-MS calcd for $C_{22}H_{49}{}^{79}BrON$ ([M+NH_4]$^+$) 422.2992, found 422.2990.

υ_{max} (thin film, cm^{-1}) 3276, 2915, 2846.

Mp 66–68 °C (lit. 72 °C)(24)

Preparation of 22-bromodocosanoic acid 21

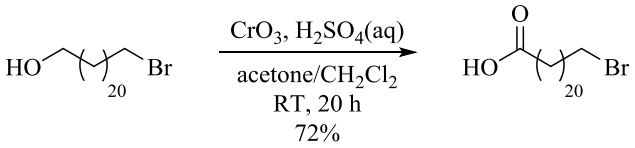

CrO_3 (696 mg, 6.96 mmol) was dissolved in concentrated H_2SO_4 (1.3 mL). Cold H_2O (2.9 mL) was added slowly and the solution stirred at room temperature for 10 min. The resulting solution was added drop-wise to a solution of alcohol **16** (703 mg, 1.74 mmol) in acetone/CH_2Cl_2 (3:1, 65 mL). The reaction was stirred at room temperature for 20 h before being H_2O (50 mL) and CH_2Cl_2 (30 mL) were added. The layers were separated and the aqueous phase extracted with CH_2Cl_2 (4 × 30 mL). The combined organics were washed with brine (30 mL), dried over $MgSO_4$, filtered and concentrated *in vacuo*. The crude residue was purified by column chromatography, eluting with 90:10 petrol/EtOAc (+0.1% AcOH), to afford the product (522 mg, 72%) as a white solid.

δ_H (400 MHz, $CDCl_3$) 3.40 (t, 2H, *J* 6.9 Hz, C*H*$_2$Br), 2.35 (t, 2H, *J* 7.5 Hz, C*H*$_2$CO$_2$H), 1.81–1.90 (m, 2H, C*H*$_2$CH$_2$Br), 1.59–1.68 (m, 2H, C*H*$_2$CH$_2$CO$_2$H), 1.25–1.44 (m, 34H, 17 × C*H*$_2$).

δ_C (101 MHz, $CDCl_3$) 179.4, 34.2, 34.1, 33.0, 29.8, 29.7, 29.6, 29.4, 29.2, 28.9, 28.3, 24.8.

LR-MS (EI+) 421.0 ([M(^{81}Br)+H]$^+$), 419.0 ([M(^{79}Br)+H]$^+$), 393.0 ([M(^{81}Br)-H_2O+H]$^+$), 391.0 ([M(^{79}Br)-H_2O+H]$^+$), 341.1 ([M-Br+H]$^+$), 293.1 ([M-Br-H_2O+H]$^+$).

HR-MS calcd for $C_{22}H_{42}{}^{79}BrO_2^-$ ([M-H]$^-$) 417.2374, found 417.2368.

υ_{max} (thin film, cm^{-1}) 2913, 2846, 1693.

Mp 78–80 °C

Preparation of 22-azidodocosanoic acid 26

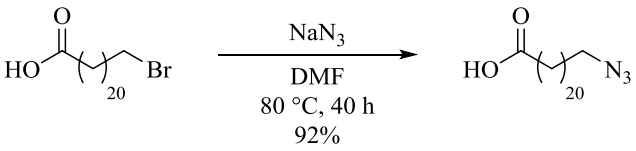

Reaction performed under a N_2 atmosphere

NaN_3 (195 mg, 3.0 mmol) was added to a solution of bromide **21** (208 mg, 0.5 mmol) in DMF (2 mL). The reaction was stirred at 80 °C for 40 h before being cooled to room temperature. A 1:1 mixture of EtOAc/H_2O (20 mL) was added, the layers separated and the aqueous phase extracted with EtOAc (3 × 10 mL) and CH_2Cl_2 (10 mL). The combined organics were washed with brine (15 mL), dried over $MgSO_4$, filtered and concentrated *in vacuo*. The crude residue was purified by column chromatography, eluting with 90:10 petrol/EtOAc (+0.1% AcOH), to afford the product (176 mg, 92%) as a white solid.

δ_H (400 MHz, $CDCl_3$) 3.25 (t, 2H, *J* 7.0 Hz, C*H*$_2$N$_3$), 2.34 (t, 2H, *J* 7.5 Hz, C*H*$_2$CO$_2$H), 1.56–1.67 (m, 4H, C*H*$_2$CH$_2$N$_3$, C*H*$_2$CH$_2$CO$_2$H), 1.25–1.37 (m, 34H, 17 × C*H*$_2$).

δ_C (101 MHz, $CDCl_3$) 179.9, 51.7, 34.1, 29.8, 29.7, 29.7, 29.6, 29.6, 29.4, 29.3, 29.3, 29.2, 29.0, 26.9, 24.8.

LR-MS (ES-) 352.3 ([M-N_2-H]$^-$), 380.3 ([M-H]$^-$).

HR-MS calcd for $C_{22}H_{42}N_3O_2^-$ ([M-H]$^-$) 380.3283, found 380.3275.

υ_{max} (thin film, cm^{-1}) 2913, 2846, 2095, 1693.

Mp 71–73 °C

14-Azidotetradecanoic acid 22 ^{1}H NMR (400 MHz, $CDCl_3$)

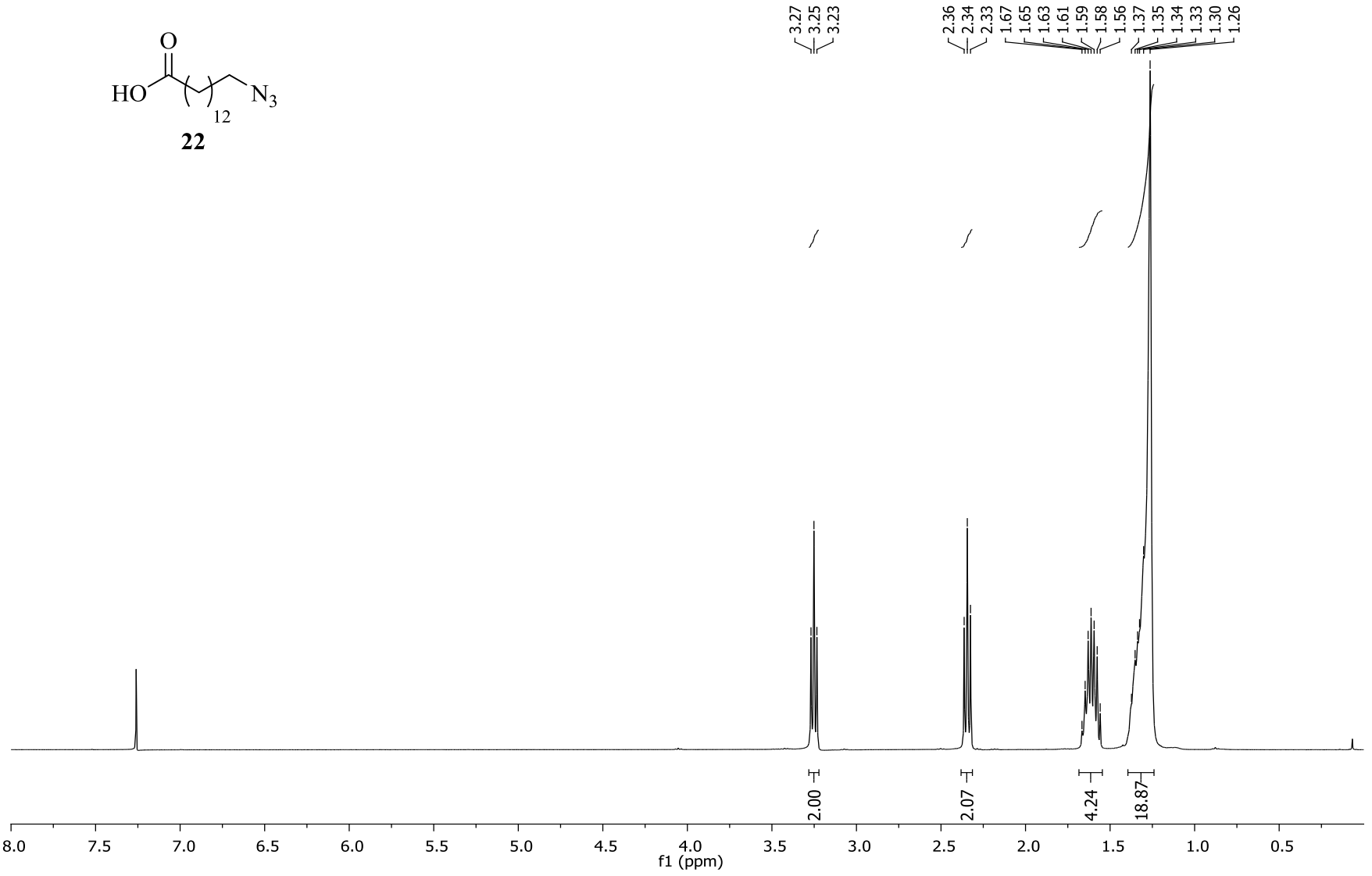

14-Azidotetradecanoic acid 22 ^{13}C NMR (101 MHz, $CDCl_3$)

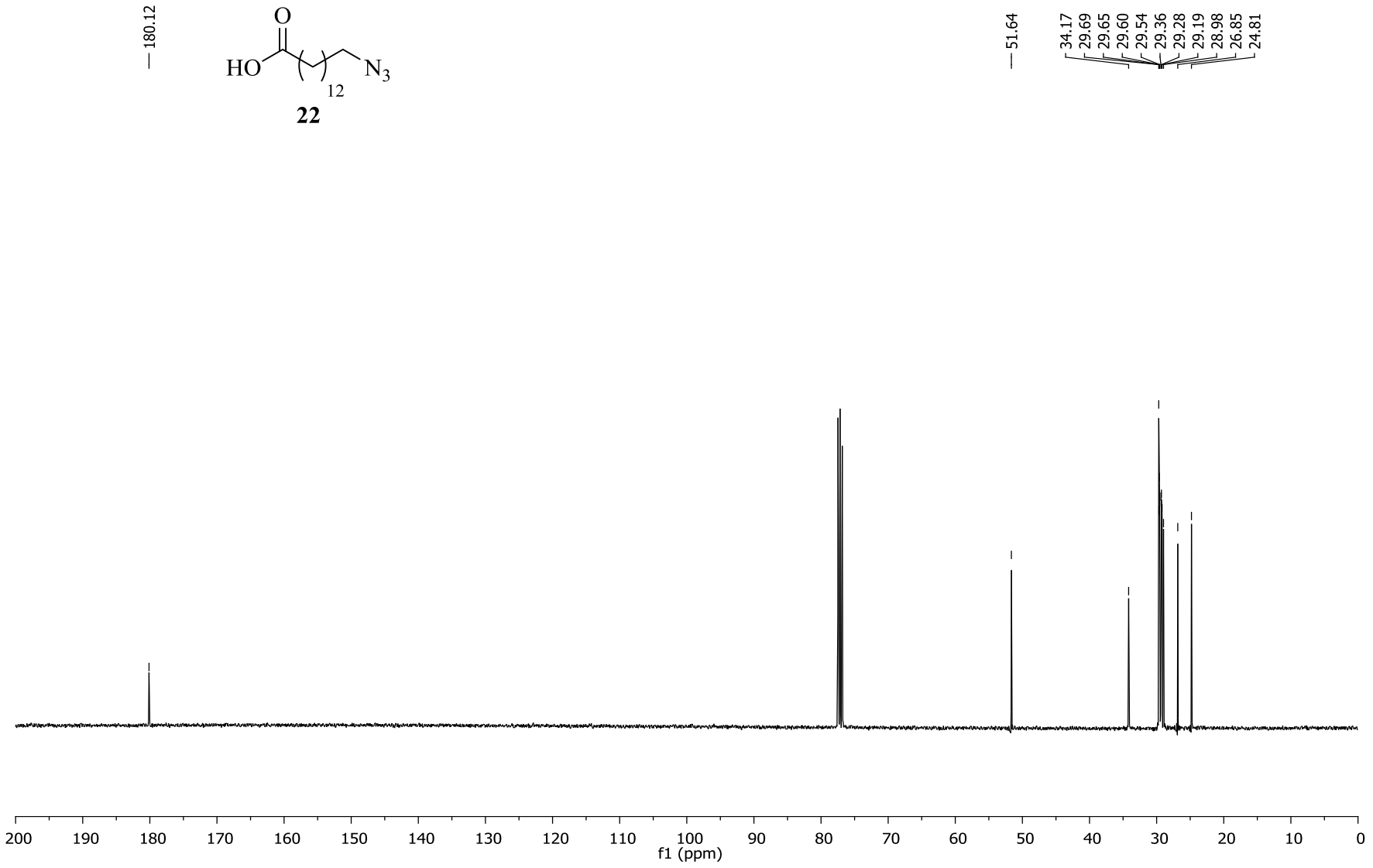

16-Azidohexadecanoic acid 23 ^{1}H NMR (400 MHz, $CDCl_3$)

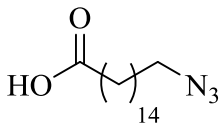

23

16-Azidohexadecanoic acid 23 ^{13}C NMR (101 MHz, $CDCl_3$)

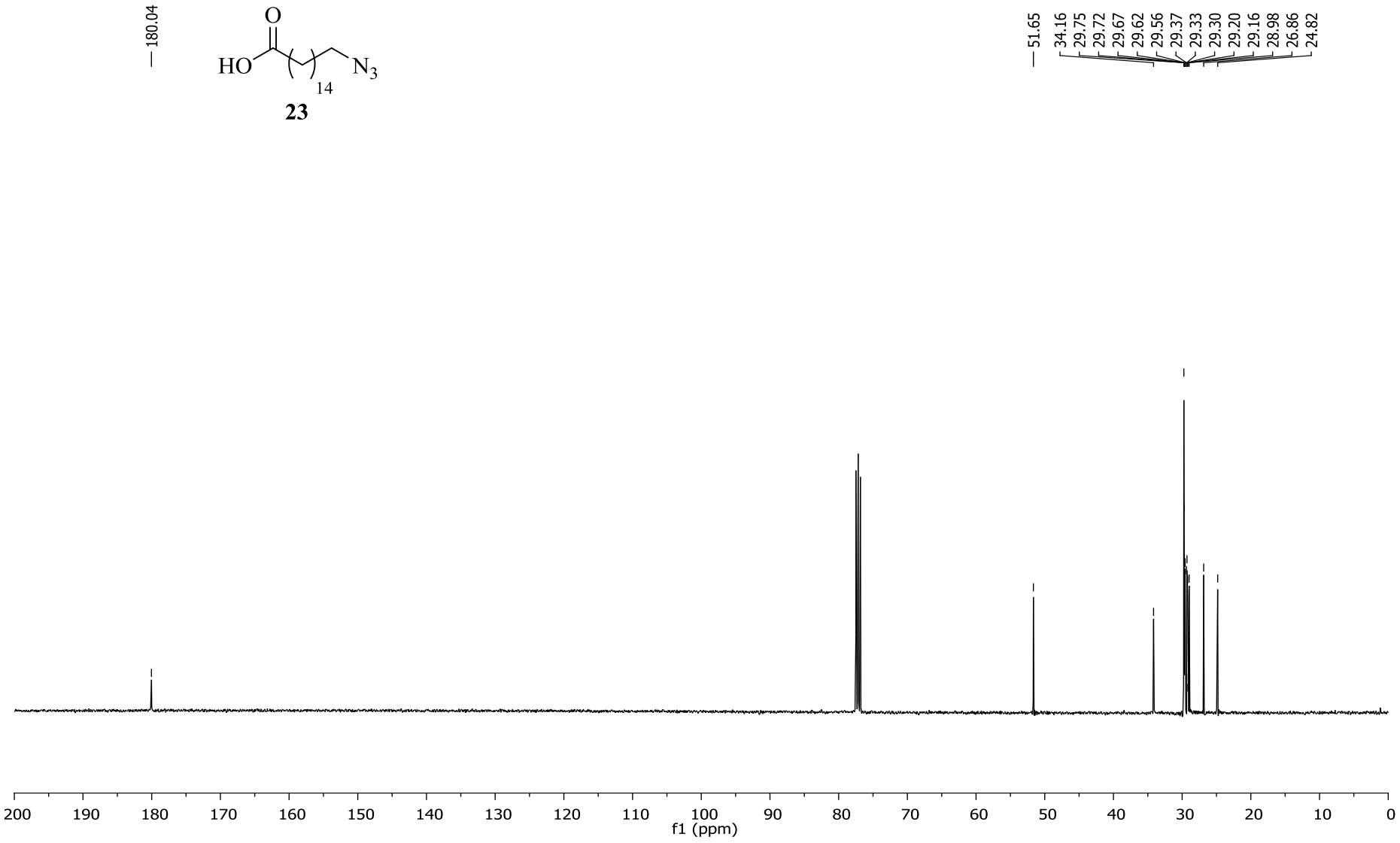

18-Azidooctadecanoic acid 24 ^{1}H NMR (400 MHz, $CDCl_3$)

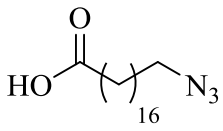

24

18-Azidooctadecanoic acid 24 ^{13}C NMR (101 MHz, $CDCl_3$)

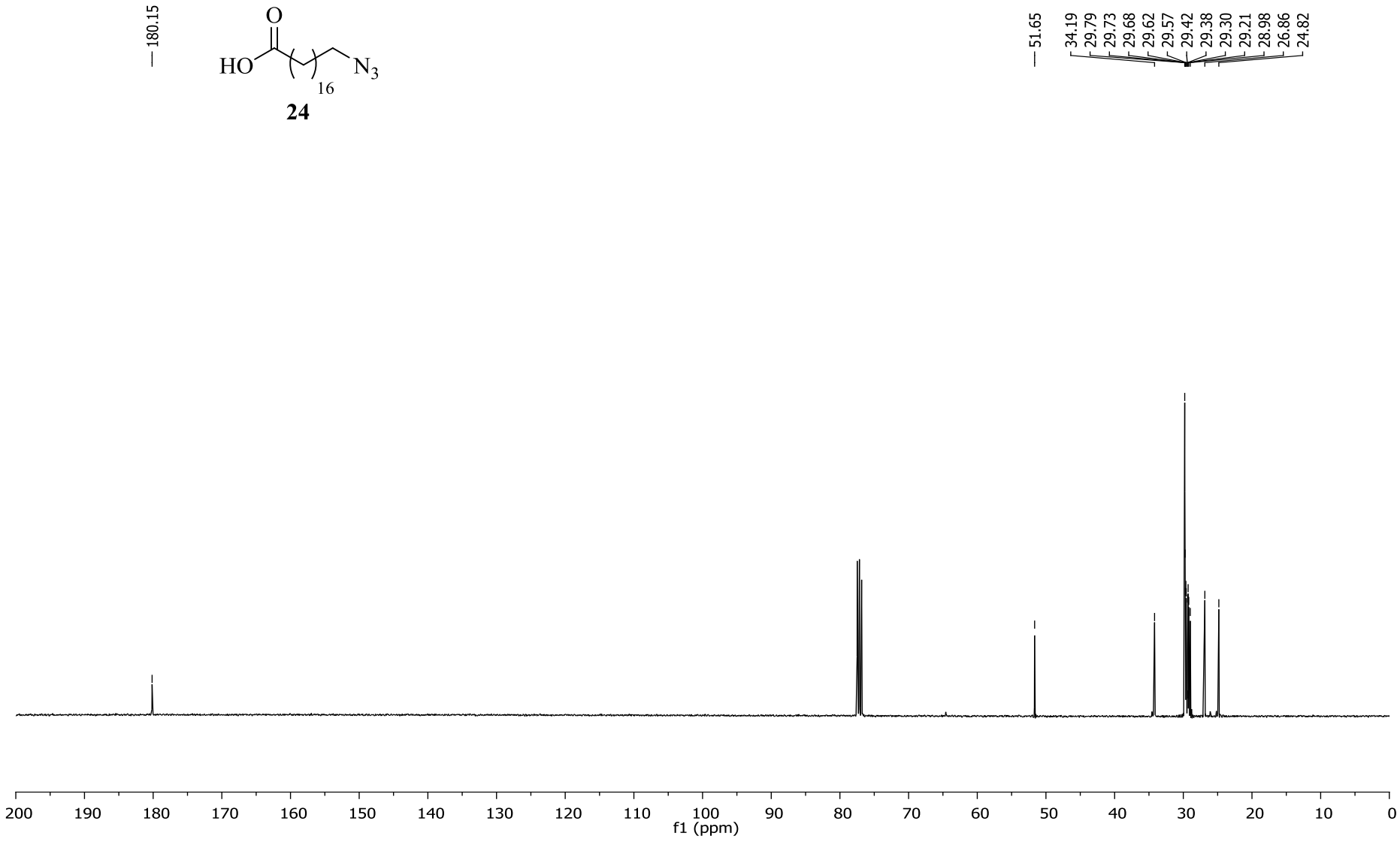

20-Azidoicoscanoic acid 25 ^{1}H NMR (400 MHz, $CDCl_3$)

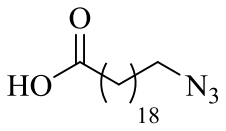

25

20-Azidoicoscanoic acid 25 ^{13}C NMR (101 MHz, $CDCl_3$)

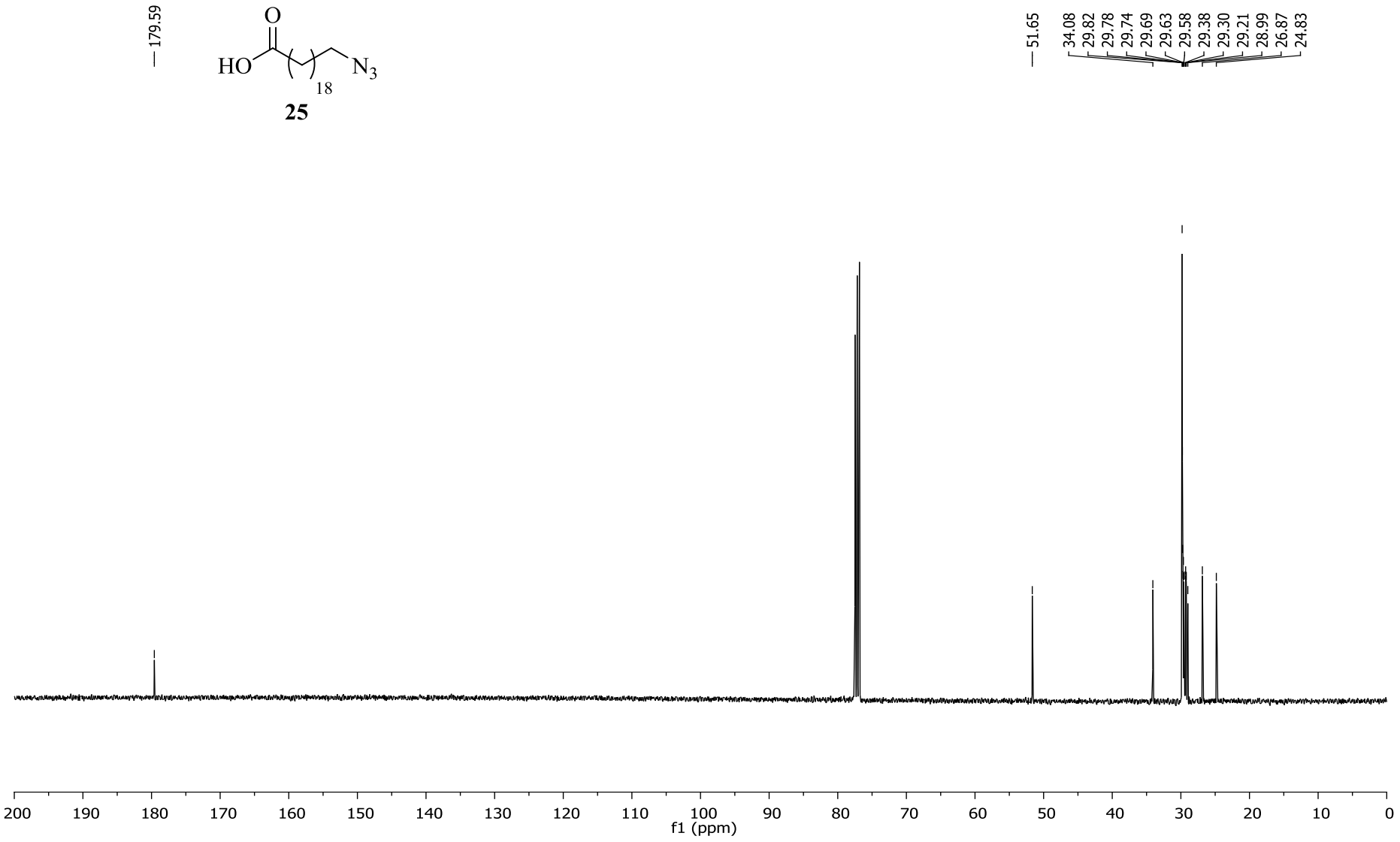

22-Azidodocoscanoic acid 26 ^{1}H NMR (400 MHz, $CDCl_3$)

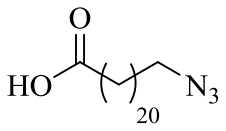

26

22-Azidodcoscanoic acid 26 ^{13}C NMR (101 MHz, $CDCl_3$)

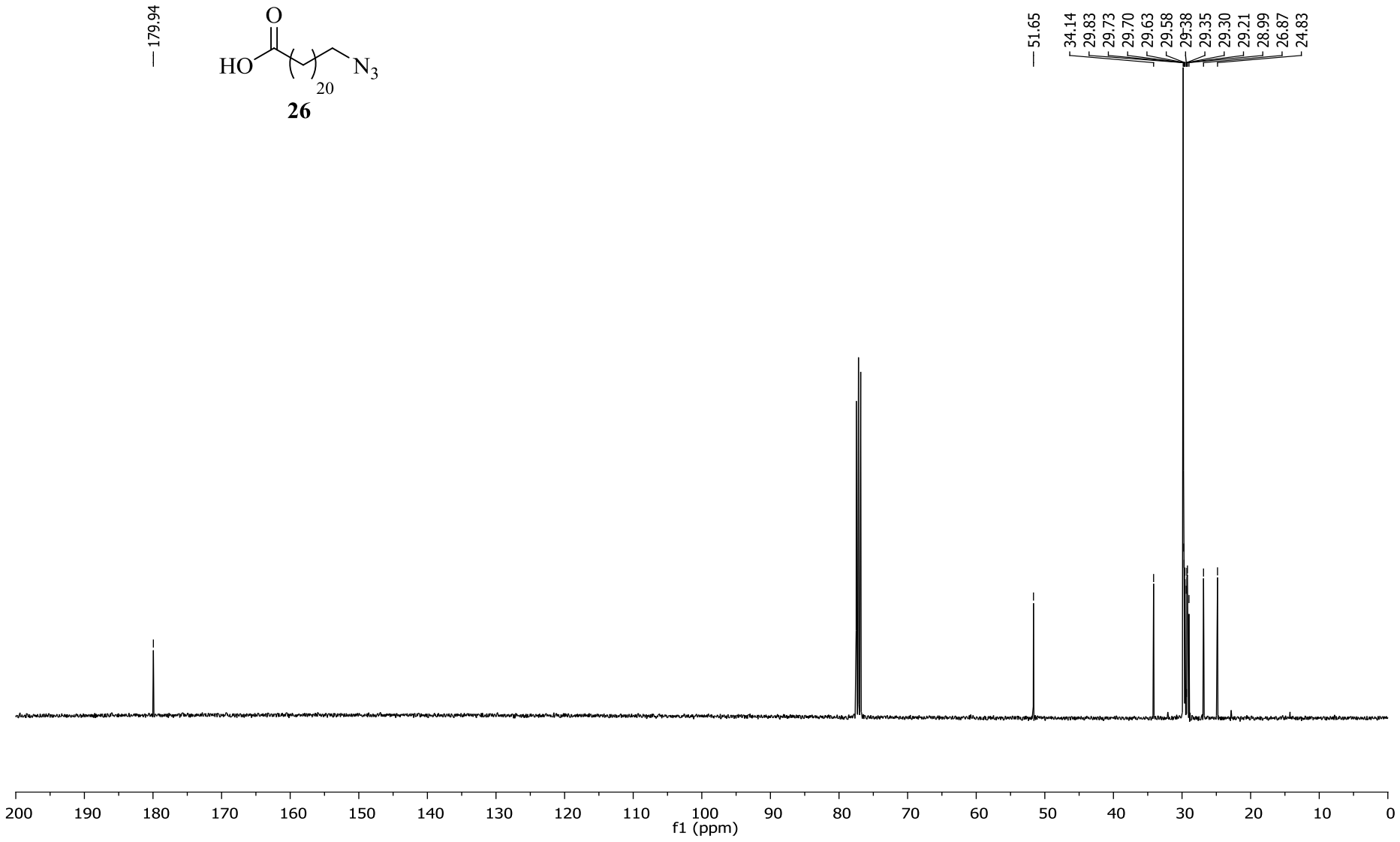

Hexadec-15-ynoic acid 30 ^{1}H NMR (400 MHz, $CDCl_3$)

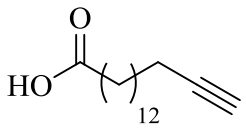

30

Hexadec-15-ynoic acid 30 ^{13}C NMR (101 MHz, $CDCl_3$)

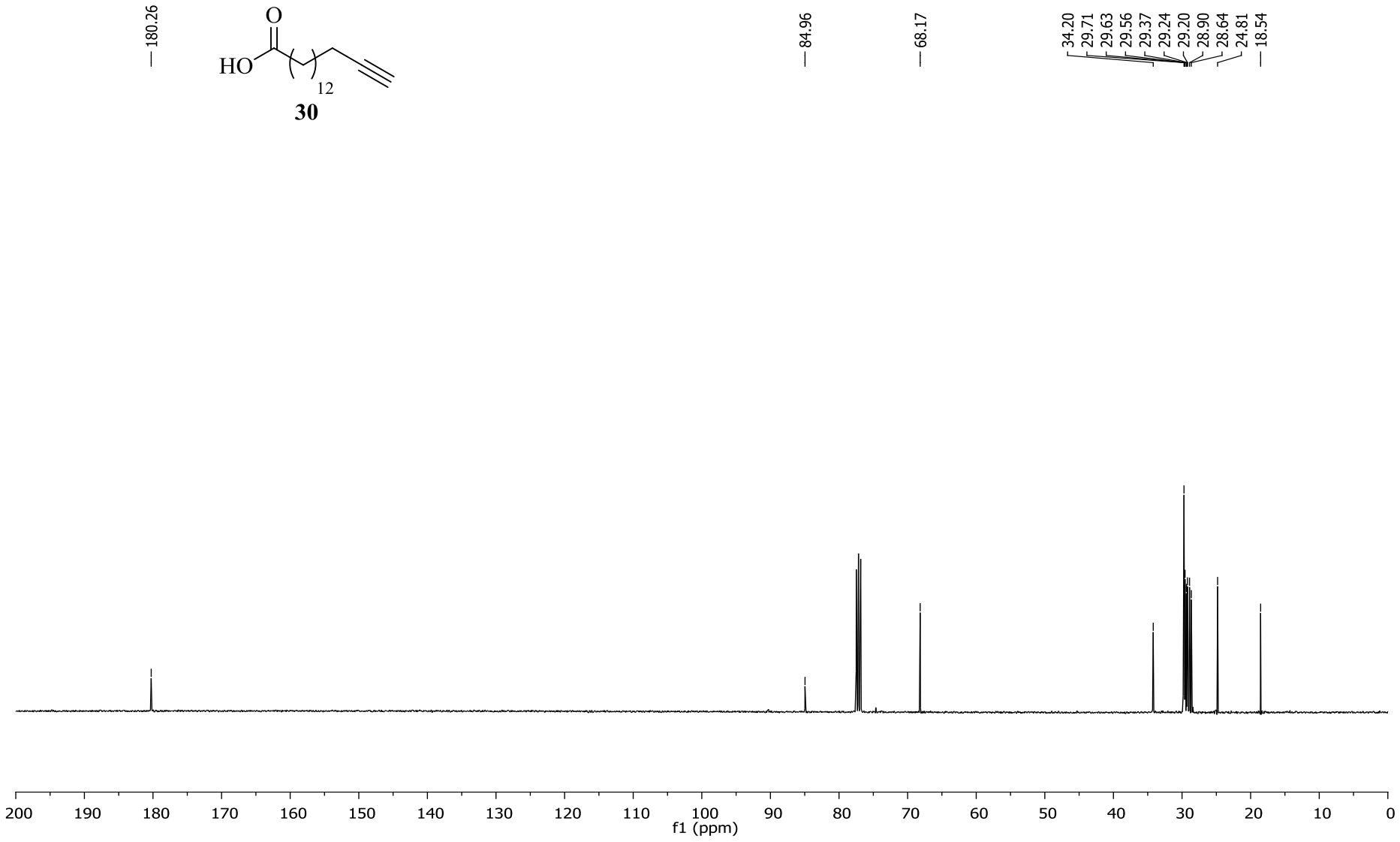

Octadec-17-ynoic acid 31 ^{1}H NMR (400 MHz, $CDCl_3$)

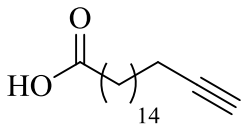

31

Octadec-17-ynoic acid 31 ^{13}C NMR (101 MHz, $CDCl_3$)

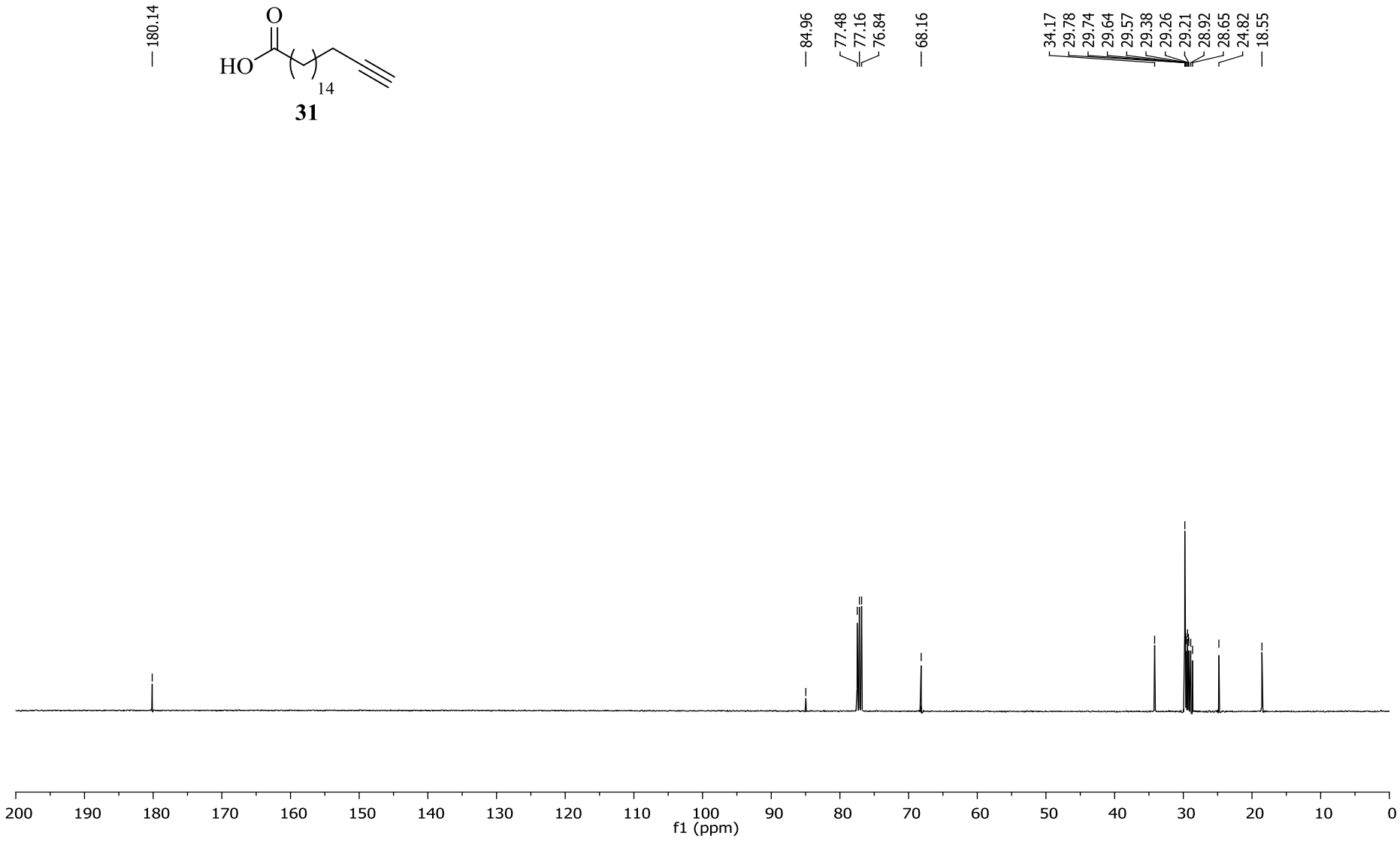

Icos-19-ynoic acid 32 ^{1}H NMR (400 MHz, $CDCl_3$)

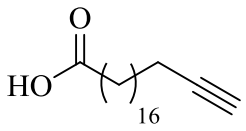

32

Icos-19-ynoic acid 32 ^{13}C NMR (101 MHz, $CDCl_3$)

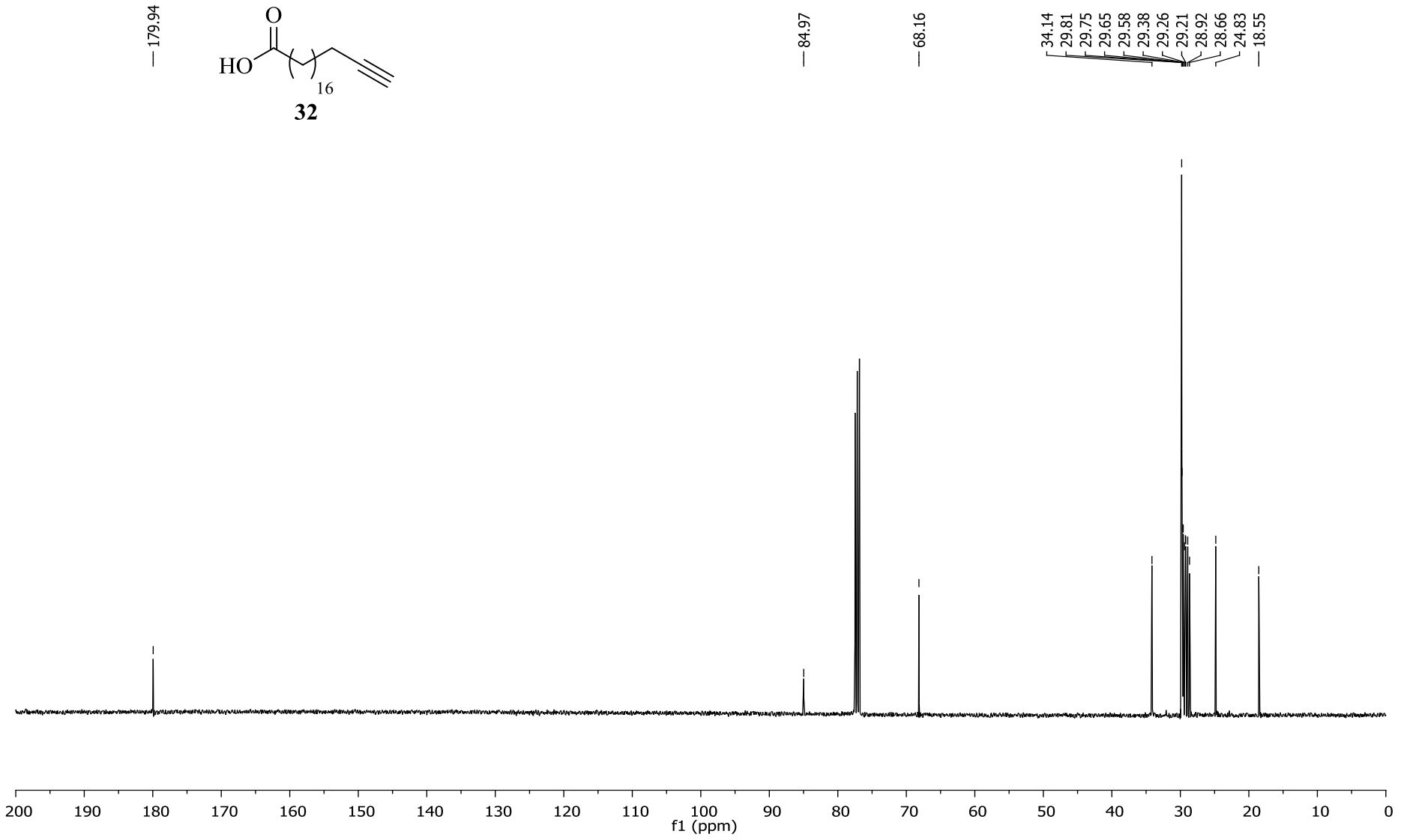

References

1. Mori K (2008) Synthesis of all the six components of the female-produced contact sex pheromone of the German cockroach, Blattella germanica (L.). *Tetrahedron* **64**(18):4060-4071.
2. Zhang T, Zheng FP, Xu XH, Huang C, Liu YP, Sun BG (2014) Synthesis of Bromoalkanols under Microwave Irradiation. *Adv Mater Res* **1051**:182-185.
3. Dong C-Z, Ahamada-Himidi A, Plocki S, Aoun D, Touaibia M, Meddad-Bel Habich N, Huet J, Redeuilh C, Ombetta J-E, Godfroid J-J, Massicot F, Heymans F (2005) Inhibition of secretory phospholipase A2. 2-Synthesis and structure–activity relationship studies of 4,5-dihydro-3-(4-tetradecyloxybenzyl)-1,2,4-4*H*-oxadiazol-5-one (PMS1062) derivatives specific for group II enzyme. *Bioorg Med Chem* **13**(6):1989-2007.
4. Davis SC, Sui Z, Peterson JA, de Montellano PRO (1996) Oxidation of ω-Oxo Fatty Acids by Cytochrome P450BM-3(CYP102). *Arch Biochem Biophys* **328**(1):35-42.
5. Ames DE, Covell AN, Goodburn TG (1965) Syntheses of long-chain acids. Part VI. Acetylenic acids and cis,cis-docosa-5,13-dienoic acid. *J Chem Soc* (0):894-899.
6. Hang HC, Geutjes E-J, Grotenbreg G, Pollington AM, Bijlmakers MJ, Ploegh HL (2007) Chemical Probes for the Rapid Detection of Fatty-Acylated Proteins in Mammalian Cells. *J Am Chem Soc* **129**(10):2744-2745.
7. Charron G, Zhang MM, Yount JS, Wilson J, Raghavan AS, Shamir E, Hang HC (2009) Robust Fluorescent Detection of Protein Fatty-Acylation with Chemical Reporters. *J Am Chem Soc* **131**(13):4967-4975.
8. Hebert N, Beck A, Lennox RB, Just G (1992) A new reagent for the removal of the 4-methoxybenzyl ether: application to the synthesis of unusual macrocyclic and bolaform phosphatidylcholines. *J Org Chem* **57**(6):1777-1783.
9. Yuen AKL, Heinroth F, Ward AJ, Masters AF, Maschmeyer T (2012) Novel bis(methylimidazolium)alkane bolaamphiphiles as templates for supermicroporous and mesoporous silicas. *Microporous Mesoporous Mater* **148**(1):62-72.
10. Opálka L, Kováčik A, Sochorová M, Roh J, Kuneš J, Lenčo J, Vávrová K (2015) Scalable Synthesis of Human Ultralong Chain Ceramides. *Org Lett* **17**(21):5456-5459.
11. Hunsdiecker H, Hunsdiecker C (1942) Über den Abbau der Salze aliphatischer Säuren durch Brom. *Chem Ber* **75**(3):291-297.
12. DeVries VG, Moran DB, Allen GR, Riggi SJ (1976) Hypolipidemic alkoxybenzoic acids. *J Med Chem* **19**(7):946-957.
13. Holder SJ, Sriskantha BC, Bagshaw SA, Bruce IJ (2012) Headgroup effects on the krafft temperatures and self-assembly of ω-hydroxy and ω-carboxy hexadecyl quaternary ammonium bromide bolaform amphiphiles: Micelles versus molecular clusters? *J Colloid Interface Sci* **367**(1):293-304.
14. Augustin KE , Schäfer HJ (1991) Conversion of oleic acid to 17- and 18-substituted stearic acid derivatives by way of the "acetylene zipper". *Liebigs Ann Chem* (10):1037-1040.
15. Lucas T , Schäfer HJ (2014) Hydroboration of unsaturated fatty acid methyl esters and conversion of the boron adducts. *Eur J Lipid Sci Technol* **116**(1):52-62.
16. Cardinale G, Laan JAM, Van der Steen D, Ward JP (1985) Bifunctional compounds from reaction of alkoxy hydroperoxides with metal salts. *Tetrahedron* **41**(24):6051-6054.
17. Musgrave OC, Stark J, Spring FS (1952) Non-saponifiable constituents of Spanish broom. *J Chem Soc* (0):4393-4397.
18. Polyakova SM, Belov VN, Yan SF, Eggeling C, Ringemann C, Schwarzmann G, de Meijere A, Hell SW (2009) New GM1 Ganglioside Derivatives for Selective Single and Double Labelling of the Natural Glycosphingolipid Skeleton. *Eur J Org Chem* (30):5162-5177.
19. Chuit P, Hausser J (1929) Réduction des éthers diméthyliques des acides polyméthylène-dicarboniques de 15 à 21 atomes de carbone, par le sodium et l'alcool. *Helv Chim Acta* **12**(1):850-859.
20. Kimura K, Takahashi M, Tanaka A (1960) Anodic Synthesis of Fatty Acids. VI. The Syntheses of ω-Hydroxylated Fatty Acids and ω,ω'-Diols. *Chem Pharm Bull* **8**(12):1059-1062.

21. Weber ME, Schlesinger PH, Gokel GW (2005) Dynamic Assessment of Bilayer Thickness by Varying Phospholipid and Hydraphile Synthetic Channel Chain Lengths. *J Am Chem Soc* **127**(2):636-642.
22. Van der Steen M, Stevens CV, Eeckhout Y, De Buyck L, Ghelfi F, Roncaglia F (2008) Undecylenic acid: A valuable renewable building block on route to Tyromycin A derivatives. *Eur J Lipid Sci Technol* **110**(9):846-852.
23. Drescher S, Meister A, Blume A, Karlsson G, Almgren M, Dobner B (2007) General Synthesis and Aggregation Behaviour of a Series of Single-Chain 1,ω-Bis(phosphocholines). *Chem Eur J* **13**(18):5300-5307.
24. Signer R , Sprecher P (1947) Die Synthese von ω-Bromdokosanol. *Helv Chim Acta* **30**(4):1001-1004.

Acyl-CoA	MRM Transition	Collision Energy (eV)	Declustering Potential (eV)	Dwell Time (ms)	Response factor
14:0	976→471	40	40	500	2.25
16:0	1006→499	40	40	500	2.38
16:1	1004→497	40	40	500	2.3
17:0	1020→513	40	40	100	2.32
18:0	1034→527	45	40	250	2.62
18:1	1032→525	45	40	250	2.5
18:2	1030→523	50	45	500	2.4
20:0	1062→555	50	45	500	2.48
20:2	1058→551	50	45	500	2.3
20:4	1054→547	50	45	250	2.23
20:5	1052→545	55	45	500	2.2
22:0	1090→583	50	45	500	2.2
22:4	1082→575	55	45	500	2.1
22:5	1080→573	55	45	500	2.1
22:6	1078→571	50	45	500	2.1
C14:0-azide	1019→512	40	40	500	2.3
C16:0-azide	1047→540	40	40	500	2.3
C16:1-azide	1045→538	40	40	500	2.3
C18:0-azide	1075→568	45	40	500	2.3
C18:1-azide	1073→566	45	40	500	2.2
C18:2-azide	1071→564	45	40	500	2.1
C20:0-azide	1113→596	50	45	500	2.3
C20:1-azide	1111→594	50	45	500	2.3
C22:0-azide	1141→624	50	45	500	2.2

Table 1. MRM Transitions:

Multiple reaction monitoring transitions were based upon optimized fragmentation in positive ion mode. Interface temp 30 C, Nanomate: gas pressure 0.5 psi, Tip voltage 1.25-1.3kV, EP 8, CXP 12.

[1] Resp Factor[1] (10^6 cpm/pmole) are based upon standard curve point (1000, 500, 100, 10, 5, 2.5 and 1 pmole(s)) has its own response in terms of number of specific ions observed by the mass spectrometer under those specific conditions. Values in blue represent estimates in the absence of actual standards and similar related response factors observed previously (doi: 10.1194/jlr.D800001-JLR200))

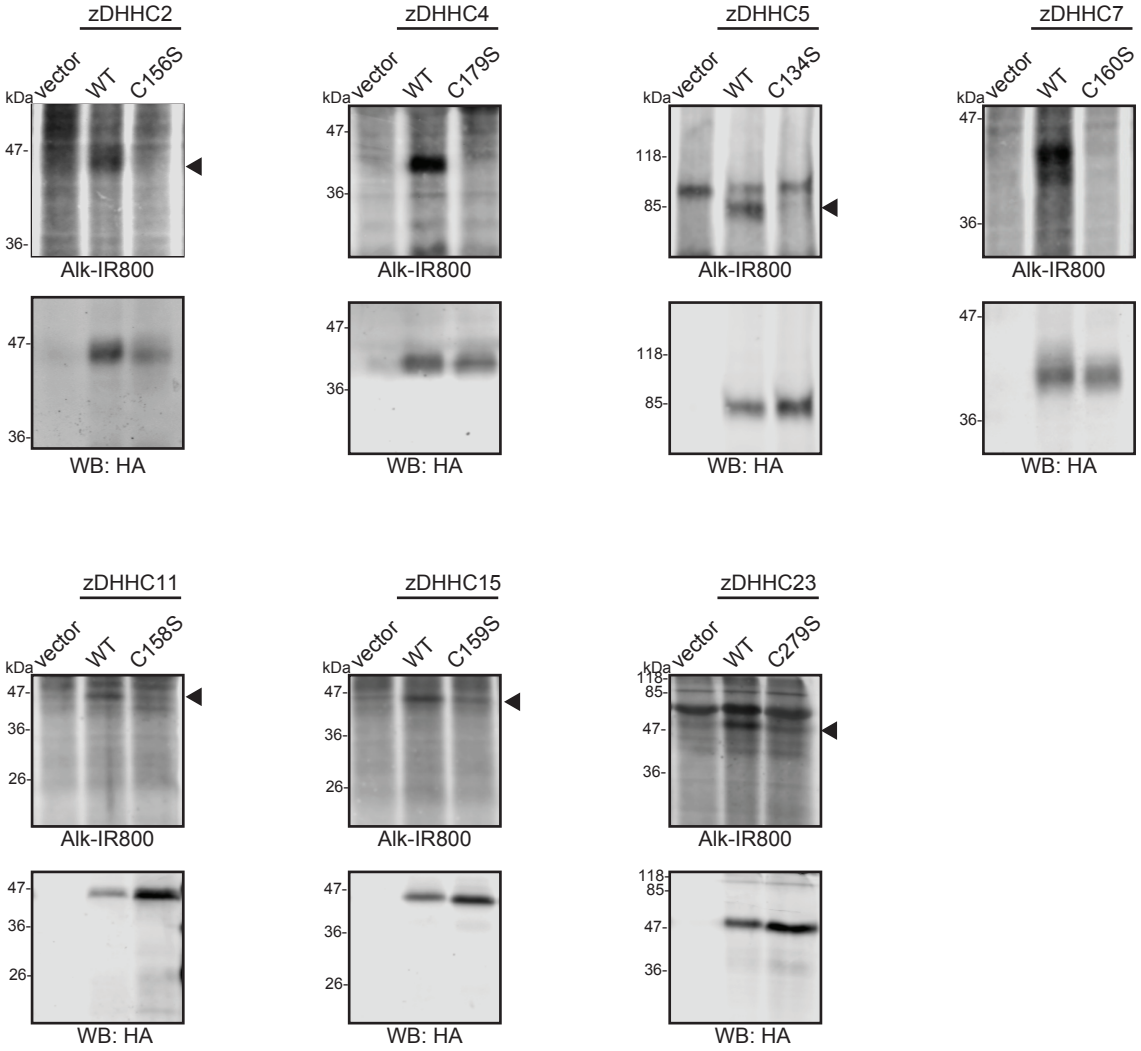

Supplementary Figure 1: *S*-acylation of wild-type and inactive zDHHC enzymes by C16:0- azides.
HEK293T cells transfected with HA-tagged wild-type or mutant zDHHC enzyme constructs containing a cysteine-to-serine mutation of the catalytic DHHC cysteine residue. Cells were then incubated with C16:0 fatty acid azides for 4 h at 37 ºC. Fatty acid azides were then labelled by click chemistry using an alkyne-800 infrared dye. Isolated proteins were resolved by SDS-PAGE and transferred to nitrocellulose membranes. Representative click signals and western blots are shown. Position of molecular weight markers are shown on the left. Arrowheads indicate the zDHHC bands that incorporate label.

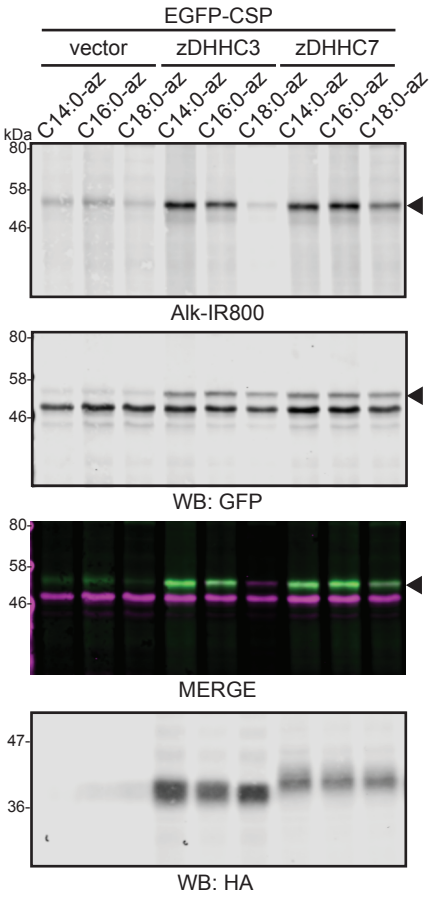

Supplementary Figure 2: *S*-acylation of EGFP-Cysteine-string protein by different zDHHC enzymes.
HEK293T cells were transfected with EGFP-CSP together with pEF-BOS-HA (vector), HA-zDHHC3 or HA-zDHHC7. Cells were then incubated with C14:0, C16:0 or C18:0 fatty acid azides as indicated for 4 h at 37 ºC. Fatty acid azides were labelled by click chemistry using an alkyne-800 infrared dye. Isolated proteins were resolved by SDS-PAGE and transferred to nitrocellulose membranes. Representative click signals and western blots are shown. Position of molecular weight markers are shown on the left. Note that CSP migrates as two bands, the upper band (*arrowhead*) is S-acylated, whereas the lower band is non-acylated.

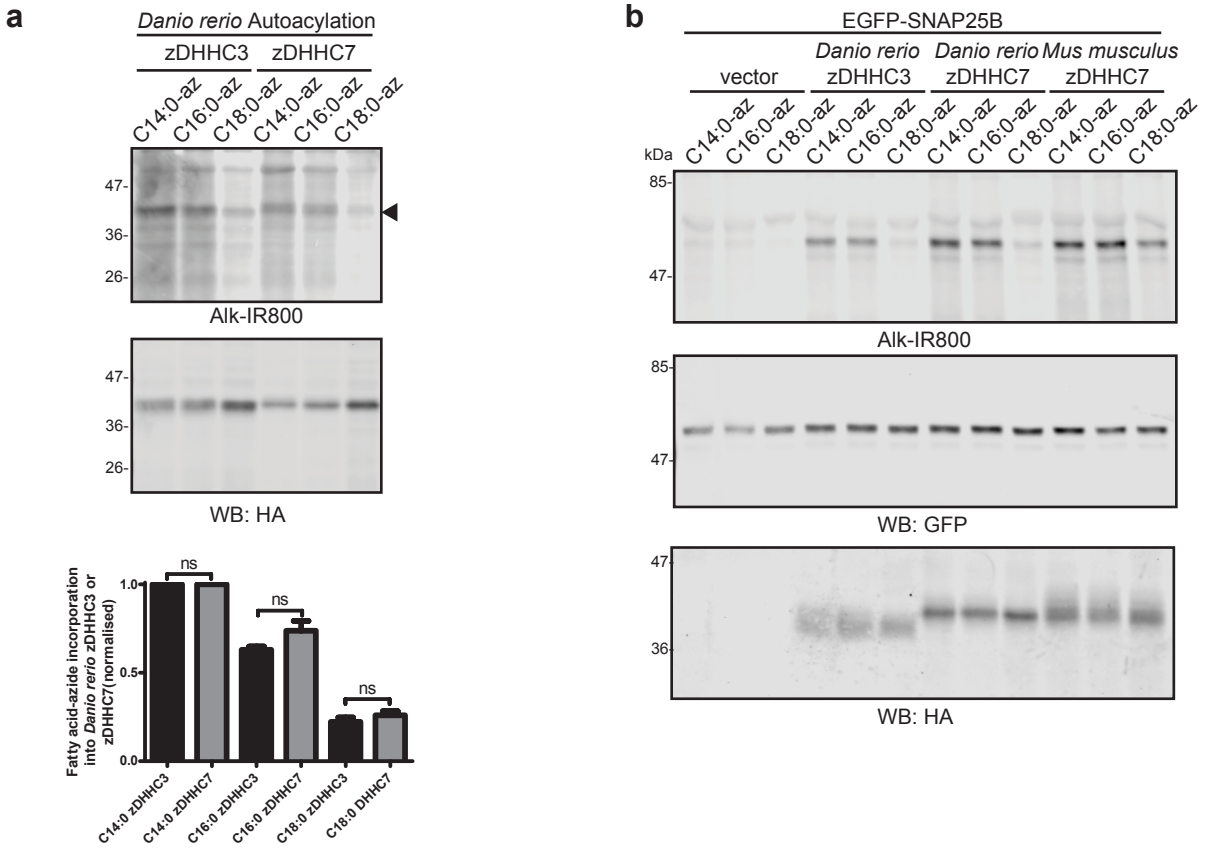

Supplementary Figure 3: S-acylation profiles of *Danio rerio* zDHHC3 and zDHHC7 by fatty-acid azides.
(A) HEK293T cells transfected with HA-tagged zDHHC3 or zDHHC7 from *Danio rerio* were incubated with C14:0, C16:0 or C18:0 fatty acid azides for 4 h at 37 ºC. Fatty acid azides were then labelled by click chemistry using an alkyne-800 infrared dye. Isolated proteins were resolved by SDS-PAGE and transferred to nitrocellulose membranes. Representative click signals and western blots and quantified data (mean ± SEM) are shown. n = 5; ns = not significant. (B) HEK293T cells were transfected with EGFP-SNAP25B together with either pEF-BOS-HA (vector control), zDHHC3 or zDHHC7 from *Danio rerio*, or mouse zDHHC7. Cells were then incubated with C14:0, C16:0 or C18:0 fatty acid azides for 4 h at 37 ºC, and fatty acid azides were then labelled by click chemistry using an alkyne-800 infrared dye. Isolated proteins were resolved by SDS-PAGE and transferred to nitrocellulose membranes. Representative click signals and western blots are shown.